The Pennsylvania State University

The Graduate School

Graduate Program in Acoustics

TIME-VARYING AUTOREGRESSIVE MODELLING FOR NONSTATIONARY ACOUSTIC SIGNAL AND ITS FREQUENCY ANALYSIS

A Thesis in Acoustics

by

Chukiet Sodsri

Submitted in Partial Fulfillment
of the Requirements
for the Degree of

Doctor of Philosophy

December 2003

We approve the thesis of Chukiet Sodsri.

Date of Signature

David C. Swanson
Senior Research Associate
Associate Professor of Acoustics
Thesis Advisor
Chair of Committee

John F. Doherty
Associate Professor of Electrical Engineering

Karl M. Reichard
Research Associate
Assistant Professor of Acoustics

Victor W. Sparrow
Associate Professor of Acoustics

Anthony A. Atchley
Professor of Acoustics
Head of the Graduate Program in Acoustics

ABSTRACT

A time-varying autoregressive (TVAR) approach is used for modeling nonstationary signals, and frequency information is then extracted from the TVAR parameters. Two methods may be used for estimating the TVAR parameters: the adaptive algorithm approach and the basis function approach. Adaptive algorithms, such as the least mean square (LMS) and the recursive least square (RLS), use a dynamic model for adapting the TVAR parameters and are capable of tracking time-varying frequency, provided that the variation is slow. It is observed that, if the signals have a single time-frequency component, the RLS with a fixed pole on the unit circle yields the fastest convergence. The basis function method employs an explicit model for the TVAR parameter variation, and model parameters are estimated via a block calculation. We proposed a modification to the basis function method by utilizing both forward and backward predictors for estimating the time-varying spectral density of nonstationary signals. It is shown that our approach yields better accuracy than the existing basis function approach, which uses only the forward predictor. The selection of the basis functions and limitations are also discussed in this thesis. Finally, the proposed approach is applied to analyze violin vibrato. Our results showed superior frequency resolution and spectral line smoothness using the proposed approach, compared to conventional analysis with the short time Fourier transform (STFT) whose frequency resolution is very limited. It was also found that frequency modulation of vibrato occurs at the rate of 6 Hz, and the frequency variations for each partial are different and increase nonlinearly with the partial number.

TABLE OF CONTENTS

LIST OF FIGURES

LIST OF TABLES

ACKNOWLEDGEMENTS

I would like to express my gratitude to the members of my committee for their constructive comments and valuable suggestions. In particular, I am indebted to my advisor, Dr. David C. Swanson, for his both insight and broad range of knowledge that he willingly shared with me during the research and writing of my dissertation. His advices are always very helpful, both academically and non-academically. It has been a great pleasure working with him. I also would like to extend my sincere thank to Dr. John F. Doherty, Dr. Karl M. Reichard, and Dr. Victor W. Sparrow, who served as my doctoral committee members. I deeply appreciate their interest in the subject and critical review of this work.

I am very grateful to my parents, all of my sisters, and other family members for their invaluable support. Lastly, I would like to thank the Royal Thai Government for financial support during my period of study.

CHAPTER 1

INTRODUCTION

1.1 Motivation

In signal analysis, a signal is usually assumed to be stationary. However, this assumption is not always accurate for acoustic signals, because such signals might have time-varying frequency and amplitude. Signals with time-varying frequency are highly nonstationary. Frequency analysis of nonstationary signals is important since the time history of frequency is a powerful approach in signal characterization. The analysis of time-varying frequency is typically performed by using a short time Fourier transform (STFT) and a time-frequency distribution (TFD).

The short-time Fourier transform is the most direct approach for computing the time-varying spectrum of a signal. In this approach, the signal is separated into small lengths fitting a sliding window, whose length must be short enough so that the signal can be assumed stationary within the window. Since the length of the window affects both the time and the frequency resolution in an opposite manner (i.e. the short window length yields a good time resolution but poor frequency resolution and vice versa for the long window length), good frequency and time resolution cannot be obtained simultaneously.

The time-frequency distribution is mathematically complicated, but it yields possible higher time and frequency resolution for a given limited length of signal, since the signal is not divided into small lengths as is done in the short-time Fourier transform.

The simplest, and possibly the most famous time-frequency distribution, is the Wigner-Ville distribution (WVD), since other types of time-frequency distribution can be derived from the WVD. While the WVD yields very high resolution in both time and frequency for a signal that has a single time-frequency component it suffers severely from artifacts when signals have two or more time-frequency components. Other types of TFD, such as Choi-Williams and other kernels, may improve the artifacts or the inter-component interference and outperform the WVD. However, their abilities to resolve the time-varying frequencies are limited by the *uncertainty principle*, $\sigma_t \sigma_w \geq 1/2$ [Cohen, 1995], where $\sigma_t^2 = \int (t - < t >)^2 \mid s(t) \mid^2 dt$ is the variance of energy in the time domain, which represents the sharpness in the time analysis, and $\sigma_w^2 = \int (w - < w >)^2 \mid S(w) \mid^2 dw$ is the variance of energy in the frequency domain, which represents the sharpness in the frequency analysis. In short, the uncertainty principle implies that there is no way to get arbitrarily sharp resolution in both the time and the frequency domains at once.

The best frequency resolution is possible by using the parametric method, in which a signal is modeled by using either the autoregressive, the moving average, or the autoregressive moving average models. The parametric method for the modern spectral estimation of stationary signals has been thoroughly studied and well documented [Kay, 1988 and Maple, 1987]. It was shown that, even though the available signal is very short, the parametric method yields very high frequency resolution in the spectral estimation. This parametric method also has been adapted so that it can be used for nonstationary signals.

Nonstationary signals are present in some applications. For example, in the pulse Doppler radar, the sonar and the ultrasound, a wideband pulse is used for target localization, range and velocity estimation. In marine or terrestrial mammal bioacoustics studies and bird vocalization, the available signal may be recorded in a short period and some might contain a chirp component. Or in the pile installation for a construction, only a short outburst of acoustic signal can be recorded and it might be analyzed for a possible crack monitoring. Frequency analysis with high frequency resolution of these short and nonstationary signals is possible by using the parametric method with the time-varying coefficients. The parametric method using the time-varying autoregressive (TVAR) model, whose transfer function is $T(z) = 1 \Big/ \left(1 + \sum_i a_i[t] z^{-1} \right)$, is considered in this research.

Estimation of the TVAR parameters may be classified into one of the two categories: namely the adaptive method and the basis function approach, based on the definition of the time-variant parameters. In the first category, the time-varying parameters are defined using a dynamic model as $a[t] = a[t\text{-}1] + \Delta a$**,** where $a[t]$ are the parameters of the TVAR model, and t is discrete time from 0 to T. In this case, the parameters $a[t]$ are updated depending on the utilized adaptive algorithms, such as the steepest gradient and the recursive least square algorithm, and can be processed in real time. The TVAR model in this category has been very popular in several research areas and appears in many applications, such as the online noise cancellation and the adaptive estimation. In the second category, the TVAR parameters are explicitly defined as a

linear combination of weighted time-dependent functions, $a[t] = \sum_k a_k f_k(t)$, where a_k are some constants or weights in the summation and $f_k(t)$ are some predefined time functions. According to Liporace [1975], this definition was first used in 1975 by Rao, who used a finite number of terms in the summation. The TVAR parameters $a[t]$ in this definition are calculated via a block estimation, done in two steps. Firstly, a_k are estimated using all data from time 0 to T, and usually involves solving a set of linear equations. In the second step, the time-varying parameters $a[t]$ are computed from their definition, which is the summation of the weighted time-functions. Different sets of time-functions have been used by different researchers, such as a low-order polynomial used by Rao [1975], an arbitrary order polynomial by Liporace [1975], the Legendre polynomial by Chabonnier et al. [1987], the non-harmonic Fourier basis by Hall et al. [1983], and the discrete cosine function by Eom [1999]. The accuracy of the parameter estimation varied, when different sets of time-functions were used [Chabonnier et al., 1987]. However, there is no criteria for selecting the proper time-function and the dimension of summation.

It was also mentioned in Boashash [1992] that the accuracy of the TVAR method for instantaneous frequency estimation is limited, but Beex and Shan, [1999] showed digitally that the estimation could be more accurate than that using the WVD at some range of signal-to-noise ratio.

Once the parameter estimates of the TVAR model for the stationary signal are computed, the estimation of the time-varying power spectral density can be calculated from the equation

$$S_{xx}(t,f) = \sigma_v^2 \Big/ \left| 1 + \sum_i a_i[t] e^{-j2\pi f \cdot i} \right|^2 ,$$

where σ_v^2 is the variance of additive zero-mean white noise. The time-varying frequency estimates can then be chosen as either the location of the highest spectral peaks or the angle of the closest roots to the unit circle of the prediction error filter polynomial.

In this thesis, the TVAR model is used for estimating the time-varying frequencies and the spectra of non-stationary signals. We propose approaches to estimate the TVAR parameters of category 2, in which the parameter variations are explicitly modeled as the sum of weighted time-functions. The proposed approaches are to improve the accuracy of the time-varying estimate, especially when the model order is over-determined. The proposed method is used to analyze a nonstationary signal (violin vibrato).

1.2 Assumption

For most physical systems, noise is unavoidable. In this research, the noise is assumed to be an additive, zero-mean Gaussian white noise. The signal-to-noise ratio (SNR) is assumed to be moderate (15 dB) to high (20 dB or higher). Although, this may not always be practical in general, it is possible in a real application. This assumption about the moderate-to-high SNR is consistent with that of the adaptive algorithm to work effectively [Swanson, 2000].

1.3 Statement of Thesis

An approach to improve the accuracy of the TVAR model estimation is proposed and tested with highly nonstationary (wideband) signals in both noise-free and noisy situations. The accuracy is compared to that of an existing approach, such as the short-time Fourier transform. Different basis functions were tested with the proposed approach. A demonstration to estimate a time-varying frequency/ spectrum of a nonstationary acoustic signal is given.

1.4 Contribution:

(1) Comparatively display ability in tracking the time-varying frequency between the adaptive algorithm and the basis function method. Also digitally show that for a signal with single time-frequency component, fixing a pole of the TVAR model on the unit circle allows the adaptive algorithm to converge faster.

(2) Derive two approaches, which are modified versions of the basis function approach to improve the accuracy of time-varying frequency estimation.

(3) Compare several basis functions and choose the best one, which could be used for general signals.

(4) Use the proposed method to analyze violin vibrato, and compare the result to that of a traditional analysis with the STFT.

1.5 Outline

The thesis is organized as follows: Chapter 2 provides a discussion on the TVAR model and its parameter estimation, and a comparison aspect between the adaptive algorithm and the time basis function method for the time-varying frequency estimation. Chapter 3 presents two proposed approaches, which are modified versions of the basis function method by using both the forward and the backward predictors for the time-variant parameter estimation. Improvements of the proposed approach to the existing basis function method are shown via simulations in this chapter as well. In chapter 4, several sets of time-functions are used as the basis function in the proposed approach, and their results for the time-varying frequency estimations are compared. The overall best basis function is chosen. Chapter 5 discusses some limitations, and chapter 6 presents a demonstration of the frequency analysis of a nonstationary acoustic signal (i.e. violin vibrato signal is analyzed), using the proposed approach. The original contributions in this thesis appear mainly in chapter 3, and partly in chapters 2, 4, 5, and 6. Some basic concepts related to this thesis are presented in an Appendix.

CHAPTER 2

Time-Varying Autoregressive Model for Nonstationary Signal

According to Wold's decomposition theorem, any stationary random process $x[t]$ may be represented by a sum of two orthogonal components, predictable and regular processes [Therrien, 1992], [Hayes, 1996]. The first component, denoted by $x_p[t]$ is deterministic or predictable, which can be calculated from an infinite number of its previous value without any estimation error (i.e. $x_p[t] = -\sum_{i=1}^{\infty} a_i x_p[t-i]$). The second component is nondeterministic, denoted by $x_r[t]$, and can be estimated as an output of a causal noise-shaping filter with infinite order (i.e. $x_r[t] = -\sum_{i=1}^{\infty} h_i w[t-i]$, where h_i is coefficient of a filter). In practice, using the infinite number of previous values and filter coefficients is impossible. A finite order has been used, depending on a chosen structure of the filter; whether auto regressive (AR), moving average (MA), or autoregressive moving average (ARMA) filter is used. Since the AR process is simple and was shown in [Key, 1988] that it is capable of approximating either the MA or the ARMA model, the AR process has been much of interest. In fact, it has been modified by allowing its coefficients to change with time for modeling non-stationary signals, and are called time-varying auto regressive (TVAR).

In this chapter, we review a TVAR process, and discuss two general methods for TVAR parameter estimation. The time-varying spectrum can be obtained from the TVAR

coefficients. Some aspects about ability, in extracting the time-varying frequency of a non-stationary signal, between the two methods are shown.

2.1 TVAR model

The TVAR process, also known as the time-varying linear predictor, is to estimate the current or future value $y[t]$ by using a linear combination of previous values $y[t\text{-}i]$. The process is written as

$$\hat{y}[t] = -\sum_{i=1}^{p} a_i[t]\, y[t-i] \tag{2.1}$$

or $$y[t] = -\sum_{i=1}^{p} a_i[t]\, y[t-i] + e[t]$$

Where $a_i[t], i = 1,2,\ldots,p$ are time-varying coefficients, p is model order, $\hat{y}[t]$ is the estimate of $y[t]$, and $e[t]$ is the estimation error. Although, there is no corresponding general theory for a nonstationary process, the TVAR has been successfully shown for modeling, analyzing, and synthesizing nonstationary signals, such as speech [Hall, 1983; Liporace, 1975]

2.2 TVAR Parameter Estimation

In order to use the TVAR as a model for nonstationary signal processing, the model order p in the equation (2.1) must be chosen, and then time-variant parameters $a_i[t]$ must be determined, if not pre-known. We will assume in this chapter that the order p is known, and only the parameters $a_i[t]$ are needed to be estimated. Since

$a_i[t]$ are time-variant, they cannot be estimated by using the same method as obtaining the solution of the Wiener-Hopf equations [Marple, 1987] or [Kay, 1988]. Available approaches for estimating the time-variant coefficients fall into one of two categories, based on the model of the $a_i[t]$ variation. In one category, a dynamic model is used for the parameter variation, and the parameters are updated each time when new data are available. An adaptive algorithm is utilized in this category. In another category, the coefficient $a_i[t]$ is explicitly defined as a linear summation of weighted time-functions. The time functions are pre-defined. Only the weight must be determined, and this can be done via block processing. Some details of these two approaches for the TVAR parameter estimation are shown below.

2.2.1 Using the dynamic model and the adaptive algorithm

Variation of the time-varying parameters $a_i[t]$ are based on a dynamic model defined as

$$\vec{a}_i[t] = \vec{a}_i[t-1] + \Delta\vec{a}_i[t]\,. \tag{2.2}$$

The parameters $a_i[t]$ are updated from their previous values $a_i[t-1]$. Terms $\Delta a_i[t]$ represent innovation terms, and they might be different depending on which rule or the adaptive algorithm being utilized (i.e., steepest descent, least mean square (LMS), recursive least square (RLS) algorithm, etc). If the steepest descent or the LMS algorithm is used, $\Delta\vec{a}_i[t]$ is equal to $\mu \cdot E\{e[t]\vec{\varphi}[t]\}$ or $\mu \cdot e[t]\vec{\varphi}[t]$, respectively, where $\vec{\varphi}[t] = \begin{bmatrix} y[t] & y[t-1] & \ldots & y[t-p] \end{bmatrix}^T$ is a vector of the sampled nonstationary signal. If

the RLS algorithm is applied, the $\Delta a_i[t]$ are a little bit more involved. Computation steps of the LMS and the RLS algorithms are listed below.

LMS algorithm:

Parameter: p = Filter order

μ = Step size

$$\vec{\varphi}[t] = \begin{bmatrix} y[t] & y[t-1] & \dots & y[t-p+1] \end{bmatrix}$$

$$\vec{a}[t] = \begin{bmatrix} a_1[t] & a_2[t] & \dots & a_p[t] \end{bmatrix}$$

Initialization: $\hat{\vec{a}}[0] = 0$

Computation: For $t = 0, 1, 2, \dots$

$$\hat{y}[t] = -\sum_{i=1}^{p} a_i[t]\, y[t-i]$$

$$e[t] = y[t] - \hat{y}[t]$$

$$\hat{\vec{a}}[t] = \hat{\vec{a}}[t-1] + \mu \cdot e[t]\vec{\varphi}[t-1]$$

RLS algorithm:

Parameter: p = Filter order

λ = Exponential weighting or forgetting factor

δ = Value used to initialize P(0)

$$\vec{\varphi}[t] = \begin{bmatrix} y[t] & y[t-1] & \dots & y[t-p+1] \end{bmatrix}$$

$$\vec{a}[t] = \begin{bmatrix} a_1[t] & a_2[t] & \dots & a_p[t] \end{bmatrix}$$

Initialization: $\hat{\vec{a}}[0] = 0$

$$\mathrm{P}(0) = \delta^{-1} I$$

Computation: For $t = 1, 2, \dots$.

$$\vec{z}[t] = P[t-1]\vec{\varphi}^{*}[t-1]$$

$$\vec{g}[t] = \frac{1}{\lambda + \vec{y}^{T}[t]\vec{z}[t]}\vec{z}[t]$$

$$e[t] = y[t] + \sum_{i=1}^{p} \vec{a}_i[t-1]y[t-i]$$
$$\hat{\vec{a}}[t] = \hat{\vec{a}}[t-1] + e[t]\vec{g}[t]$$
$$p[t] = \frac{1}{\lambda}\left[P[t-1] - \vec{g}[t]\vec{z}^{H}[t]\right]$$

Step size and forgetting factor affect the convergence rate of the LMS and the RLS algorithm, respectively. To ensure stability, the step size μ must be in the range $0 < \mu < 2/\lambda_{\max}$, where $\lambda_{\max}$ is the largest eigenvalue of the correlation matrix[1] R. However, in general application, knowledge of the $\lambda_{\max}$ is unavailable. Therefore, a simple working rule, stepsize in the range $0 < \mu < 2/tap\_input\_power$ where $tap\_input\_power = \sum_{i=0}^{p-1} E[|y(t-i)|^2]$, can be used [Haykin, 1996]. For the RLS algorithm, the exponential weighting or forgetting factor λ must be chosen in the range of $0 < \lambda \leq 1$. The factor λ is to ensure that the data in a distant past are forgotten. Details about these factors, the LMS, and the RLS algorithm are available, [Haykin, 1996], [Hayes, 1996], or [Swanson, 2000].

The adaptive methods may be sufficient for the TVAR parameter estimation, if the nonstationay part of a signal changes slowly. However, due to its nature as an adaptive system, they are sensitive to noise. Increasing the step size or the forgetting factor can help in reducing sensitivity to the noise, but the convergence rate of the

---

[1] Correlation matrix is defined as $R = E\left\{\vec{y}[t-1]\vec{y}^{H}[t-1]\right\}$, where
$\vec{y}[t-1] = [y[t-1] \quad y[t-2] \quad \ldots \quad y[t-p]]^{T}$

algorithm decreases as well, and this may result in a diminished ability in tracking the parameter change.

2.2.2 Using the basis function and the block processing (called "the basis function approach")

Instead of using the dynamic model and the adaptive algorithm for estimation, $a_i[t]$ are explicitly modeled as a summation of weighted time functions as

$$a_i[t] = \sum_{k=0}^{q} a_{ik} f_k(t) \tag{2.3}$$

where a_{ik}, $i = 1,2,\ldots, p$, k $= 0,1,\ldots, q$ are constants, q is expansion dimension, and $f_k(t)$ are some predefined time-functions that are used as the basis function in the expansion.

With $a_i[t]$ defined in (2.3), equation (2.1) can be rewritten as

$$\hat{y}[t] = -\sum_{i=1}^{p}\left(\sum_{k=0}^{q} a_{ik} f_k(t)\right) y[t-i] \tag{2.4}$$

and the estimation error is

$$e[t] = y[t] + \sum_{i=1}^{p}\left(\sum_{k=0}^{q} a_{ik} f_k(t)\right) y[t-i].$$

Parameters a_{ik} are calculated by solving a set of $p(q+1)$ linear equations, equation (2.5), which is the result from minimizing the mean squared error $\varepsilon = \frac{1}{2(T-p)}\sum_{t=p}^{T} |\, e[t]\,|^2$

$$\sum_{i=1}^{p}\sum_{k=0}^{q} a_{ik} c_{kl}(i,j) = -c_{0l}(0,j), \quad j = 1,2,\ldots p \text{ and } l = 0,1,\ldots q. \tag{2.5}$$

Here $$c_{kl}(i,j) \doteq \frac{1}{T-p}\left(\sum_{t=p}^{T} f_k(t) f_l^*(t) y[t-i] y^*[t-j]\right). \qquad (2.6)$$

The parameter estimates $\hat{a}_i[t]$ are obtained by $\hat{a}_i[t] = \sum_{k=0}^{q} a_{ik} f_k(t)$. Details of this method are in [Hall et al., 1983].

It should be noted that, in this method not only the model order p, but also the basis time-function $f_k(t)$ and the expansion dimension q must be chosen. Some existing functions that can be used as a basis for parameter expansion are the time-polynomial, the Legendre, the Cosine, the Fourier function, and the discrete prolate spheroidal sequence. It was unclear, which function and dimension were the best for the parameter expansion. A study about the effects of these functions and dimension number on the frequency estimation is shown in chapter 4.

2.3 Time-varying frequency/spectral estimation extraction

The time-varying frequency can be extracted from the TVAR parameters $a_i[t]$. Since the nonstationary signal is modeled as the output of the TVAR process, with a zero-mean white noise input $w[t]$, the power spectral density $S_{yy}[t,f]$ of the stationary signal is given by

$$S_{yy}[t, f] = \frac{\sigma_w^2}{\left|1 + \sum_{i=1}^{p} a_i[t] e^{-j2\pi f \cdot i}\right|^2} \qquad (2.7)$$

where σ_w^2 is the variance of the white noise $w[t]$. In practice, this variance is unknown, but can be approximated by

$$\sigma_w^2 \sim \sigma_e^2 = \frac{1}{T-p}\sum_{t=p+1}^{T}\left(y[t]+\sum_{i=1}^{p}a_i[t]y[t-i]\right)^2. \qquad (2.8)$$

Time-varying frequencies can be extracted from the power spectral density by locating the peak of the $S_{yy}[t,f]$. If there are *m* frequency components in the signal, one can choose the frequency estimate as the locations of the *m* largest spectral peaks. Note that a threshold could be also set so that the peak below this threshold would be considered as that of an additive noise.

Another way to extract the time-varying frequency from the TVAR, is by calculating the roots z_i of the estimation error filter polynomial $z^p + a_1[t]z^{p-1} + a_2[t]z^{p-2} + ... + a_p[t] = 0$, and choosing the frequency estimate as the angles of the root z_i. For a real signal, the roots may be complex conjugate to each other. So only the roots in either upper or lower half of complex plane are selected. For example, if the number of the frequency components is *m*, the closest *m* poles to the unit circle in the upper half of the z-plane are chosen. The time-varying frequencies $f_i[t]$ are then calculated by $f_i[t] = \text{angle}\left(z_i[t]\right) \cdot Fs/2\pi$. According to Kay [1988], estimating the frequency in this way is slightly more accurate than locating the frequency as the largest spectral peak location.

2.4 Aspect about Ability in estimating time-varying frequency: Adaptive algorithm vs Basis Function method.

As explained in previous sections, the frequency estimation via the TVAR model was accomplished in two steps, the TVAR parameter estimation and the frequency extraction. There exist several methods in the two general categories, and available for the estimation. One may wonder which approach should be chosen for estimating the time-varying frequency of a nonstationary signal. The adaptive algorithms are known for their ability to track time-variation in the statistics of the signal, provided that the variations are sufficiently slow, and its computation can be done on-line.

For block estimation, processing is done on a block-to-block basis. Traditionally, the length of the block is usually chosen short enough to maintain a pseudo-stationary assumption. However, for the basis function approach the TVAR parameters that contain the nonstationarity information of a signal are changed to the summation of a set of unknown constants multiplied by predefined time-functions. As a consequence, the block estimation in the basis function approach is to calculate these unknown constants, not the time-variant parameter, and the calculation is the same as if it is for a stationary signal. Hence the length of the block for the basis function approach can be of any length (i.e., the length of the block could be very long), provided that computational complexity and time are not restricted.

The following are some comparisons between the adaptive algorithm and the basis function approach about their ability in estimating the time-varying frequency of

three nonstationary signals. The first signal was a chirp with a unit amplitude and had a frequency increasing linearly. The next signal was a sinusoidal that its frequency varied periodically, and the last signal was a sinewave that has a frequency jump. All the signals were real and had one frequency component, then the TVAR model of the second order (p = 2) was used. Three adaptive algorithms, namely the LMS, the RLS, and the RLS with a pole constrained on the unit circle, were used to estimate the time-varying frequency of signals 1, 2, and 3, respectively. The step size for the LMS algorithm was set to 0.5 and the forgetting factor for the RLS method was set to 0.7. The results from using these algorithms are shown in Figures 2.1, 2.2 and 2.3.

Figure 2.1 shows the frequency estimate of the chirp signal where the frequency increase linearly, in (a) noise-free and (b) noisy (20dB-SNR) situations. As seen in figure 2.1(a) all algorithms can track the true frequency that changed slowly. However, the frequency estimate is in no way equal to the true frequency, since there is always a delay when the adaptive algorithms were utilized. Among the algorithms, the LMS was slowest in the rate of convergence. The step size of the LMS algorithm could be increased so that it would converge faster, but the oscillation would be higher. The RLS algorithm yielded fast convergence, especially when a pole of the TVAR(2) model was constrained to be on the unit circle. The reason that the RLS with the constrained pole converged very fast, was because after a pole was constrained, there was only another parameter needed to be estimated, instead of 2 parameters. Figure 2.1(b) shows the frequency estimate of the chirp in a noisy situation with the SNR ~20dB. Compared to the result in the noise-free situation, it is obvious that the adaptive algorithm is sensitive

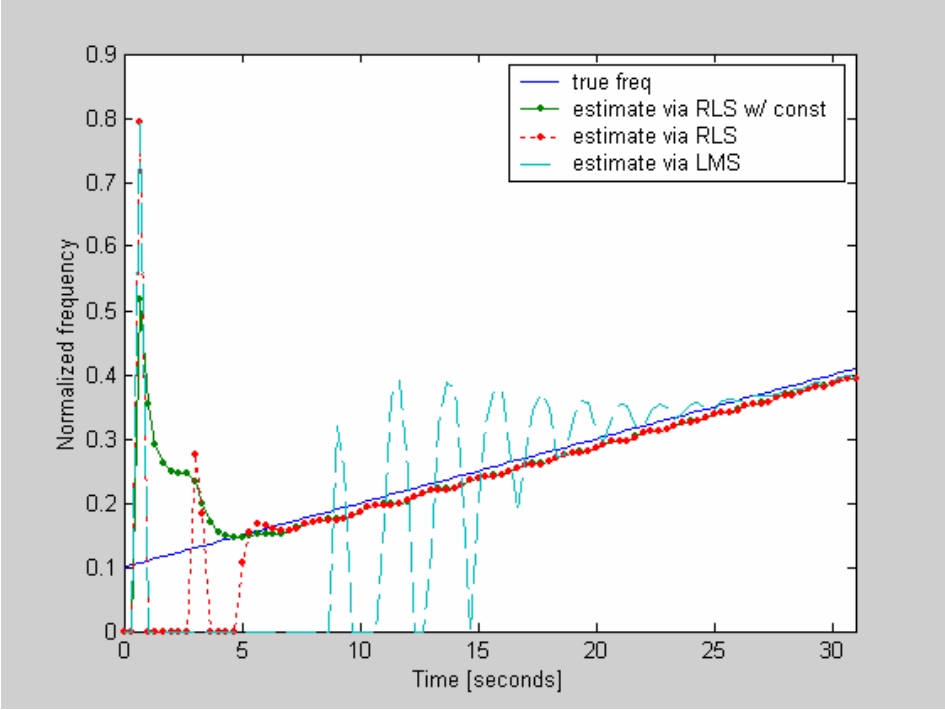

(a) Noise-free case

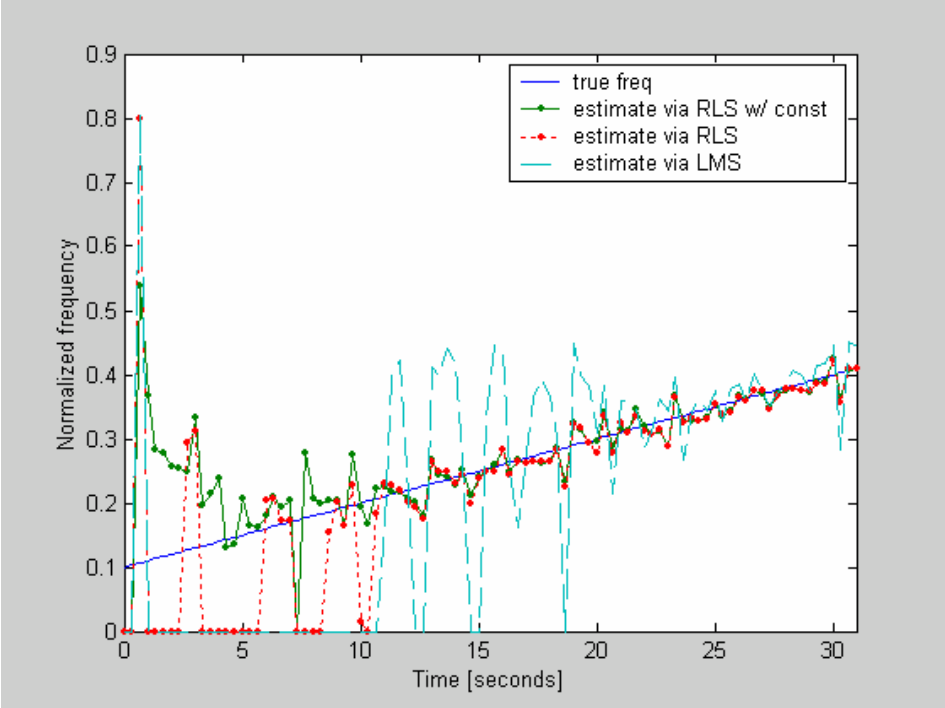

(b) Noisy case

Figure 2.1: Frequency estimate of linear chirp (f = 0.01+0.1*t* Hz) using 1. RLS algorithm with forgetting factor =0.75 with a pole constrained on unit circle, 2. RLS algorithm with forgetting factor =0.75 (no constraint), 3. LMS algorithm with step size = 0.5

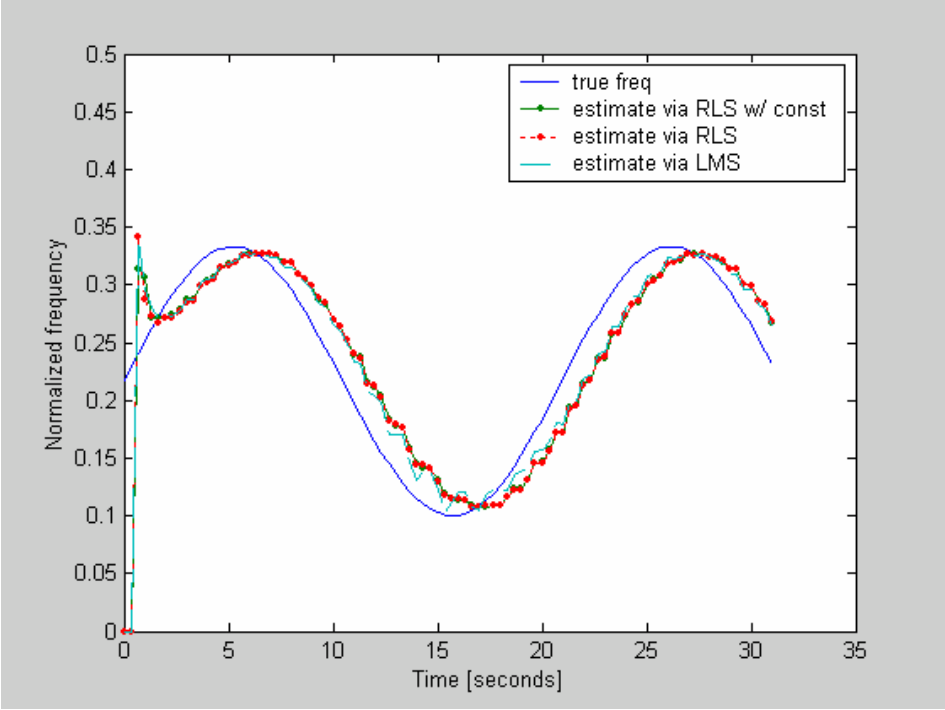

(a) True frequency f = 0.*35*sin(0.3*t)+.65*

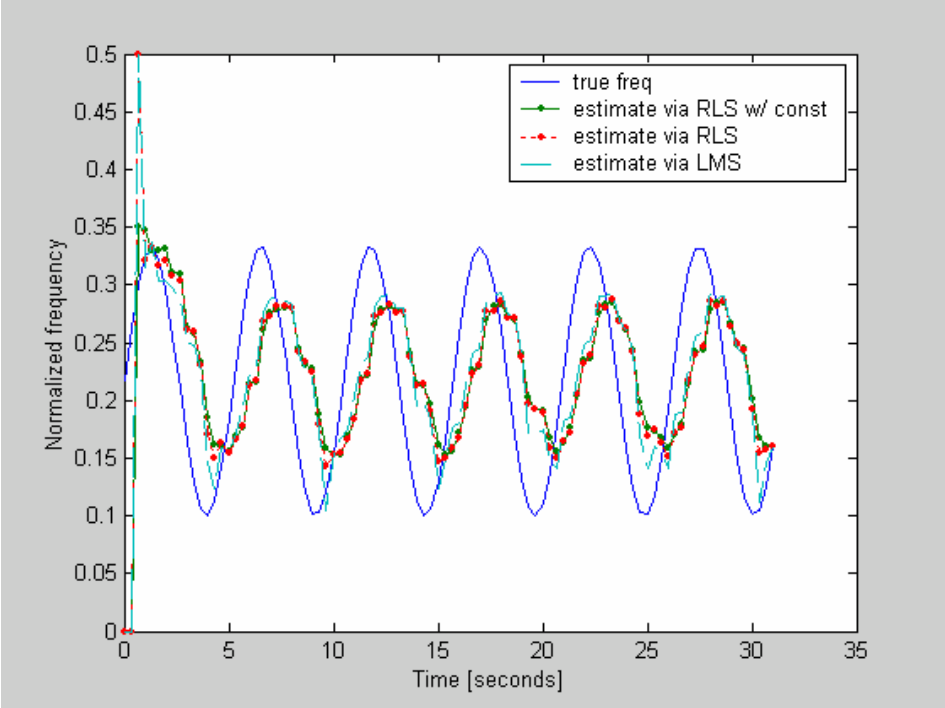

(b) true frequency *f = 0.35*sin(1.2*t)+.65*

Figure 2.2: Frequency estimate of a real sinusoid where frequency changes periodically, in noise-free environment, using adaptive algorithm. a) Frequency change slowly. b) Frequency changes very fast, 4 times faster than in (a).

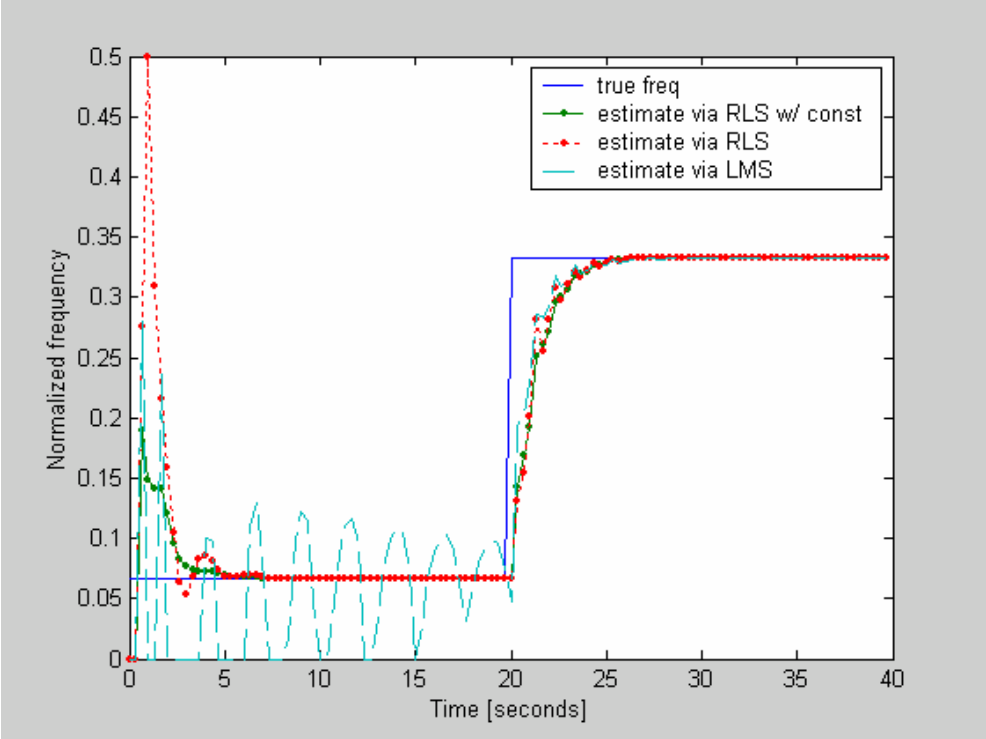

Figure 2.3 Frequency estimate of sinusoidal signal which has frequency jump, using adaptive algorithm

to the additive noise. This is due to the nature of its adaptive mechanism that automatically adjusted itself to the change.

The ability of the adaptive algorithm in tracking the time-varying frequency is more clearly seen from the result in figure 2.2, where the signal has a periodically changing frequency. When the frequency of the signal changes slowly (figure 2.2a), the adaptive algorithms yield the frequency estimate that is about the delayed version of the true time-varying frequency. However, when the frequency changes very fast (figure 2.2b), 4 times faster than that in figure 2.2a, the adaptive method fails to track the frequency change. This was obviously seen (in figure 2.2 a) that the frequency estimate,

neither from the LMS nor the RLS algorithm, reaches the peak and valley of the true frequency curve.

Figure 2.3 displays the frequency estimate of the signal that has a frequency discontinuity at about 20 seconds. The RLS and the RLS with a pole constraint can track the frequency jump, and so does the LMS algorithm. However, the LMS algorithm seems to have trouble in tracking the frequency that varies close to zero (as seen in figure 2.3 that the frequency estimate from the LMS algorithm does not converge to the true frequency when the true frequency is at 0.067Fs, where Fs is the 3 Hz sampling frequency used in this chapter). This is because the eigenvalues of the autocorrelation matrix **R** for this signal spread wildly. The biggest and smallest eigenvalues are so different. The step size of the LMS algorithm must be set small, corresponding to the biggest eigenvalue, so that a convergence could be attained. Hence, while the LMS does converse, it converges slowly at low frequency and is seen as if it cannot track the low frequency for a given signal range.

Results from using the basis function method are shown in Figures 2.4, 2.5, and 2.6. In using the basis function approach, the time function $f_k(t)$ and the expansion dimension q must be chosen. For the chirp signal, we used the time-polynomial function $f_k(t) = \left(\frac{t-1}{N}\right)^k$ and the dimension q = 2. For the sinusoid with the periodically time-varying frequency, the cosine function $f_k(t) = \cos\left(\pi k \frac{t}{N}\right)$ was used, and the dimension of q =8 and q =16 were utilized for the slow and fast time-varying frequencies.

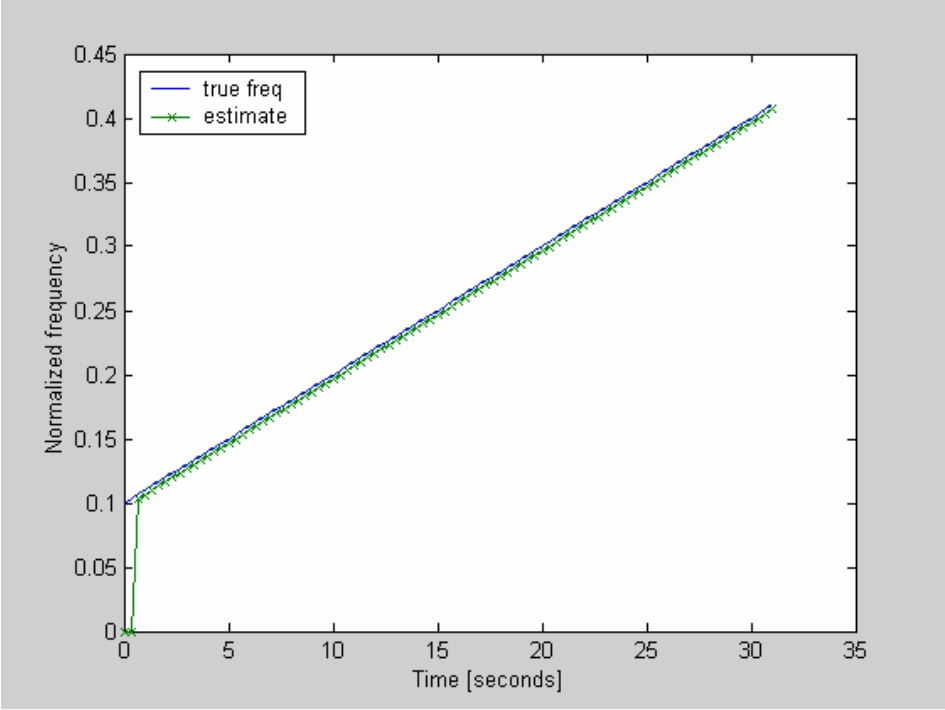

(a) No-noise

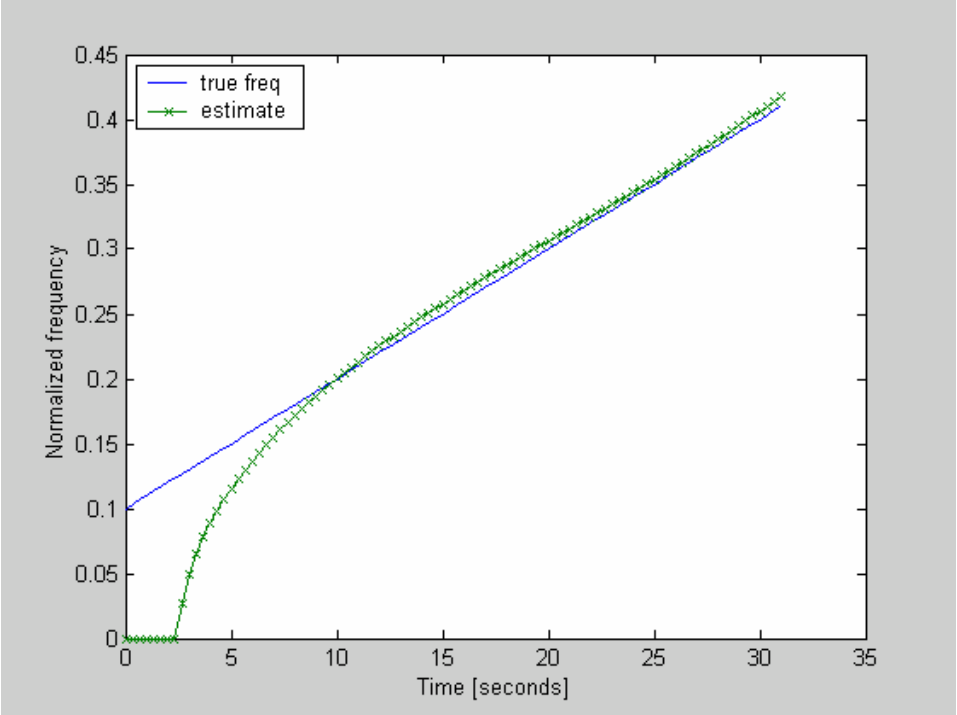

(b) Noisy case (20dB-SNR)

Figure 2.4: Frequency estimation of the chirp signal, using the TVAR parameter as a summation of the weighted time-function.

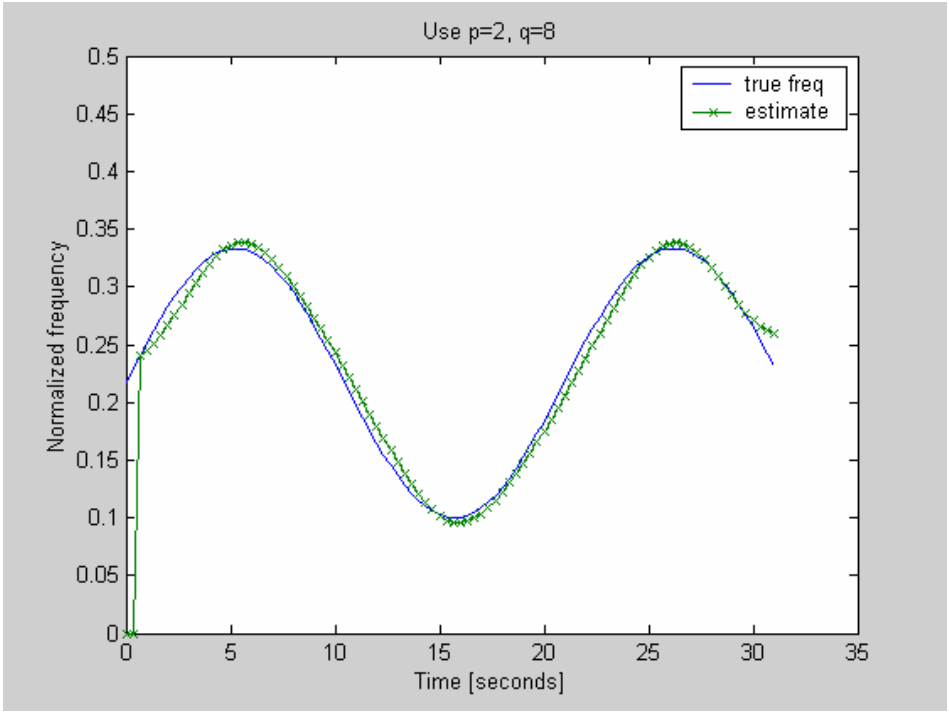

(a) True frequency $f = 0.35*sin(0.3*t)+.65$

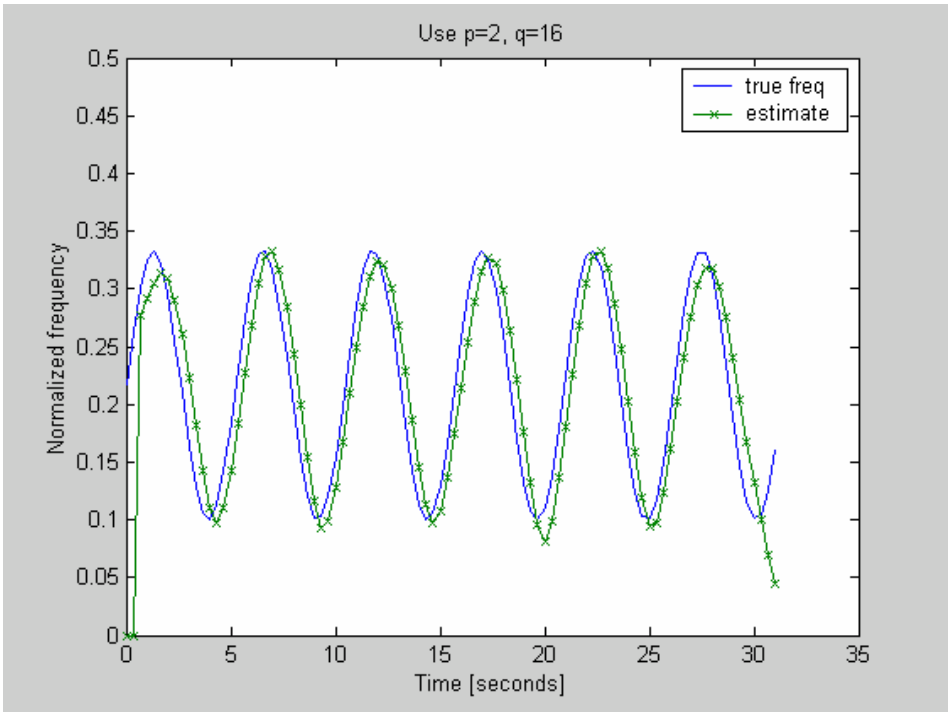

(b) True frequency $f = 0.35*sin(1.2*t)+.65$

Figure 2.5: Frequency estimate of the sinusoid where frequency changes periodically, in noise-free environment, using the basis function method. a) Frequency change slowly. b) Frequency changes very fast, 4 times faster than in (a).

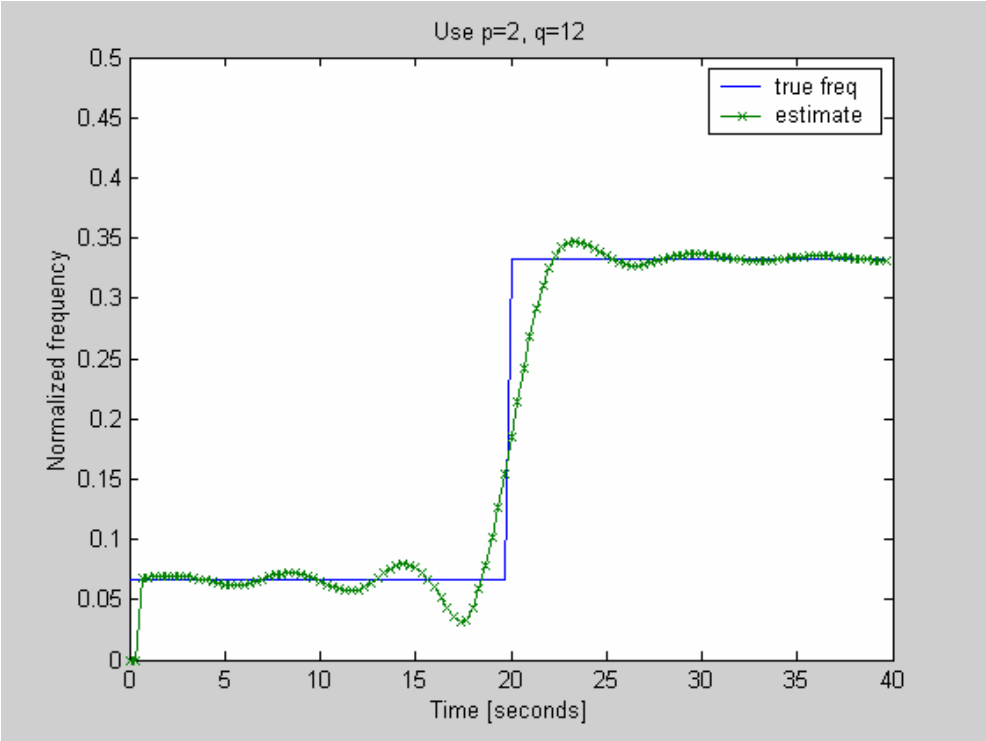

Figure 2.6: Frequency estimate of the signal that has a frequency jump, using the basis function method.

The cosine function was also applied for the case of frequency jump.

As seen from figure 2.4 (a) of the noise-free case, the frequency estimate is about the true frequency. The convergence rate was not a problem for the basis function method in the estimation, since the computation was done in a processing block. However, the estimate at the beginning (about p steps) was not available, since it required p initial values of the data before the calculation started, as it is for the AR(p) process. Figure 2.4 (b) displays an ability of the basis function method to estimate the time-varying frequency in a noisy situation, 20dB-SNR. However, as also can be seen from the figure, the noise resulted in the shift of the frequency estimate from the true frequency, and

many incorrect frequency estimates at the beginning. The ability of the basis function method in tracking the time-varying frequency that varies broadly can be more obviously seen from the results in Figure 2.5(a) and (b). The frequency estimates are close to the true frequencies for both slow and fast varying.

Figure 2.6 displays frequency estimate from using the basis function method in a situation where there is a frequency jump. The expansion dimension is $q = 12$. As shown, the frequency estimate bounces around the true frequency before and after the jump. The estimate could be closer to the true frequency, if a higher expansion dimension was used.

2.5 Chapter summary

TVAR processes are used as models for nonstationary signals. Then information, especially the time-varying frequency or spectrum, of the nonstationary signals are contained in the time-variant coefficients of the TVAR model. Extracting the frequency information consists of two steps: first, the TVAR parameter estimation, and then the power spectrum density or frequency calculation. Approaches for estimating the TVAR parameters may generally be classified into one of two categories; namely adaptive algorithms employing a dynamic model for parameter variation, and the basis function method utilizing the explicit model for the parameter variation. It was demonstrated that while the adaptive algorithms had the ability to track the slowly time-varying frequency, it was sensitive to the noise. They also failed to track the time-varying frequency of the signal, if the frequency changed very fast or broadly. However, they were efficient in tracking the frequency jump.

The basis function method, in which the time-variant parameters are expanded as a summation of the weighted time-functions, are capable of tracking both the fast or the slow time-varying frequencies. However, the selection of the expansion dimension and the basis function is questionable since there is no fundamental theorem on how to choose them. It is ideally expected that when the expansion dimension is infinite, the result of the frequencies estimation from any basis function is the same, which will exactly equal to the true frequency. But this is impractical, since the computation may require infinite memory, and infinite computational time consumption. A result from the previous section showed that the effect of an additive noise could cause the shift of the frequency estimate from the true frequency. Also it was observed that the frequency estimate was not exactly equal to the true frequency, but it was a step-delayed version of the true frequency.

CHAPTER 3

The Modified Basis Function Method

The TVAR model, $\hat{y}[t] = -\sum_{i=1}^{p} a_i[t]y[t-i]$ where $a_i[t] = \sum_{k}^{q} a_{ik} f_k(t)$, was observed to have yielded a frequency estimate, which was about one-step delay of the true frequency. In addition, by using this TVAR model, the frequency estimate at the time t = 0,1, …, p-1 was unavailable, since the calculation must be delayed p steps before it could be started. In this chapter, we propose a method by applying a combination of a backward and a forward linear estimator that results in no delay of the frequency estimate (i.e. frequency can be estimated from t = 0,1, …, T, and the frequency estimate is also about the true frequency). In the case in which the model order was over determined, our simulation showed superiority in the time-varying frequency estimation of the proposed method over that from the model using only the forward linear prediction. The accuracy of the estimation may also be further improved, if a slight modification of the model was made. As will be seen in the simulation, the forward and the backward linear predictors, which are defined as $\hat{y}^f[t+1] = -\sum_{i=1}^{p} a_i[t]y[t-i+1]$ and $\hat{y}^b[t-1] = -\sum_{i=1}^{p} b_i[t]y[t+i-1]$ as in equations (3.10) and (3.12) respectively, attain better frequency estimation. The reason for this is explained later in the chapter.

3.1 Proposed approach: Two slightly different versions are proposed

The TVAR model that has been used for the non-stationary signal in [Eom, 1999] and others, such as [Hall et al., 1983] and [Beex and Shan, 1999], utilizes only the forward linear estimation. It could be observed in Figure 2.3(a) and Figure 2.4 that the estimates of the time-varying frequency of the non-stationary signals were one-step delay from the true frequency, even though it was processed via block estimation. We anticipate to get rid of the time delay in the frequency estimate by using two slightly different approaches. In the first approach, the same TVAR model, as in the previous chapter is used, but we employ a combination of forward and backward estimators to estimate the TVAR parameters and then the time varying frequencies. In the second approach, the TVAR model is slightly modified so that the estimate is about the true frequency. The combination of both the forward and the backward estimators is also used in the second approach.

3.1.1 Approach 1: uses the same TVAR model as in chapter 2, and applies both the forward and the backward estimators.

First, the forward linear estimation is re-written as

$$\hat{y}^f[t] = -\sum_{i=1}^{p} a_i[t]\,y[t-i] \;,\; t = p,\, p+1,\, \ldots,\, T \tag{3.1}$$

$$a_i[t] = \sum_{k=0}^{q} a_{ik} f_k(t) \tag{3.2}$$

and the forward estimation error is

$$\begin{aligned} e^f[t] &= y[t] - \hat{y}^f[t] \\ &= y[t] + \sum_{i=1}^{p}\left(\sum_{k=0}^{q} a_{ik} f_k(t)\right) y[t-i] \end{aligned} \tag{3.3}$$

For the same set of data $y[t]$, *t = 0, 1, …, T,* a linear backward estimator can be defined as

$$\hat{y}^b[t] = -\sum_{i=1}^{p} b_i[t]y[t+i] \text{ , } t = 0, 1, \ldots, T\text{-}p \tag{3.4}$$

Where $b_i[t], i = 1,2,...,p$ are time-varying coefficients in the backward estimator, and $\hat{y}^b[t]$ are the estimates of $y[t]$ using future information. An obvious difference between the forward and the backward predictor is that the forward predictor is causal while the backward predictor is anti-causal.

For stationary signals, the backward and the forward parameters are time-invariant, and they are related to each other. As a matter of fact, for stationary signals, the backward parameters b_i are simply complex conjugates of the forward parameters a_i. In the case of the non-stationary signal, the backward and the forward coefficients are not time-invariant, and they may or may not be equal to the complex conjugate of each other. However, to develop our approach, we will force them to be equal by using a constraint $b_i[t] \cong a_i^*[t]$. Therefore, we can rewrite the backward estimator as

$$\hat{y}^b[t] = -\sum_{i=1}^{p} a_i^*[t]y[t+i] \tag{3.5}$$

and the backward estimation error as

$$\begin{aligned} e^b[t] &= y[t] - \hat{y}^b[t] \\ &= y[t] + \sum_{i=1}^{p}\left(\sum_{k=0}^{q} a_{ik} f_k(t)\right)^* y[t+i] \end{aligned} \tag{3.6}$$

In section 2.3, the estimation of a_{ik} is achieved by minimizing the mean square of only the forward prediction error, but here both the forward and the backward prediction errors are combined. We redefine the mean squared error as the combination of both the forward estimation error and the backward estimation error,

$$\varepsilon \doteq \frac{1}{2(T-p)}\left\{\sum_{t=p}^{T}|\, e^{f}[t]\,|^2 + \sum_{t=0}^{T-p}|\, e^{b}[t]\,|^2\right\} \tag{3.7}$$

Since $|\, e^{b}[t]\,|^2$ and $|\, (e^{b}[t])^{*}\,|^2$ are equal, the mean squared error can be rewritten as

$$\begin{aligned}\varepsilon &= \frac{1}{2(T-p)}\left\{\sum_{t=p}^{T}|\, e^{f}[t]]^2 + \sum_{t=0}^{T-p}|\, (e^{b}[t])^{*}\,|^2\right\} \\ &= \frac{1}{2(T-p)}\left\{\sum_{t=p}^{T}\left|y[t]+\sum_{i=1}^{p}\sum_{k=0}^{q}a_{ik}f_k(t)y[t-i]\right|^2 + \sum_{t=0}^{T-p}\left|y^{*}[t]+\sum_{i=1}^{p}\left(\sum_{k=0}^{q}a_{ik}f_k(t)\right)y^{*}[t+i]\right|^2\right\}\end{aligned}$$

Taking derivative of ε with respected to a_{jl}, $j = 1,2,...p, l = 0,1,...q$, and equate to zero.

$$\begin{aligned}\frac{\partial\varepsilon}{\partial a_{jl}} = 0 = \sum_{t=p}^{T}&\left(y[t]+\sum_{i=1}^{p}\sum_{k=0}^{q}a_{ik}f_k(t)y[t-i]\right)f_l^{*}(t)y^{*}[t-j] \\ &+\sum_{t=0}^{T-p}\left(y^{*}[t]+\sum_{i=1}^{p}\sum_{k=0}^{q}a_{ik}f_k(t)y^{*}[t+i]\right)f_l^{*}(t)y[t+j]\end{aligned}$$

Rearrange the above equation

$$\begin{aligned}&\sum_{i=1}^{p}\sum_{k=1}^{q}a_{ik}\left(\sum_{t=p}^{T}f_k(t)f_l^{*}(t)y[t-i]y^{*}[t-j]+\sum_{t=0}^{T-p}f_k(t)f_l^{*}(t)y^{*}[t+i]y[t+j]\right) \\ &\qquad = -\left(\sum_{t=p}^{T}f_l^{*}(t)y[t]y^{*}[t-j]+\sum_{t=0}^{T-p}f_l^{*}(t)y^{*}[t]y[t-j]\right)\end{aligned}$$

Define

$$c_{kl}(i,j) \doteq \sum_{\mathrm{t=p}}^{\mathrm{T}} f_k(t) f_l^*(t) y[t-i] y^*[t-j] + \sum_{t=0}^{T-p} f_k(t) f_l^*(t) y^*[t+i] y[t+j] \qquad (3.8)$$

Then, the previous relation becomes

$$\sum_{i=1}^{p} \sum_{k=0}^{q} a_{ik} c_{kl}(i,j) = -c_{0l}(0,j), \quad j = 1,2,...p \text{ and } l = 0,1,...q . \qquad (3.9)$$

Equation (3.9) is important and neededd to be solved to obtain a_{ik}. After getting a_{ik}, the TVAR coefficients, $\hat{a}_i[t]$, for t = 0, 1, 2, ... , T, are obtained by computing $\hat{a}_i[t] = \sum_{k=0}^{q} a_{ik} f_j(t)$.

3.1.2 Approach 2: The previous estimator is slightly modified and both the forward and the backward estimation are also utilized as follows:

Forward estimation:

$$\hat{y}^f[t+1] = -\sum_{i=1}^{p} a_i[t] y[t-i+1] \ , \ t = p\text{-}1, p, \ldots, T\text{-}1 \qquad (3.10)$$

$$a_i[t] = \sum_{k=0}^{q} a_{ik} f_j(t)$$

Forward estimation error:

$$e^f[t+1] = y[t+1] - \hat{y}^f[t+1] = y[t+1] + \sum_{i=1}^{p} \left(\sum_{k=0}^{q} a_{ik} f_k(t) \right) y[t-i+1] \qquad (3.11)$$

Backward estimation:

$$\hat{y}^b[t-1] = -\sum_{i=1}^{p} b_i[t] y[t+i-1]$$

$$= -\sum_{i=1}^{p} a_i^*[t]y[t+i-1], \quad t = 1, 2, \ldots, T\text{-}p+1 \tag{3.12}$$

Backward estimation error:

$$e^b[t-1] = y[t-1] - \hat{y}^b[t-1] = y[t-1] + \sum_{i=1}^{p}\left(\sum_{k=0}^{q} a_{ik} f_k(t)\right)^* y[t+i-1] \tag{3.13}$$

In the above equations, the $b_i[t]$ are again forced to equal to $a_i^*[t]$. The mean squared error is defined as

$$\varepsilon \doteq \frac{1}{2(T-p)}\left\{\sum_{t=p-1}^{T-1} |\, e^f[t+1]]^2 + \sum_{t=1}^{T-p+1} |\, e^b[t-1]\,|^2\right\} \tag{3.14}$$

Similar to the derivation of approach 1, by minimizing ε with respect to a_{ik}, we have

$$\sum_{i=1}^{p}\sum_{k=0}^{q} a_{ik} c_{kl}(i,j) = -c_{0l}(0,j), \quad j = 1,2,\ldots p \text{ and } l = 0,1,\ldots q \tag{3.15}$$

where

$$c_{kl}(i,j) \doteq \sum_{t=\text{p-1}}^{\text{T-1}} f_k(t) f_l^*(t) y[t-i+1] y^*[t-j+1] + \sum_{t=1}^{T-p-1} f_k(t) f_l^*(t) y^*[t+i-1] y[t+j-1] \tag{3.16}$$

Solving the equation (3.15) yields the constant parameters a_{ik}, and then the estimates of the time-variant parameters, $\hat{a}_i[t] = \sum_{k=0}^{q} a_{ik} f_j(t)$. As can be noticed, equation (3.15) is exactly the same as equation (3.9), but the $c_{ik}(i,j)$ defined in (3.16) are totally different from that in (3.8). Furthermore, the parameter estimate $\hat{a}_i[t]$ from the

approaches 1 and 2 are also different in either their values or time-availability. In approach 1, $\hat{a}_i[t]$ are available from time t = 0 until t = T, but in approach 2, $\hat{a}_i[t]$ can be calculated only from time t = 1 to t =T-1.

Equations (3.9) and (3.15) are sets of $p(q+1)$ linear equations. Solving them for a_{ik} might be tedious, especially if p and q are large. However, they can be changed into a matrix form, and then linear algebra techniques can be applied for achieving the solutions. One can write (3.9) or (3.15) in a matrix form as

$$\mathbf{Ca = -d} \tag{3.17}$$

Where

$$\mathbf{C} = \begin{bmatrix} \Phi(1,1) & \Phi(2,1) & \cdots & \Phi(p,1) \\ \Phi(1,2) & \Phi(2,2) & \cdots & \Phi(p,2) \\ \vdots & \vdots & \ddots & \vdots \\ \Phi(1,p) & \Phi(2,p) & \cdots & \Phi(p,p) \end{bmatrix} \text{ is of } p(q+1) \text{ x } p(q+1) \text{ size.}$$

$$\Phi(i,j) = \begin{bmatrix} c_{00}(i,j) & c_{10}(i,j) & \cdots & c_{q0}(i,j) \\ c_{01}(i,j) & c_{11}(i,j) & \cdots & c_{q1}(i,j) \\ \vdots & \vdots & \ddots & \vdots \\ c_{0q}(i,j) & c_{1q}(i,j) & \cdots & c_{qq}(i,j) \end{bmatrix} \text{ is of } q+1 \text{ x } q+1 \text{ size.}$$

$$\mathbf{a} = \begin{bmatrix} \vec{a}_1 \\ \vec{a}_2 \\ \vdots \\ \vec{a}_p \end{bmatrix}, \ \vec{a}_i = \begin{bmatrix} a_{i0} \\ a_{i1} \\ \vdots \\ a_{iq} \end{bmatrix}, \quad \mathbf{d} = \begin{bmatrix} \vec{\chi}_1 \\ \vec{\chi}_2 \\ \vdots \\ \vec{\chi}_p \end{bmatrix}, \text{ and } \vec{\chi}_j = \begin{bmatrix} c_{00}(0,j) \\ c_{01}(0,j) \\ \vdots \\ c_{0q}(0,j) \end{bmatrix}.$$

Steps of transforming (3.9) or (3.15) into the matrix form (3.17) are shown in the appendix.

3.2 Computation (linear algebra) for solving Ca =-d

Computational aspects were discussed by Hall et al. [1983], in which a symmetric property was utilized to reduce the steps of computation. For the proposed approach, the matrix **C** is still symmetric. Therefore, the computational reduction, mentioned in Hall et al. [1983], can still be used in our approach. However, since we employed both the forward and the backward estimations, the computation for forming the matrix **C** in (3.15) is unavoidably two times as much of that mentioned in Hall's paper.

For solving the linear matrix equation **Ca**=**-d** for **a**, in general, two methods are available; namely, the direct and the indirect (iterative) methods. The direct method or non-iterative approach involves a finite number of calculation steps that must be completed before the solutions are obtained. It usually requires a finite number of calculations of the order of m^3, where m is the size of the square matrix **C**. This computation might be too much in a sense that m^3 is huge when m is large. Examples for the direct method are the Guassian elimination, QR, and SVD factorizations. The indirect method or the iterative approach, relies on calculating a sequence of approximations to the solution **a**. The iteration can be stopped whenever a desired accuracy is achieved or a number of iteration steps is completed. The iteration method is suitable for large and/or sparse systems. Works required for attaining solutions are of the order of m^2, where m is the size of the matrix **C**. An example of the indirect method is the conjugate gradient method, whose detail of calculation can be found in [Datta, 1995] or [Trefethen and Bau, 1997]

3.3 Test and Results – show an improvement in frequency estimation. Noise-free and noisy (20dB SNR) situations.

The proposed approaches were tested, in a noise free situation, to estimate the time varying frequencies of two synthetic signals that have only a single frequency component. The synthetic signals were real and generated such that their frequencies were exactly known as shown in Figure 3.1. The first signal is a real (not complex) chirp signal whose normalized frequency increased linearly from 0.1*Fs* to 0.41*Fs* over 32 samples, where *Fs* = sampling frequency. The second signal is sinusoid whose frequency varies periodically from 0.1*Fs* to 0.3*Fs* with a sweep rate of 0.05*Fs*. We estimated the time-varying frequency by first,

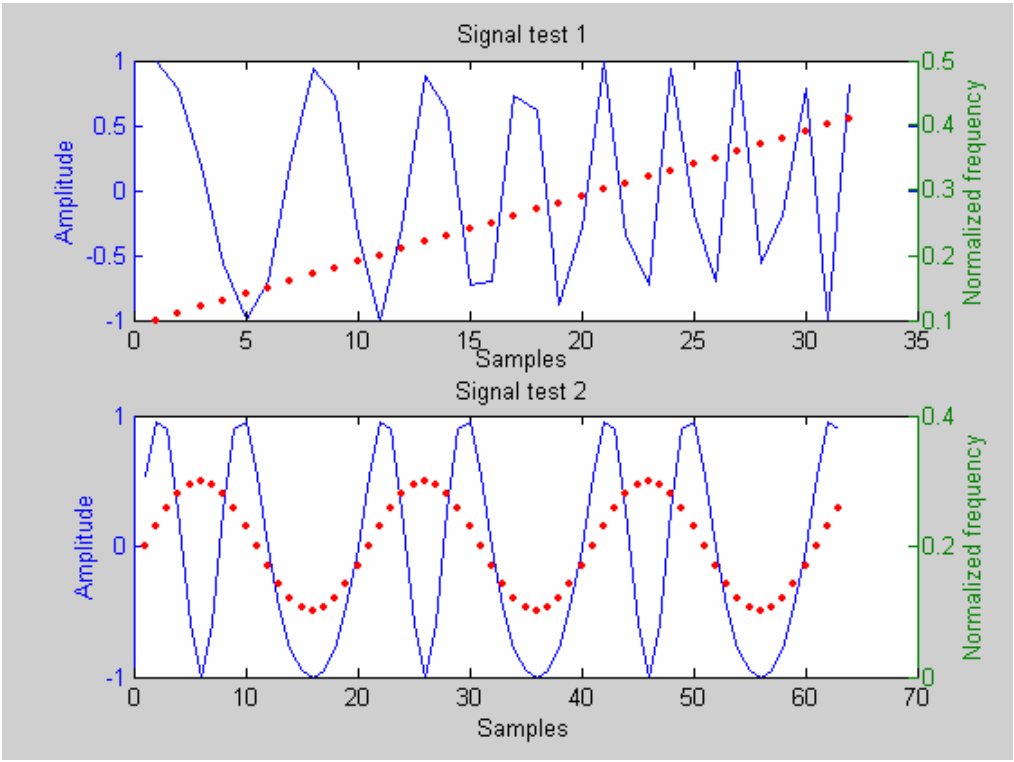

Figure 3.1: Two signals used for the test. Solid = real signals. Dot = Normalized frequency varying with time.

solving for the vector **a** in equation (3.17), and then computing the TVAR parameter estimate by using $\hat{a}_i[t] = \sum_{k=0}^{q} a_{ik} f_j(t)$, i = 1, 2, …, p. Once $\hat{a}_i[t]$ were available, the time-varying frequency estimate was obtained from $\hat{f}[t] = angle(z_o) \cdot Fs/(2\pi)$, where z_o is the closest pole to the unit circle in the complex z-plane, and is a root of the prediction error filter polynomial $z^p + a_1[t]z^{p-1} + a_2[t]z^{p-2} + ... + a_p[t] = 0$.

Figure 3.2 shows results from using approach 1 to estimate time-varying frequency. For signal test 1 (Figure 3.2a), we used the polynomial basis function $f_k(t) = \left(\frac{t-1}{N}\right)^k$ where N is the total sample number, and chose p = 2, q =4, while for the signal test 2, we used the cosine function defined as $f_k(t) = \cos\left(\frac{\pi kt}{N}\right)$, and selected p = 2, q =12. The errors shown in the Figure are the average errors, calculated from equations i) $err = \frac{1}{N-p}\sum_{n=p+1}^{N}\left|f[n] - \hat{f}[n]\right|$, for the forward estimator, ii) $err = \frac{1}{N-p}\sum_{n=1}^{N-p}\left|f[n] - \hat{f}[n]\right|$, for the backward estimator, and iii) $err = \frac{1}{N}\sum_{n=1}^{N}\left|f[n] - \hat{f}[n]\right|$. As seen, the proposed approach 1, which uses both the forward and the backward estimators yields less estimation error, compared to that from using either only the forward or the backward estimator. In fact, for the signal test 1, the average error from using either the forward or the backward is about one-step difference between the adjacent true frequencies, $\left|f[n] - f[n-1]\right| = 0.01$. This error verifies that the parameter estimates from

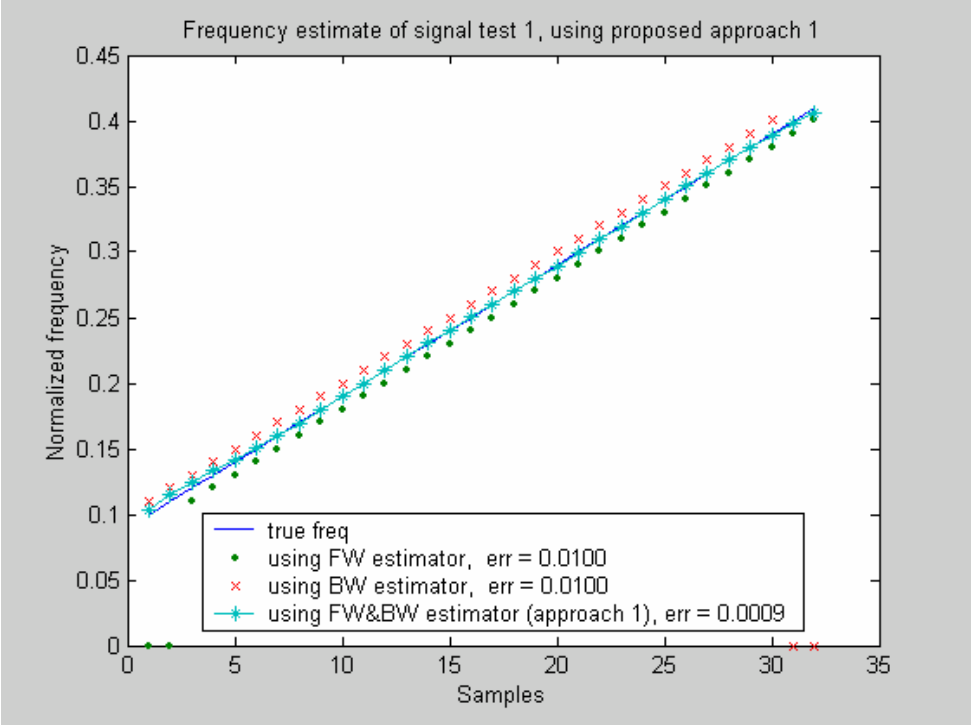

(a)

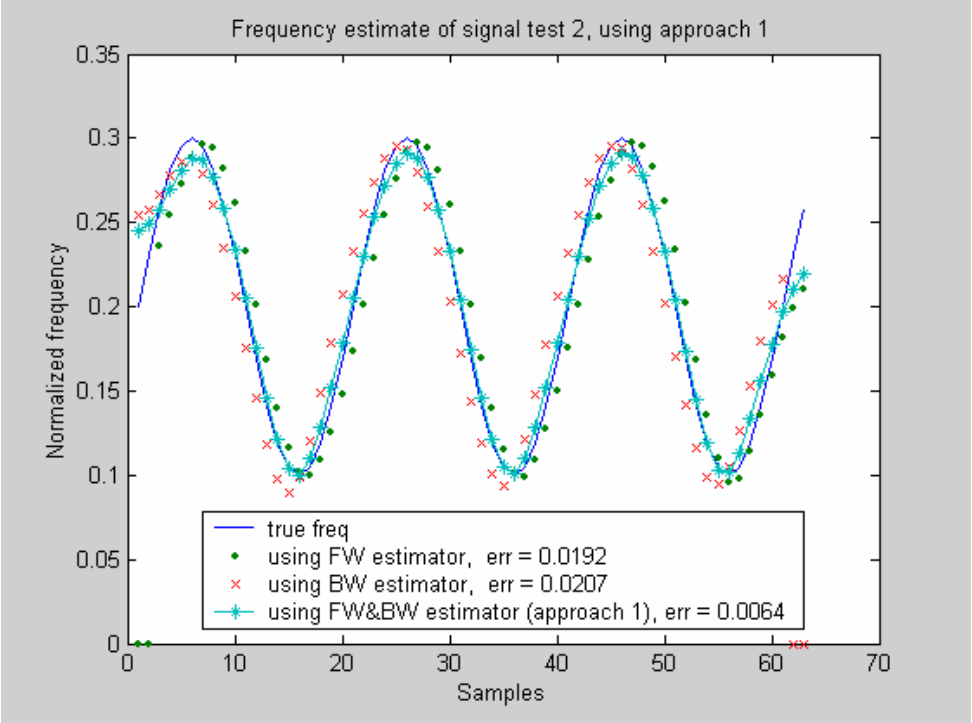

(b)

Figure 3.2: Results from using proposed approach 1 to estimate the time-varying frequency of signal test 1 and signal test 2.

using the model in chapter 2, that have been used by several researchers, is, in fact, at best a step-delay version of the true parameter. However, this error is negligible when the sampling frequency is high. Also noted was that neither the forward nor the backward yielded a frequency estimate from the start to the end (t = 0 until t =T) due to the p-delay required at the initial state, but the proposed approach 1 allowed the frequency estimate available for all sampled times t = 0,1,…,T.

Figure 3.3 displays the results from using the modified TVAR model, equation (3.15) and (3.16) in approach 2, to estimate the time-varying frequencies of the signal test 1 and signal test 2. As is seen, the frequency estimates from using either the forward, the backward or the forward-backward estimators are about the same. They are approximately equal to the true frequency. Note that the averaged errors shown in figure 3.3(a) and 3.3(b) were computed by using i) $err = \frac{1}{N-p}\sum_{n=p}^{N-1}\left|f[n]-\hat{f}[n]\right|$ for the forward estimator, ii) $err = \frac{1}{N-p}\sum_{n=2}^{N-p+1}\left|f[n]-\hat{f}[n]\right|$, for the backward estimator, and iii) $err = \frac{1}{N-2}\sum_{n=2}^{N-1}\left|f[n]-\hat{f}[n]\right|$, for the forward-backward estimator.

By comparing the accuracy in the time-varying frequency estimation between approaches 1 and 2, it can be seen that the estimation from approach 2 has less errors than from the approach 1. This is because the modified model was used in approach 2. However, as mentioned earlier, the frequency estimates using the modified model are

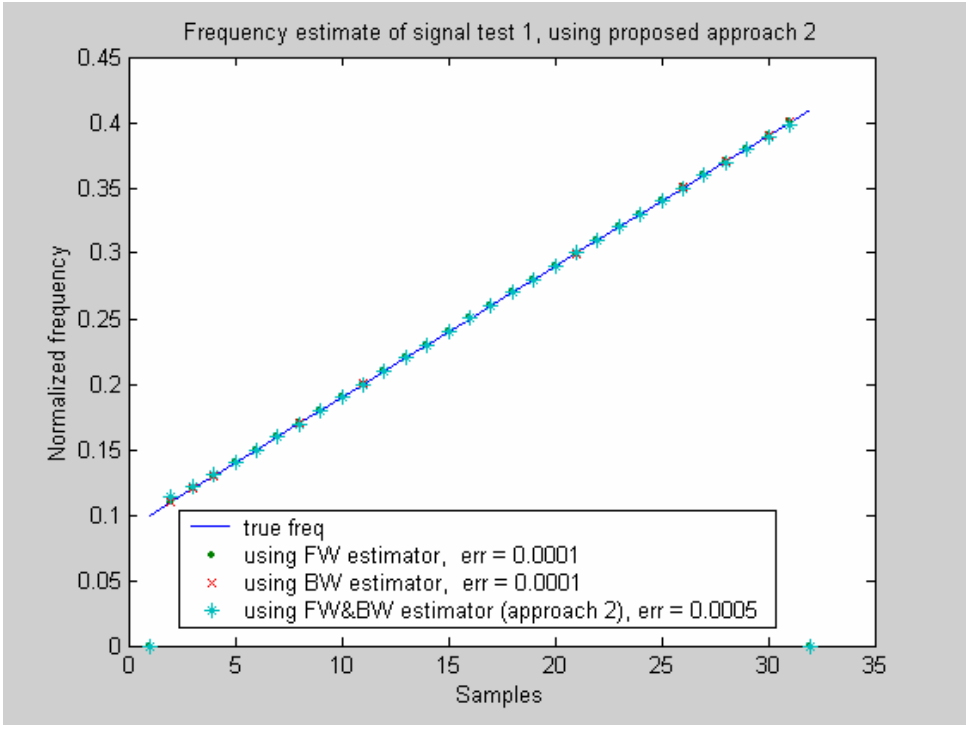

(a)

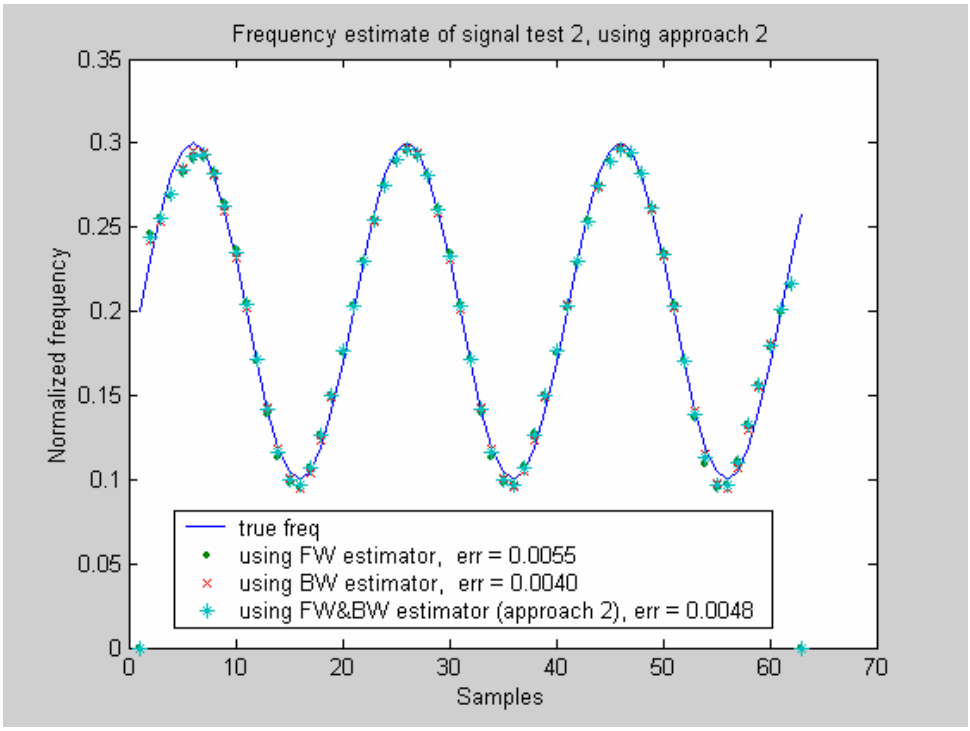

(b)

Figure 3.3: Results from using the proposed approach 2 to estimate the time-varying frequencies of the signal tests 1 and 2.

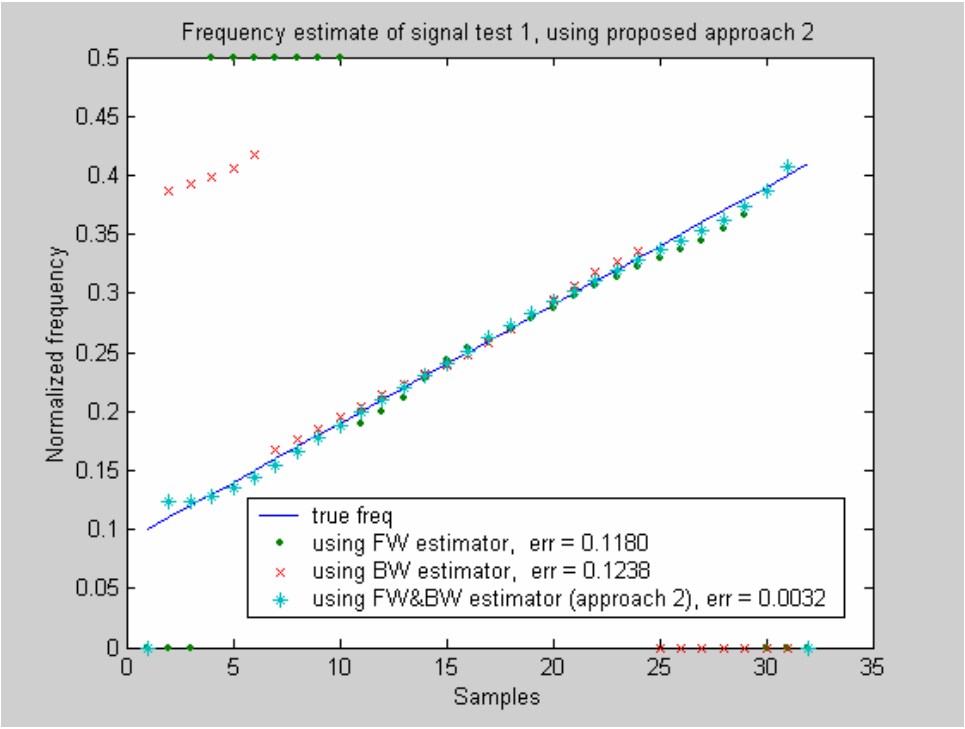

(a) for signal test 1

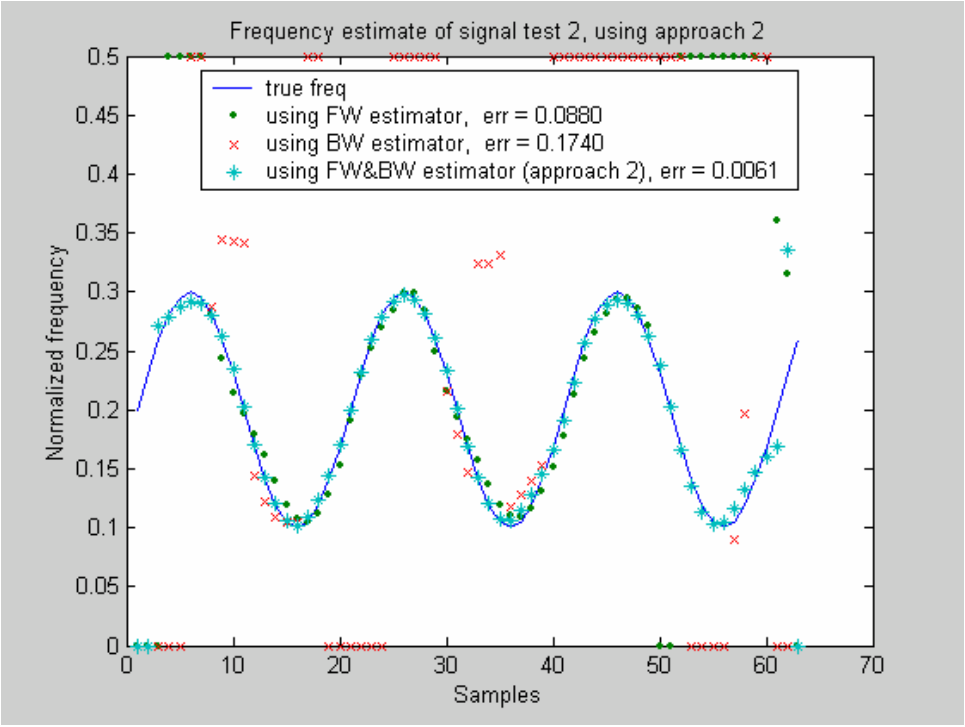

(b) for signal test 2

Figure 3.4: Results from using the 2nd proposed approach, when the model ordered is over-determined (true model order $p = 2$, but use over-determined model order $p = 4$).

available only from sample = 2 to the time sample N-1, contrasted to the approach 1 in which the estimation can be obtained for all the time samples.

Next, we used the 2nd proposed approach to estimate the frequency of the signal test 1 and 2 in the additive white noise that has signal-to-noise ratio (SNR) = 20 dB. We assumed that the true model order p is unknown, so we used p >2, which is over-determined. We can see a benefit of the proposed approach that utilizes both the forward and the backward estimators, when the model order is over-determined.

Figure 3.4 displays results when the model order p = 4, q = 4 for signal test 1, and p = 4, q =12 for signal test 2. Both cases are of over-determined model orders. As seen from Figures 3.4(a) and 3.4(b), when the model order is over-determined, neither the forward nor the backward estimators can successfully estimate the time-varying frequency. However, the proposed approach yields the frequency estimate that is reasonably accurate.

3.4 Discussion

Two approaches were proposed and used to estimate the time-varying frequency of two real (not complex) testing signals in the previous sections. The first approach uses the model that has been used by several researchers, and was characterized as a linear forward estimator. This forward estimator, which was defined in equation (3.1), estimates the current data from the previous p values of the available data. The p time-variant coefficients of the forward estimator were unknown, and then were optimally estimated

in a mean square sense by minimizing the mean squared error between the estimate and the true values of the data. The frequency estimates that were shown in the previous section were calculated from the location of poles, closest to the unit circle and are roots of the polynomial equation $z^p + a_1[t]z^{p-1} + a_2[t]z^{p-2} + ... + a_p[t] = 0$. In the noise-free case, with the signal test 1, it was seen from the simulation that the frequency estimates either from the forward or the backward estimators were not equal to the true frequency, but about one-step delay of the true frequency. However, by utilizing both the forward and the backward estimators for estimating the time-varying parameter and then the frequency, the frequency estimate about the true frequency was achieved. This can be explained empirically. Since the forward estimator yielded the parameter estimate $\hat{a}_i[t]$, which was about $a_i[t-1]$, and the backward estimator yielded the parameter estimate $\hat{b}_i[t]$, which was about $a_i[t+1]$, by combining both the forward and the backward estimation error together and minimizing this error with respect to both the forward and the backward parameters, which were constrained to be equal (i.e $b_i[t] = a_i[t]$, for the real signal), this resulted in an optimal parameter estimate in the mean squared sense, which were approximately the average of $a_i[t-1]$ and $a_i[t+1]$, as could be seen from the plot of estimated frequency in Figure 3.2 (a) and 3.2 (b). The result that showed the one step delay in the frequency estimation either from the forward or the backward estimator (3.1) or (3.4), suggested the modification of the estimation model used in approach 2.

The second approach used a modified model that resulted in no delay between the estimated and the true frequencies, even though only the forward or the backward

predictor was used. The differences between the first approach and second approach are displayed in Figure 3.5. The first approach was to estimate the time-variant parameter a[*t*] by using the forward and the backward estimation of y at the time *t*, but the second approach estimates the parameter a[*t*] by using a combination of the forward estimation of y at time *t*+1 and the backward estimation of y at time *t*-l.

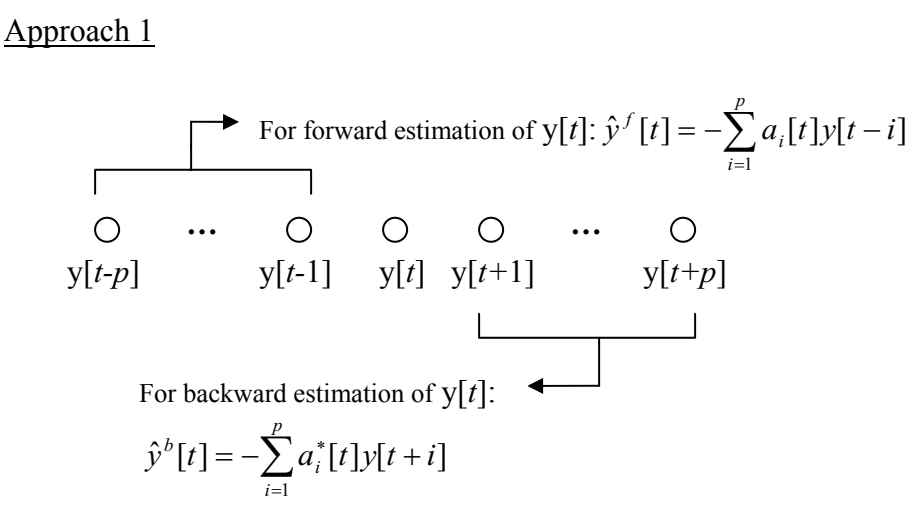

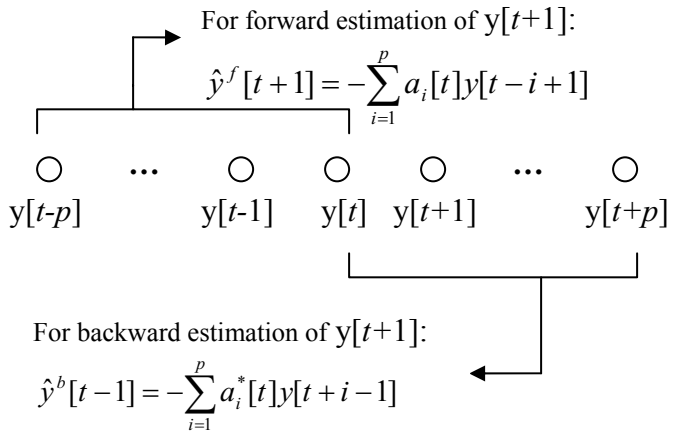

Figure 3.5: Displays the differences between the first and the second proposed approaches for estimating the TVAR parameters $a_i[t]$ at time *t*.

The proposed approach 2 yielded the frequency estimate of the signal test 2 more accurate than that from the proposed approach 1. This could be explained as follows: the forward and the backward parameter estimates from the first approach were $\hat{a}_i[t] \sim a_i[t-1]$, and $\hat{b}_i[t] \sim a_i[t+1]$, and the minimizer to the combination of the forward and backward prediction errors (with the constraint $\hat{b}_i[t] = \hat{a}_i[t]$) was approximately ~ $1/2(a_i[t-1]+a_i[t+1])$. For approach 2, the forward parameter estimate $\hat{a}_i[t]$ was about the true parameter $a_i[t]$, and the backward parameter estimate $\hat{b}_i[t]$ was also about $a_i[t]$. The minimizer to the combination of the forward and backward error (with the $\hat{b}_i[t] = \hat{a}_i[t]$ constraint) was, therefore, also about the true parameter $a_i[t]$. Since $1/2(a_i[t-1]+a_i[t+1])$ is not always equal to $a_i[t]$, therefore, the approach 2 yielded more accuracy in parameter and frequency estimation for nonstationary signals.

It could also be noted that, in the second approach, utilizing a combination of the forward and the backward predictors does not help to deal with the delay, because no delay occurred, even though only the forward or the backward predictor was used. However, it was seen in Figure 3.4, where the model order was over-determined, that neither the forward nor the backward could yield a frequency estimate, while the proposed approach yielded the frequency estimation with reasonable accuracy. One might argue that the reason that the forward or backward predictor failed to estimate the time-varying frequency in Figure 3.4, was because of the total number of parameters that were needed to be estimated ($p.q$) was not small, compared to the number of available

data, and that did not follow the rule of thumb or the implication of the parsimony principle, recommended by Niedzwiecki [2000][1]. This argument may be true because we used for the signal test 1, $p = 4$, $q = 4$ ($p.q = 16$), while the number of data = 32 samples, and for the signal test 2 $p = 4$, $q = 12$ ($p.q = 48$) while the number of available data = 96 samples.

To see that the proposed approach did actually improve the frequency estimation when the model order was over-determined, we did a few more tests in noisy 20dB-SNR environments where the sample number of signal test 1 and signal test 2 were increased to be 128, and 224 samples, respectively. The increase in the sample number is to satisfy the parsimony principle. The results of these tests are shown in Figures 3.6 and 3.7. We remarked that the true model order was 2, since the signal test 1, or the signal test 2 only had a single time-frequency component. As is seen, when the true model order p=2 was selected, the estimation errors from the forward, the backward, or the proposed approach were about the same, but when the used model order was increased (over-determined), the estimation errors from the proposed approach were smaller than that from either the forward or the backward predictor alone. This confirms that the proposed method did improve the frequency estimation.

It should be noted that, as the model order p increases (still satisfying the principle of parsimony), the estimation errors from the proposed approach tends to

---

[1] Niedzwiecki, M. [2000] suggested that, based on the principle of parsimony, the total number of estimated parameters should be much smaller than the number of available data points or satisfy the inequality $pq \leq 0.2N$, where p is the model order, q is dimension in time-function expansion, and N is total number of data. {Source: Maciej Niedzwiecki, *Identification of Time-varying processes*, Chapter 6, John Wiley & Sons, Ltd., 2000}

decrease. This can be explained as well. Since the signal was in an additive noise, the TVAR model order-2 that could sufficiently represent the noise-free signal was no longer valid for the signal in the additive noise. In fact, the AR model with limited order is not completely valid to represent a process in an additive noise, since the signal in the additive noise algebraically becomes the ARMA process. This was shown for the stationary case in Kay [1988]. In this thesis we show for the nonstationary case in the Appendix. For an AR to sufficiently represent the ARMA(p), the model order of the AR process must be increased.

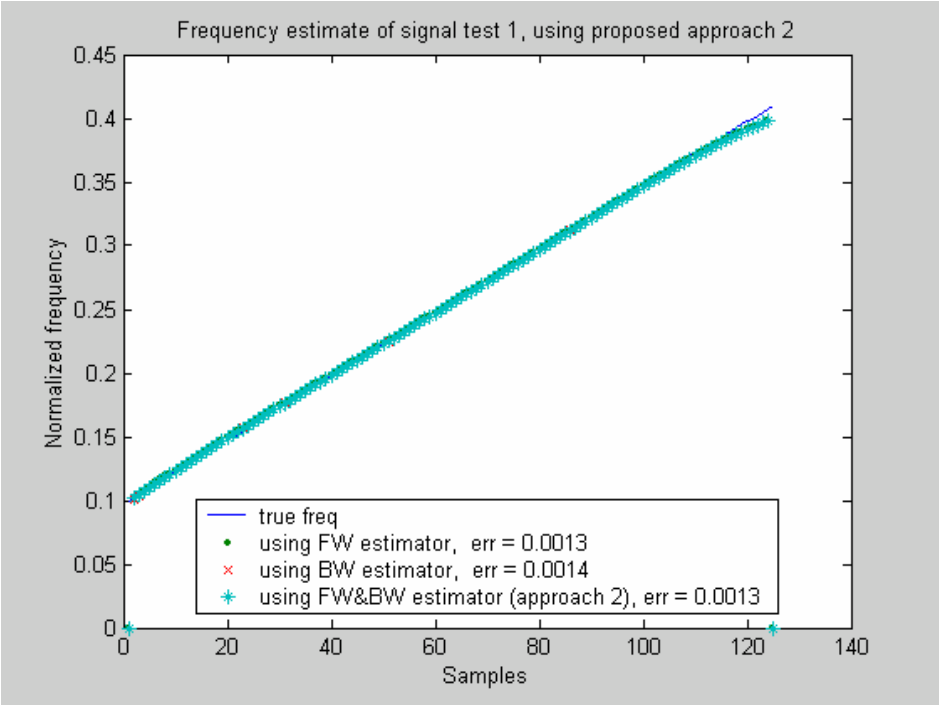

(a) p=2, q=4

Figure 3.6 Results for the signal test 1 (parsimony principle is satisfied), showing improvement in the frequency estimation of the proposed approach, when p is over-determined.

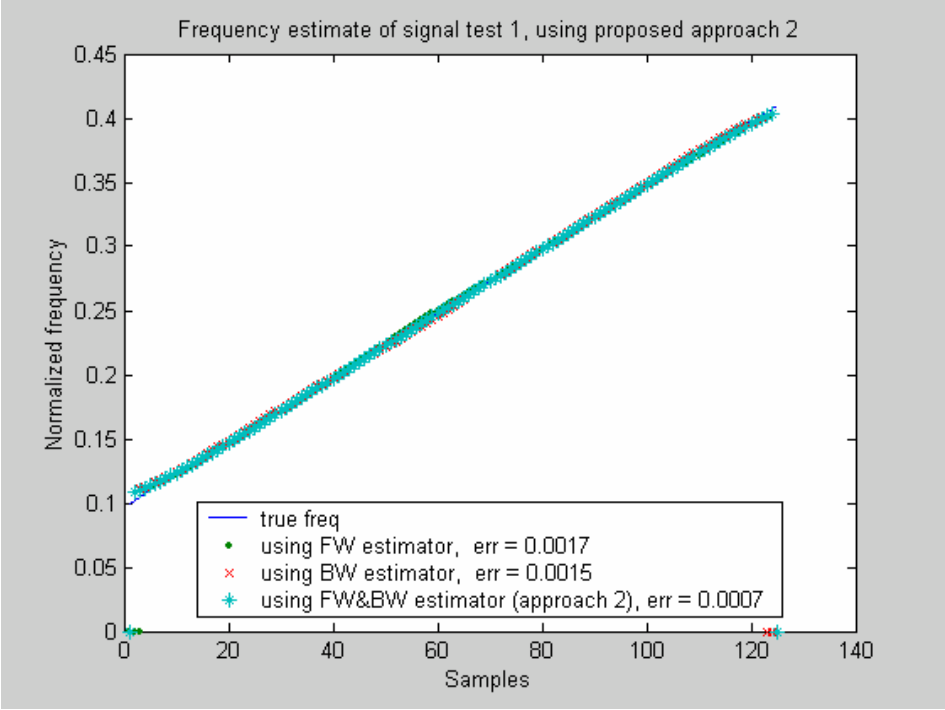

(b) $p = 4$, $q = 4$

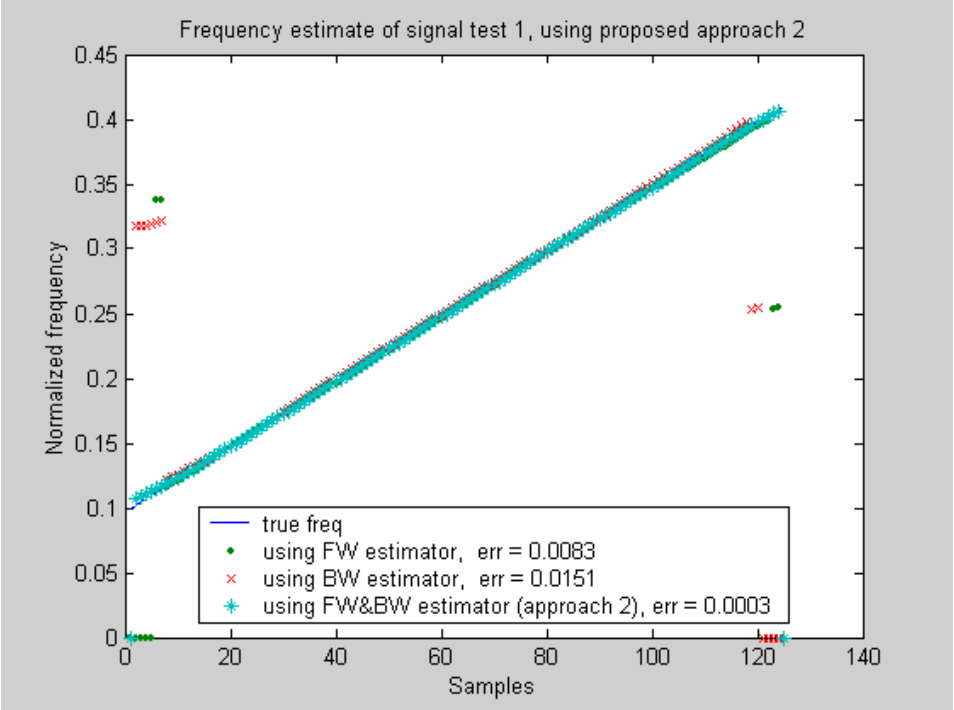

(c) $p = 6$, $q = 4$.

Figure 3.6 Results for the signal test 1 (parsimony principle is satisfied), showing improvement of the proposed method in the frequency estimation, when p is over-determined. (Continued)

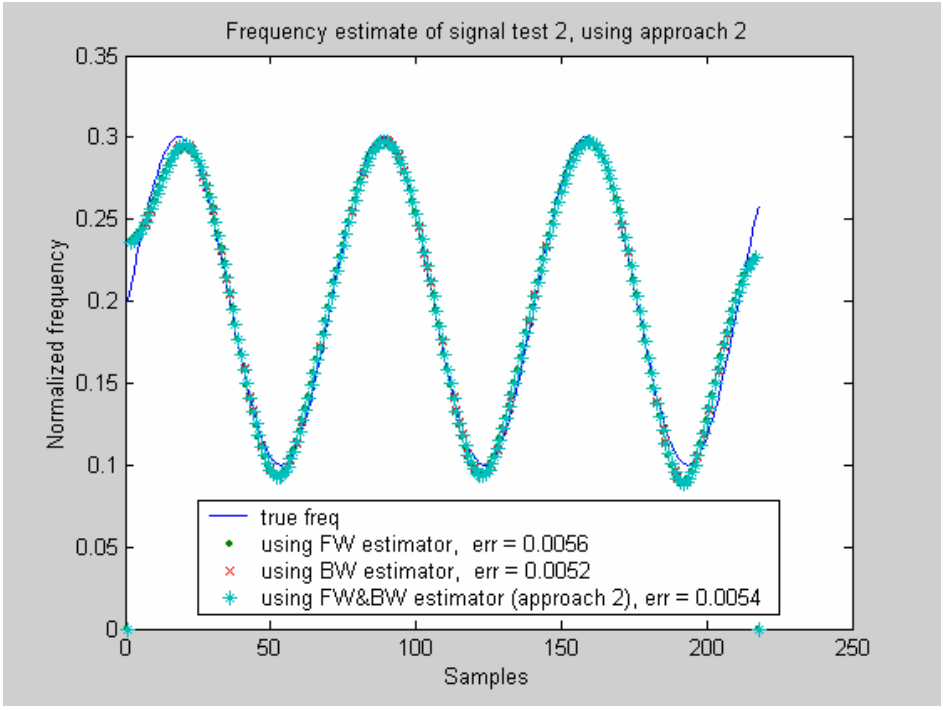

(a) $p = 2$, $q = 12$

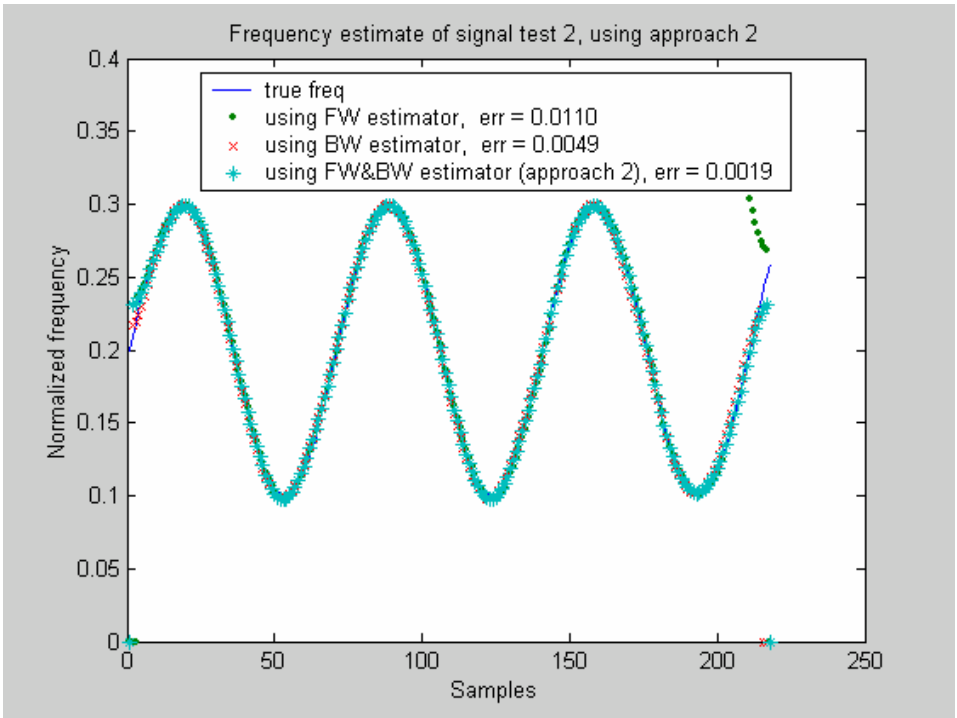

(b) $p = 4$, $q = 12$

Figure 3.7 Results for the signal test 2 where the parsimony principle is satisfied, for showing that the proposed method does improve the frequency estimation when the model order p is over-determined.

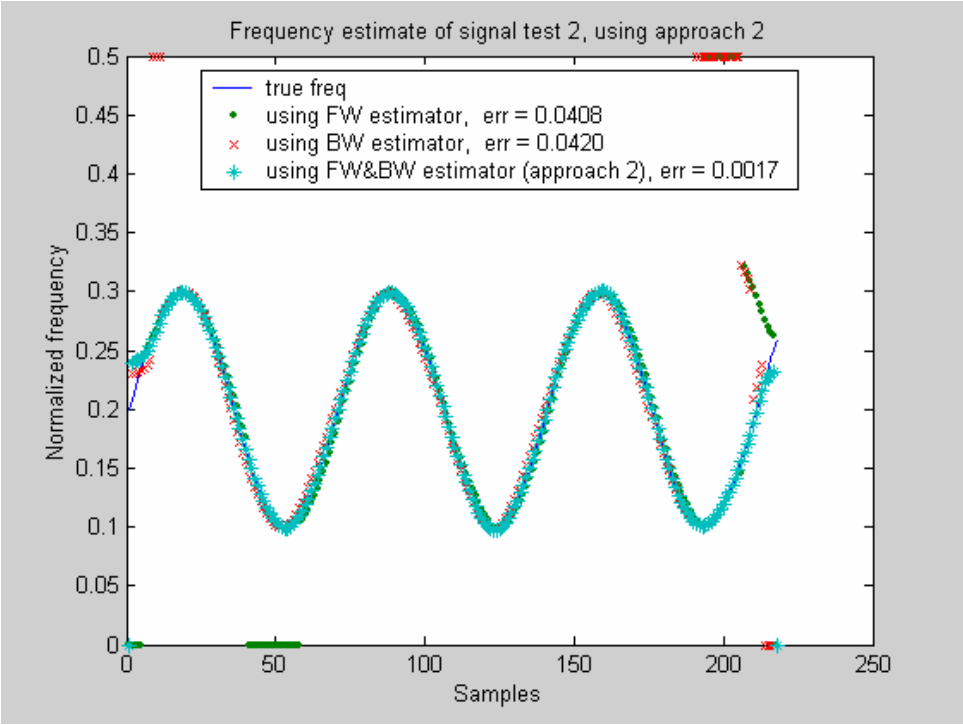

(c) $p = 6$, $q = 12$

Figure 3.7 Results for the signal test 2 where parsimony principle is satisfied, for showing that the proposed method does improve the frequency estimation when model order p is over-determined. (Continued)

3.5 Chapter summary

Two slightly different TVAR models were used in our modified basis function method that utilizes both the forward and the backward estimators to estimate the TVAR parameters, and then the time-varying frequencies. Posing the constraint $\hat{b}_i[t] = \hat{a}_i^*[t]$ to the minimization of the summation of the forward and the backward error, was beneficial to the frequency estimate in that the estimates were approximately equal to the true frequency and could be obtained for all samples t = 0, 1, 2, … T, as seen from the results

of the approach 1. In approach 2, the benefit of the constraint $\hat{b}_i[t] = \hat{a}_{i_i}^*[t]$ for minimization of forward and the backward error summation was not so obvious, since the frequency estimate from either only forward or backward predictor was already about the true frequency. However, by comparing the frequency estimate from approach 1 and approach 2, we have found that approach 2 yielded more an accurate frequency estimate. In addition, for the case where the model order was over-determined, our proposed approach showed better results in estimating the time-varying frequency than using either solely the forward or the backward estimator.

CHAPTER 4

Comparison of Different Time-Functions in Frequency Estimation

Since there were many existing time-functions that could be used as basis for the TVAR parameter expansion, one might be interested in knowing how to choose them and what difference they may cause. A work done by Charbonnier et al. [1987], showed a result of using three different time-basis functions, which are the Fourier, the Legendre, and the discrete prolate spheroidal sequence (DPSS), for the AR-modeling of non-stationary signals. Their comparison was based on a goodness of fit between the signal estimate and the true signal.

In this chapter, five basis functions (time polynomial, Legendre polynomial, non harmonic Fourier function, discrete cosine function, and DPSS are compared based on the accuracy in estimating the time-varying frequency of testing signals. The proposed approach (approach 2), from chapter 3 is used. It was found that these basis time-functions, except the polynomial and the Legendre functions, yielded different frequency estimates when the expansion order (q) is small. However, when the order of expansion is large, the difference in frequency estimate from the different basis function is insignificant, since when the dimension is large, all the basis functions approximately span the sub-space equally. The time-polynomial and the Legendre functions yield the same result. This is because both functions are linearly related and capable of spanning exactly the same subspace. Proof of this is provided for the proposed approach.

4.1 Basis Functions

Opposite to the adaptive algorithms, the function-expansion method was based on an explicit model of the parameter variation, i.e. parameters were approximated by a linear combination of the basis time-functions. The time functions (denoted by $f_k(t)$), that can be used as basis for expansion, conceptually must be independent and non-zero for all t = 0, 1, …, T. At t = 0, $f_k(t)$ must be unity. Some currently available basis functions are listed as follows:

Time polynomial function:

$$f_k(t) = \left(t/N\right)^k$$

or

$$f_k(t) = \left\{1, \frac{t}{N}, \left(\frac{t}{N}\right)^2, \left(\frac{t}{N}\right)^3, \ldots\right\} \tag{4.1}$$

Legendre polynomial function:

$$f_k(t) = \left\{1, \frac{t}{N}, \frac{1}{2}\left(\left(\frac{t}{N}\right)^2 - 1\right), \frac{1}{2}\left(5\left(\frac{t}{N}\right)^3 - 3\frac{t}{N}\right), \ldots\right\} \tag{4.2}$$

Non-harmonic Fourier function:

$$f_k(t) = \begin{cases} \cos\left(\dfrac{k\pi t}{2N}\right), & \text{k is even} \\ \sin\left(\dfrac{(k+1)\pi t}{2N}\right), & \text{k is odd} \end{cases} \tag{4.3}$$

Discrete cosine:

$$f_k(t) = \cos\left(\frac{\pi k t}{N}\right) \tag{4.4}$$

Discrete prolate spheroidal sequence (DPSS) or Slepian sequence:

$f_k(t) =$ k^{th} sequences most concentrate in the frequency band $|w| \le 2\pi W$, where W is half bandwidth.

All $t = 0,1,2,\ldots,T$ are sampling times, N is the total number of sampled data ($N = T+1$), and $k = 0,1,2,\ldots,q$ is the dimension number for expansion.

Comparison of these five basis functions in the time-varying frequency estimation has not been shown. However, it is generally mentioned in [Niedzwiecki, 2000] that there are possibly two ways for selecting the basis function. If some prior knowledge about the physical process of time variation is available, the basis functions should be chosen such that the prominent trends in parameter change is retained. An example of this, is in [Tsatsanis and Giannakis, 1996], where the knowledge about the periodic time-variation of the process is employed, and complex exponential functions are used for identification and equalization of mobile fading radio channel. If a priori information is unavailable, which might be the case for complicated physical systems, Niedzwiecki [2000] suggests that the selection of the basis function should rely on general approximation, such as the Taylor and Fourier series approximation, and the function most commonly used are the time polynomial and the Fourier, or the cosine functions.

For our comparison in the time-varying frequency estimation, all the five basis functions are tested with synthetic signals without noise. Our objective is to find an efficient basis for all testing signals in the sense that, for a small number of basis or expansion dimension, the basis yields the least error in frequency estimation.

4.2 Experiment (via Simulation) and Result

Basis functions were tested in a noise-free situation with five synthetic signals, shown in Figure 4.1. These five signals were generated such that their time-varying frequencies were exactly known.

- *Signal test 1* was a linear chirp that has a linearly-varying frequency from .01Fs to 0.45Fs over 101 samples. This signal was generated by using equation $x_1(t) = \cos(\pi\mu \cdot t^2 + 2\pi f_1 t)$ where $\mu = 4.4e5$, $f_1 = 100\,\text{Hz}$, and sampling rate Fs = 10000 Hz
- *Signal test 2* was a chirp signal with a normalized frequency variation in a parabolic shape from 0.02 to 0.46 over 101 samples. It was created by using the equation $x_2(t) = \cos(\frac{2}{3}\pi\mu_3 t^3 + 2\pi f_1 t)$, where $\mu_3 = 4.4e7$.
- *Signal test 3* was a sinusoid with a normalized frequency change in parabolic shape from 0.01 to a maximum at 0.45 and then back to 0.01 over 101 samples. This signal may be thought of as an example of an ideal Doppler signal. It was given by $x_3(t) = \cos(-\frac{2}{3}\pi\mu_2 t^3 + 2\pi\mu_2 t_d t^2 - 2\pi\mu_2 t_d^2 t + 2\pi f_2 t)$ where $\mu_2 = 1.76e8$, $f_2 = 4500\,\text{Hz}$, and t_d = time delay which is of 51 samples.
- *Signal test 4* was a sinusoid and its normalized frequency periodically varies from 0.1 to 0.4 with a sweeping rate of 0.025Fs, given by $x_4(t) = \cos(2\pi t - \frac{0.6}{f_4}\cos(2\pi f_4 t))$, where $f_4 = 0.1\,\text{Hz}$, and sampling rate Fs = 4 Hz.
- *Signal test 5* was a highly nonstationary sinusoid that has a normalized frequency,

jumping from 0.1 to 0.4 and then linearly decreasing from 0.4 to 0.1. The length of this signal was 156 samples.

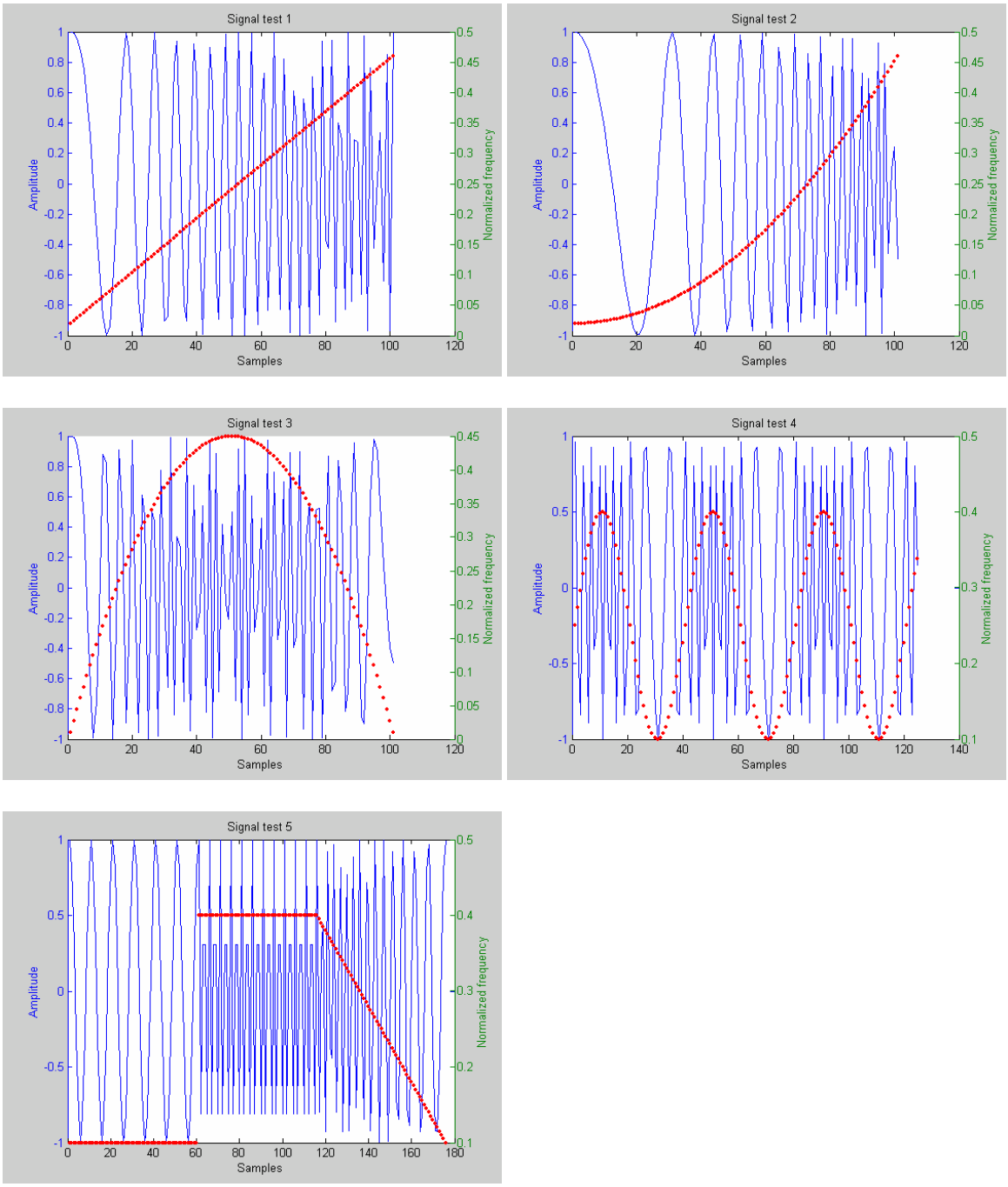

Figure 4.1: Five signal tests.

Since the synthetic signals are real (not complex) and have one frequency component varying with time, the model order $p = 2$ is used. In order to identify the TVAR parameter and the time-varying frequency, the expansion dimension q must be selected. Because an appropriate q was not known, various q will be used for each basis time-function. Effect of q for different basis functions in frequency estimation can be observed by comparing the frequency estimation error, defined by:

$$\textit{frequency estimation error} = \frac{1}{N}\sum_{t=0}^{N-1}\left|f - \hat{f}\right|. \tag{4.5}$$

Figure 4.2 shows the frequency estimate for *signal test 1*. As seen, for the low expansion order (q= 2), the Fourier basis yields the least estimation error, while the DPSS yields the biggest error. For q = 4, except the cosine function, all other basis functions have small errors in estimating the time-varying frequency of the signal test 1. Figure 4.3 is the result for *signal test 2*. The expansion dimension q shown in this figure starts from q = 4, since for q less than 4, the frequency estimation errors for all the basis functions were big and not useful for comparison. As can be observed, similar result to that of signal test 1, the Fourier basis yielded the least error when the dimension is small (q = 4), but the polynomial and the Legendre functions yielded biggest error for q=4. However, when the dimension increased, the estimation errors from all the basis functions were not much different, as seen for q = 8. Figure 4.4 displays the frequency estimate and its error for the *signal test 3*. Same as the results for signals 1 and 2, at high dimension (q =8) all the basis functions yielded about the same estimation errors, but in this case, the cosine function was slightly better in frequency estimation than other basis functions for both the low and the high expansion dimension (q = 4 and q=8).

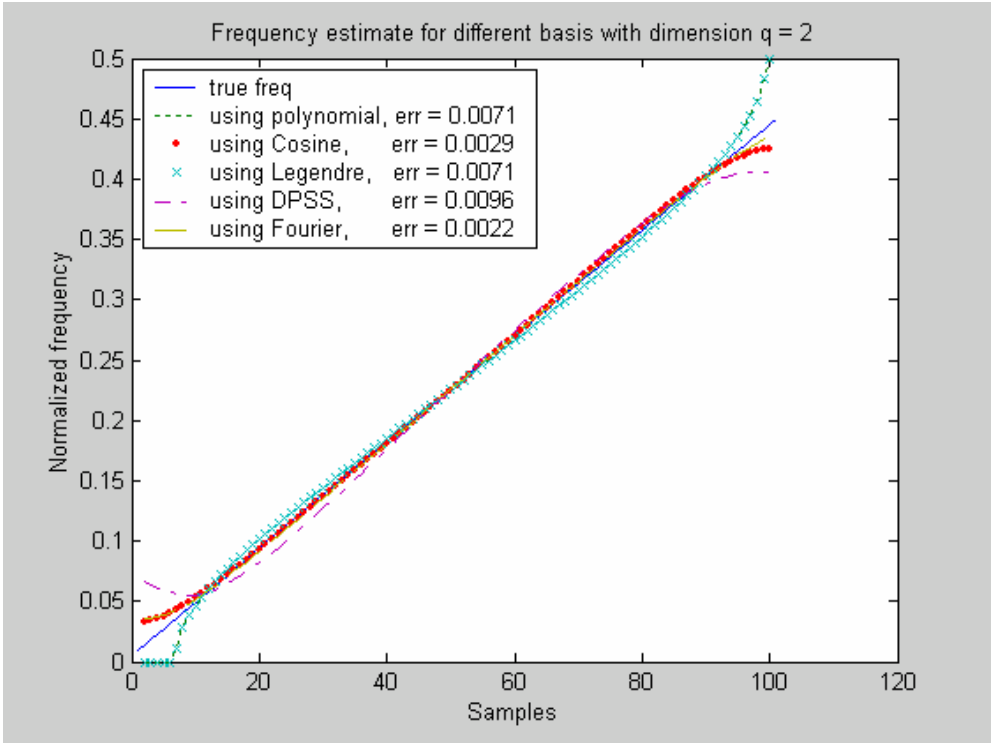

(a)

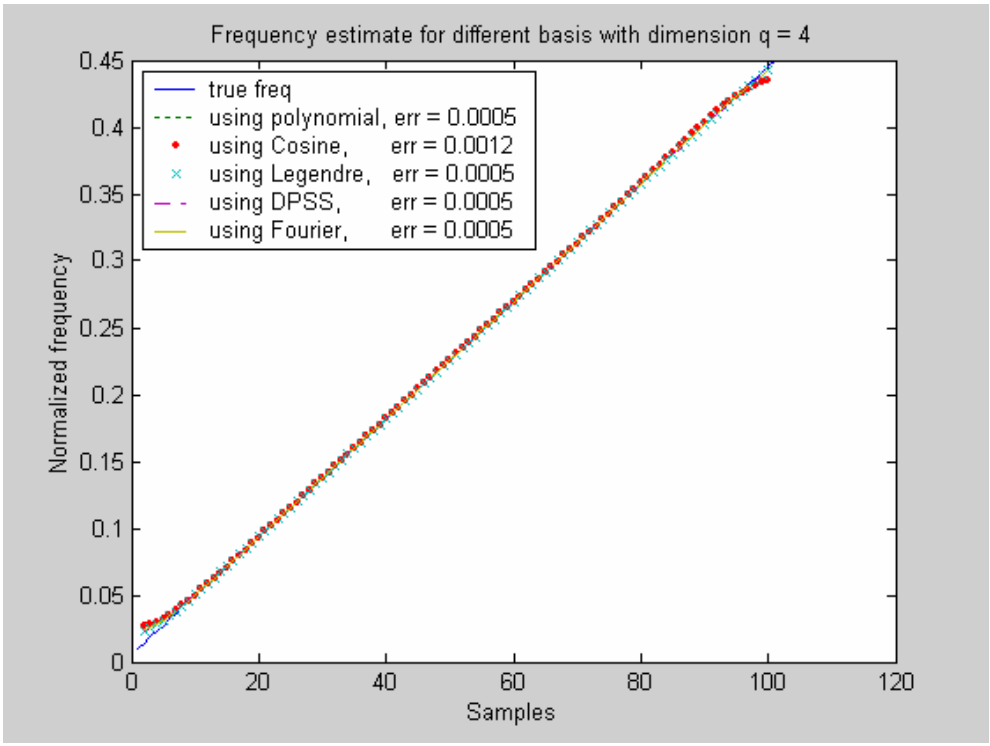

(b)

Figure 4.2: Frequency estimate of signal test 1

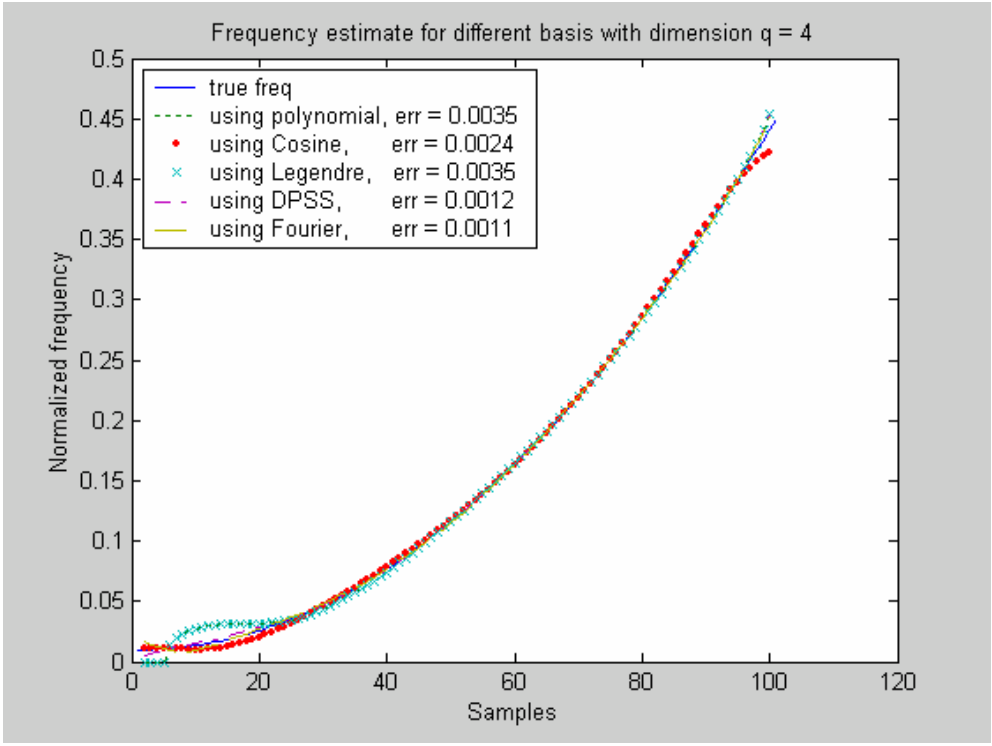

(a)

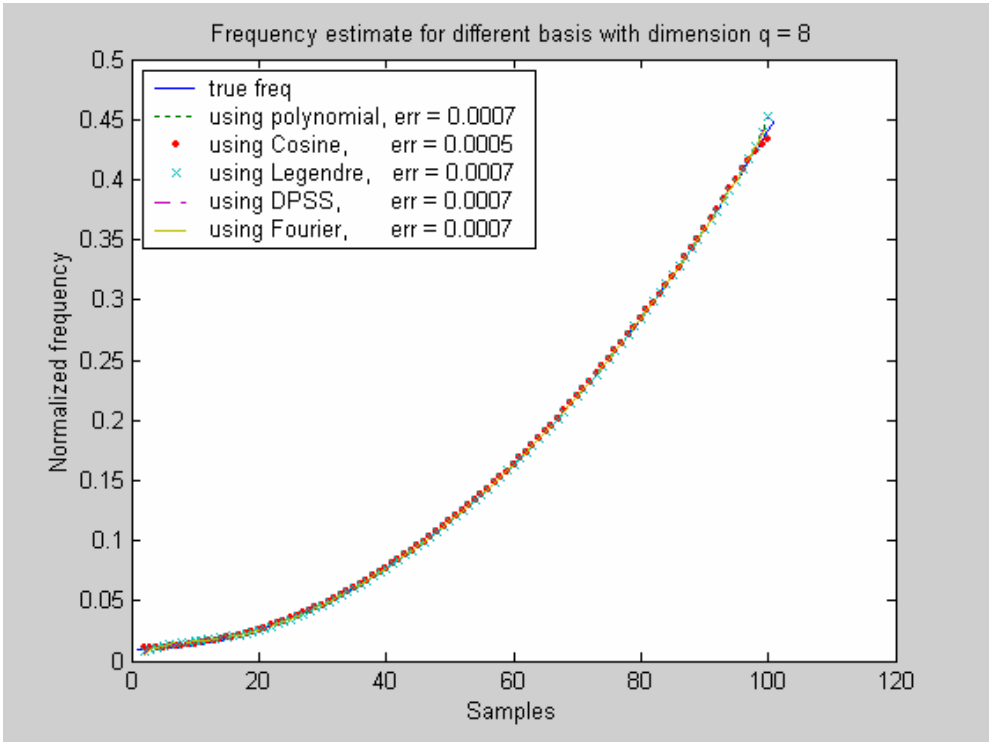

(b)

Figure 4.3: Frequency estimate of *signal test 2*

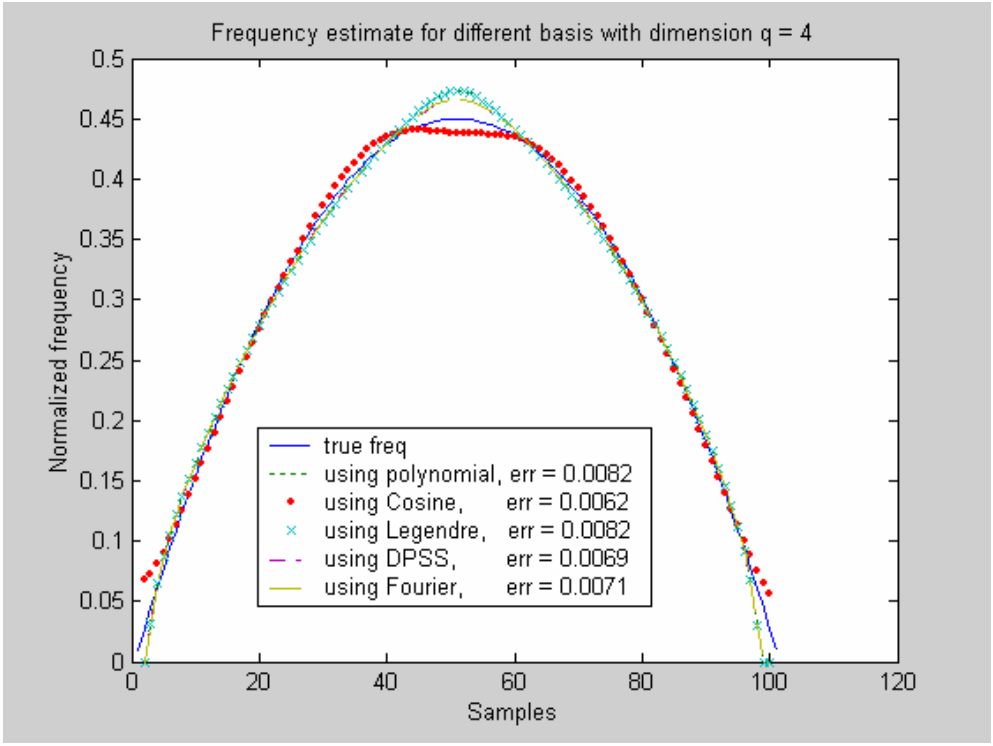

(a)

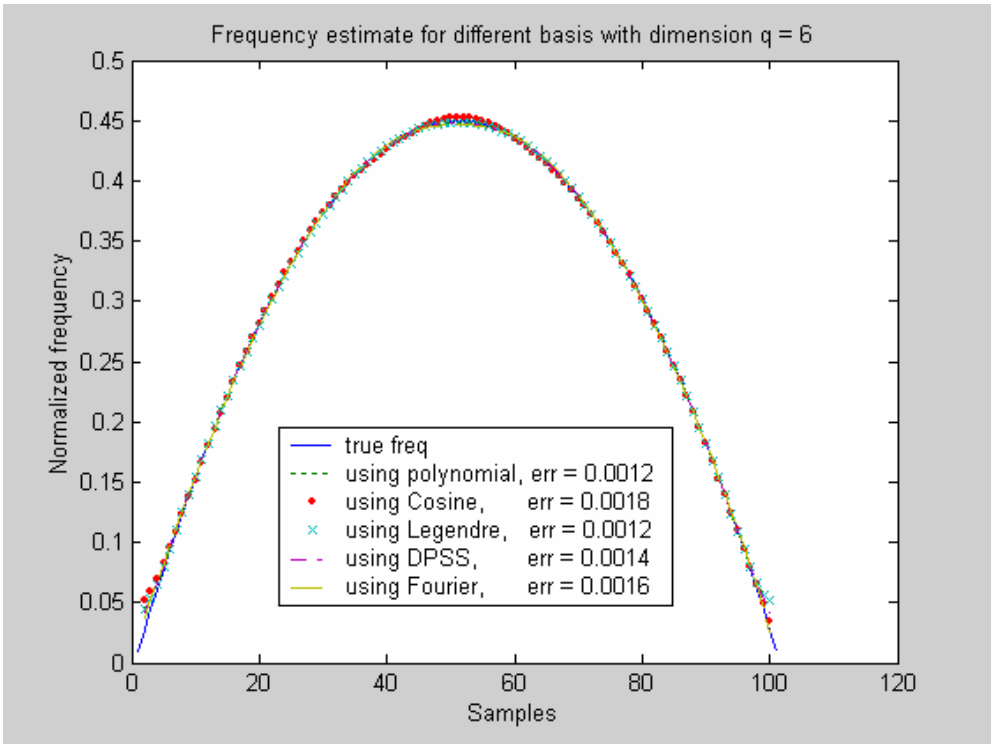

(b)

Figure 4.4 Frequency estimate of *signal test 3*

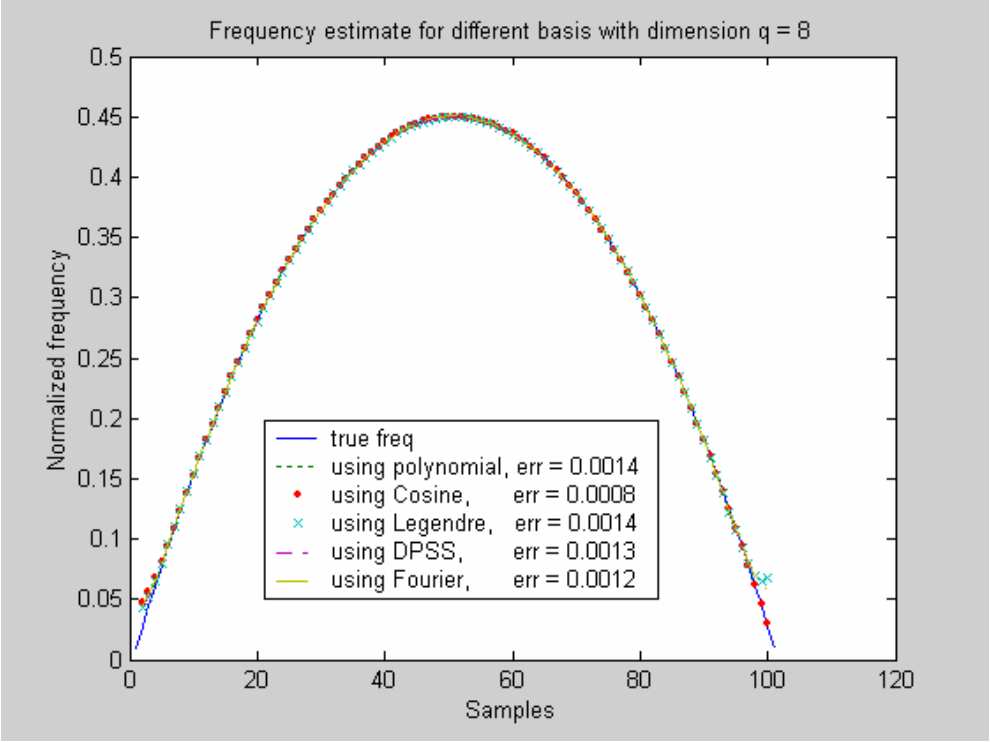

(c)

Figure 4.4: Frequency estimate of *signal test 3* (continued)

The result for *signal test 4* is shown in Figure 4.5. As noticed, none of the basis functions yields reasonable accuracy in frequency estimation of the signal test 4, when the expansion dimension is low, dimension $q < 8$. When the dimension is large, for example $q = 10$, 12 or higher, the Fourier function yields the best result in frequency estimation compared to that from the other functions. However, the difference decreases as q increases. Figure 4.6 displays the result for signal test 5 that has frequency discontinuity at the 60^{th} sample. As is seen, the expansion dimension must be equal to or higher than eight ($q \geq 8$) so that the frequency estimate is reasonably acceptable. For this signal test, the cosine function yielded the least error, but the Fourier and the DPSS functions are also not far behind in frequency estimation.

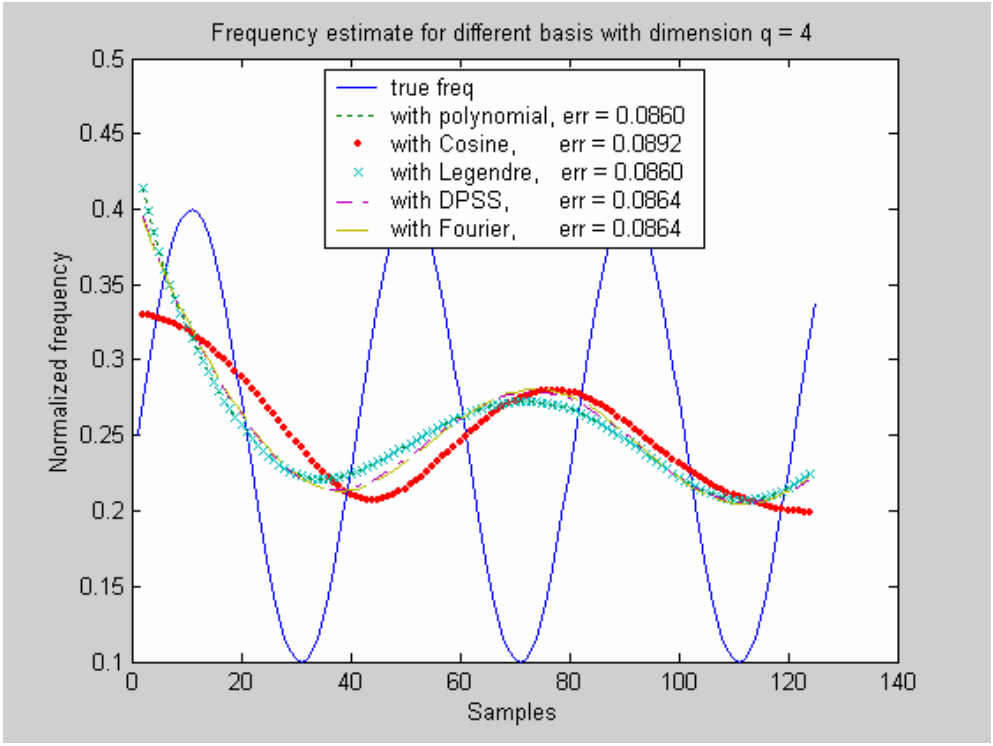

(a)

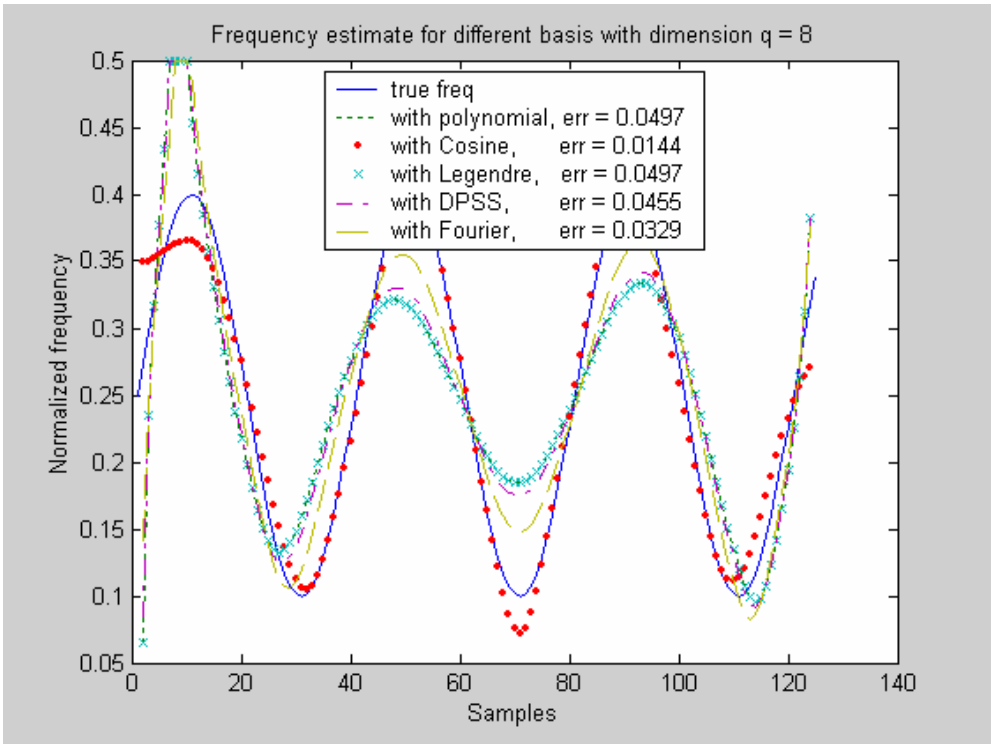

(b)

Figure 4.5: Frequency estimate of *signal test 4*

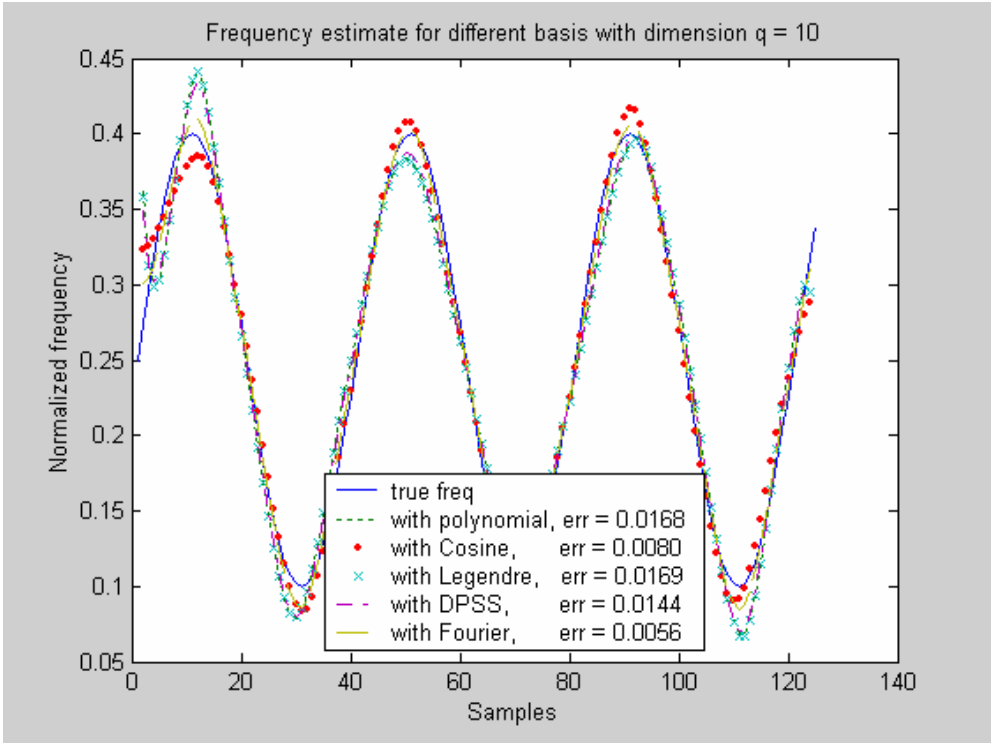

(c)

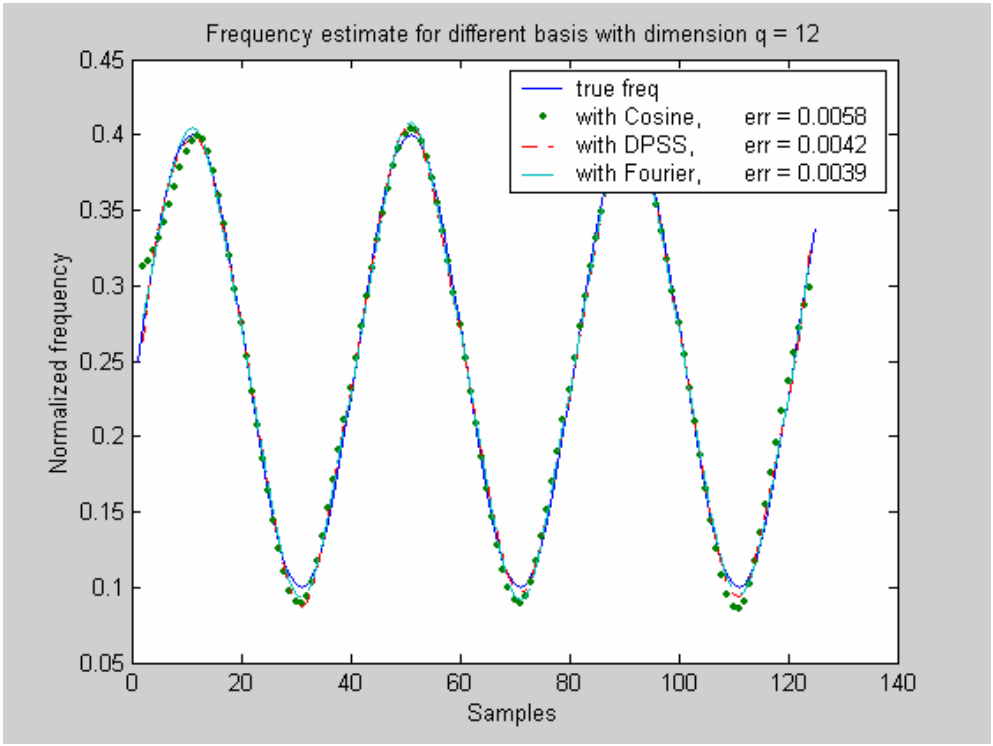

(d)

Figure 4.5: Frequency estimate of *signal test 4 (continued)*

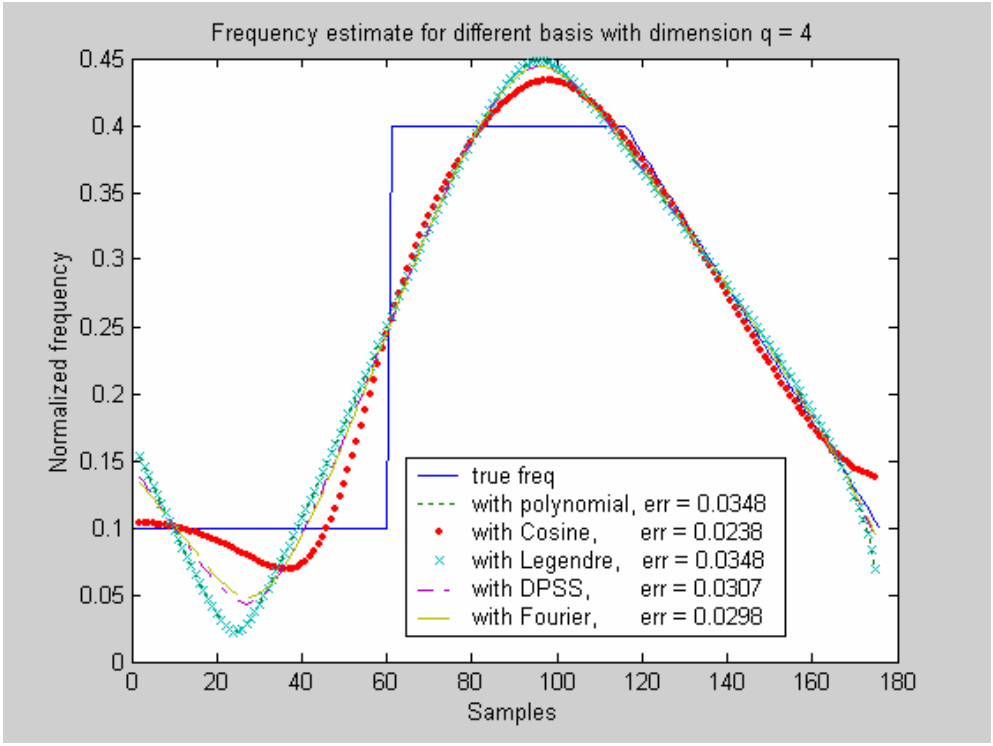

(a)

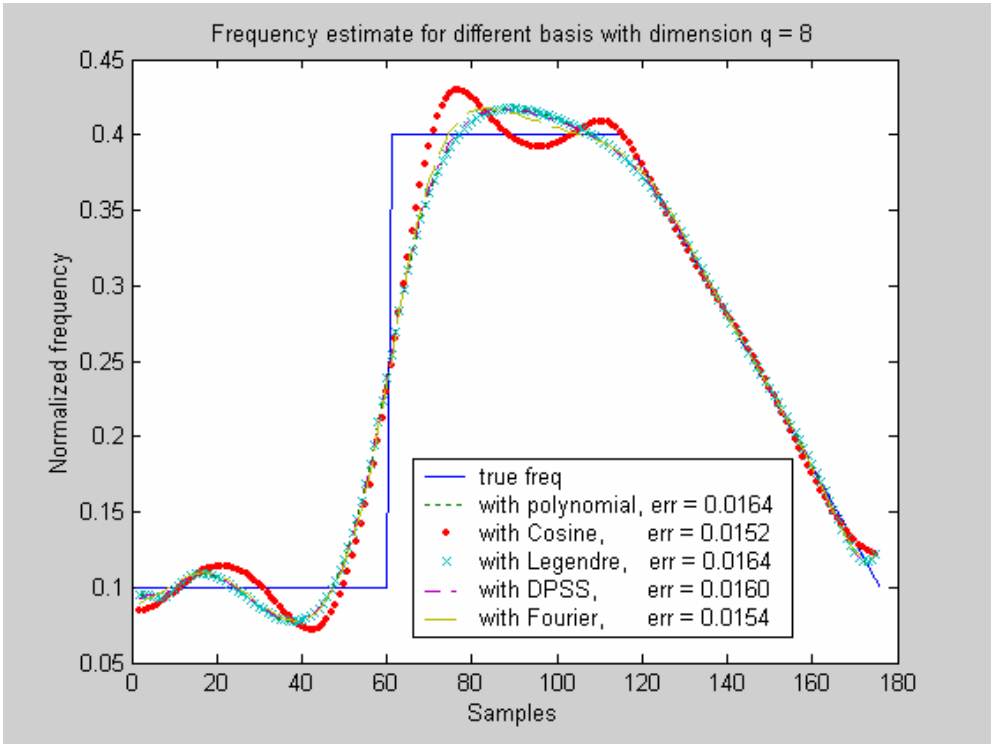

(b)

Figure 4.6: Frequency estimate of *signal test 5*

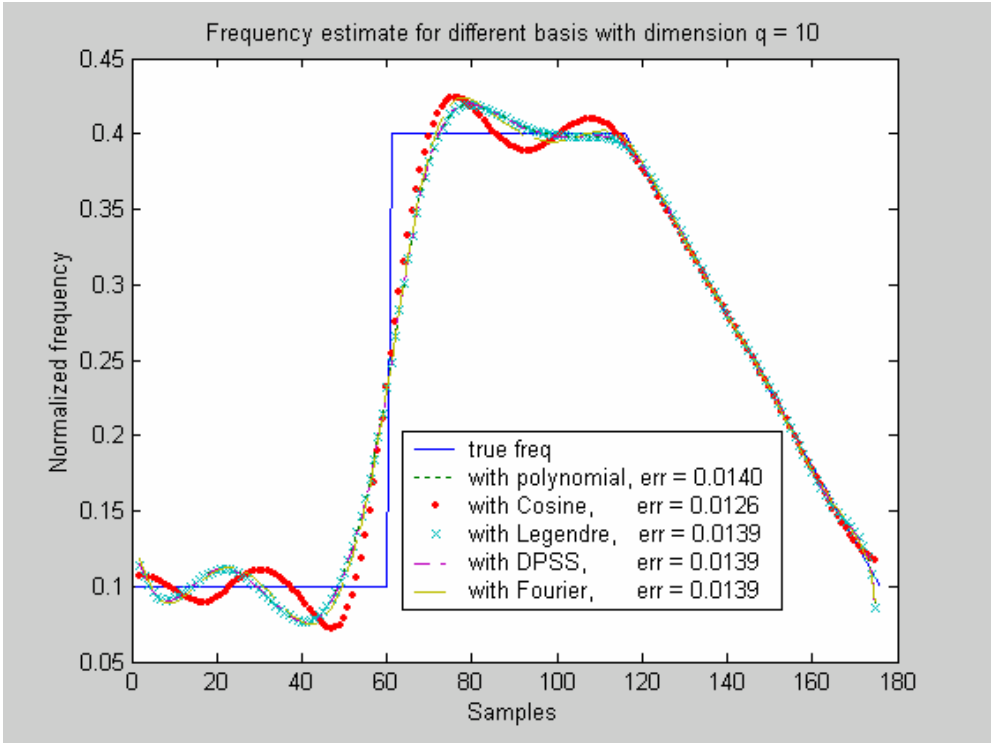

(c)

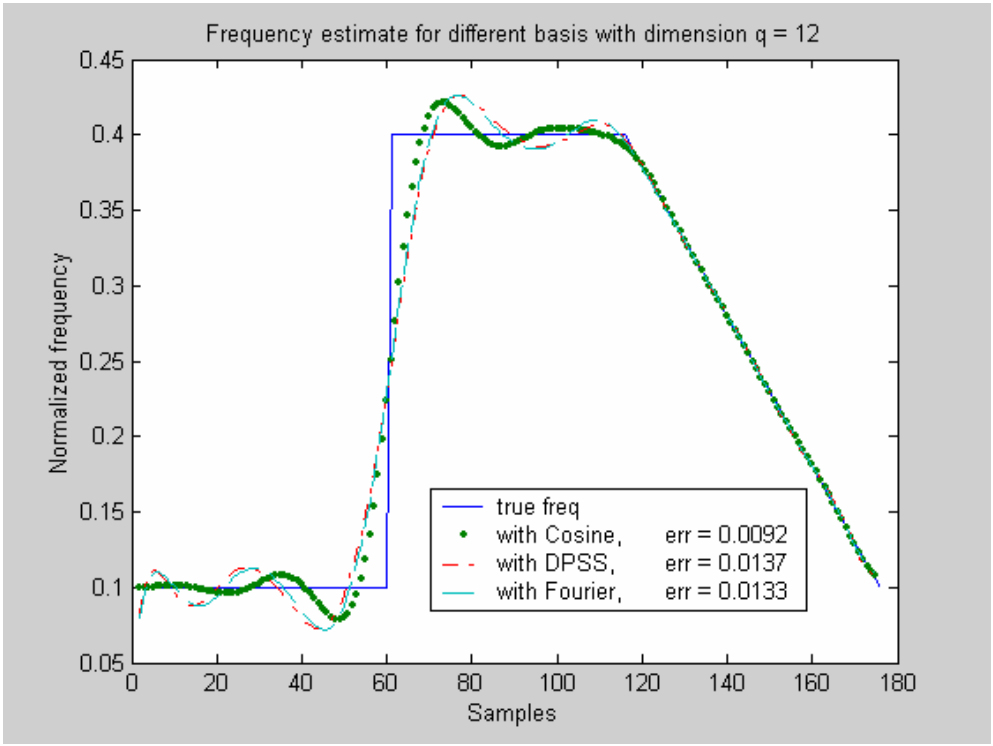

(d)

Figure 4.6: Frequency estimate of *signal test 5* (continued)

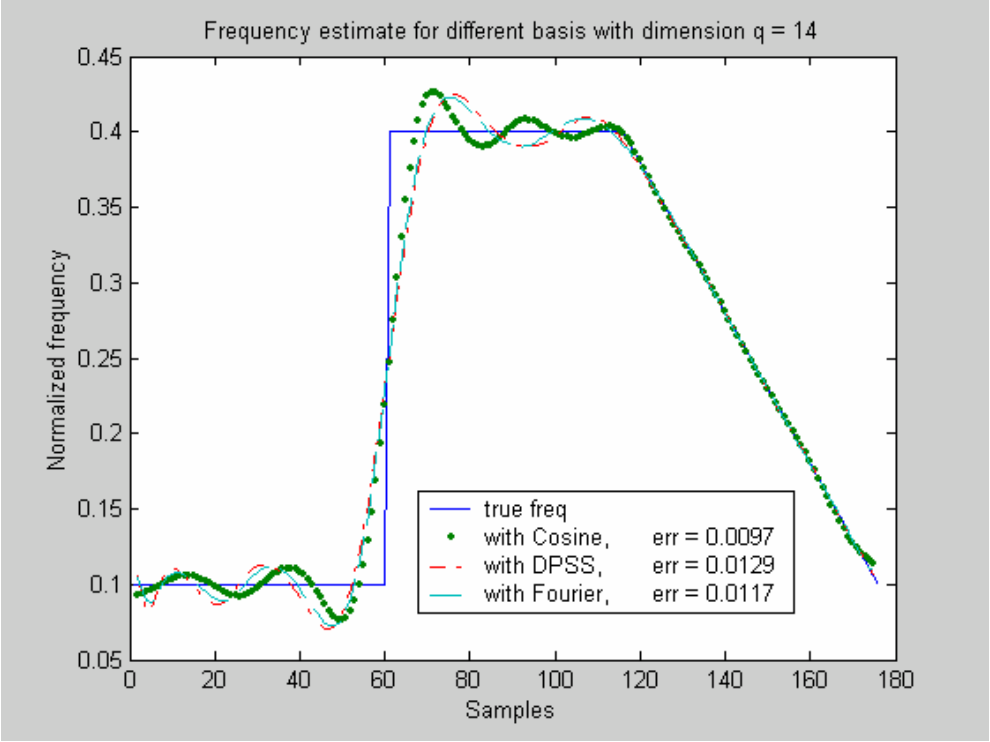

(e)

Figure 4.6: Frequency estimate of *signal test 5* (continued)

4.3 Discussion

We have tested 5 basis functions, and found that they yielded different estimation errors when low dimensions were used, except for the polynomial and the Legendre functions that always yielded exactly the same estimation errors. The difference in the estimation error for the different basis function decreases, when the basis dimension increases. This is logical because these time-functions are not equal or linearly related to each other (except the Polynomial and the Legendre function). So when they are used as a basis in a subspace, they cannot equally represent a signal in that subspace, especially for a low dimensional subspace. However, when the dimension of the subspace is high (q

is big), the difference in spanning the subspace for different functions decreases. This is because these functions may be approximate as a high-order summation of others. For example, the cosine or the Fourier function can be approximated as the m-term summation of the polynomial function for m is sufficiently large or infinite.

If two bases can span the same subspace, they will equally represent the same information of a signal. This was the case for the polynomial and the Legendre function that yield exactly the same frequency estimate and estimation error. The ability of the polynomial and the Legendre in spanning the same subspace can be observed from equations (4.1) and (4.2), stated as follows:

Let us consider a subspace in which the dimension is 4 (q = 3) and let the basis function $U_4^1(t) = \left\{1, \frac{t}{N}, \left(\frac{t}{N}\right)^2, \left(\frac{t}{N}\right)^3\right\}^T$ span the subspace $S_3(N)$ that is a 4 dimensional subspace of squared summable *N*-length sequence.

The Legendre function $U_4^2(t) = \left\{1, \frac{t}{N}, \frac{1}{2}\left(\left(\frac{t}{N}\right)^2 - 1\right), \frac{1}{2}\left(5\left(\frac{t}{N}\right)^3 - 3\frac{t}{N}\right)\right\}^T$ can be linearly related to $U_4^1(t)$ by the following equation:

$$U_4^2(t) = \begin{bmatrix} 1 & 0 & 0 & 0 \\ 0 & 1 & 0 & 0 \\ 0 & -1/2 & 1/2 & 0 \\ 0 & -3/2 & 0 & 5/2 \end{bmatrix} \cdot U_4^1(t)$$

Therefore, $U_4^2(t)$ and $U_4^1(t)$ span exactly the same subspace $S_3(N)$.

In fact, any two sets of the basis functions (*U* and *F*) that can relate to each other by *U*=A*F*, where A is a constant matrix, always give the same result in frequency estimation using our proposed approach. The proof of this is provided as follows, and similar to that in [Niedzwiecki, 2000] that shows that the estimated time-variant parameter is invariant to the different basis functions.

Proof:

First, we rewrite the proposed method in a different form. From equations (3.11) and (3.13)

$$\begin{aligned} e^f[t+1] &= y[t+1] + \sum_{i=1}^{p}\left(\sum_{k=0}^{q} a_{ik} f_k(t)\right) y[t-i+1] \\ &= \mathrm{y}[\mathrm{t}+1] + \vec{\psi}^T[t]\vec{\gamma} \end{aligned}$$

$$\begin{aligned} e^b[t-1] &= y[t-1] + \sum_{i=1}^{p}\left(\sum_{k=0}^{q} a_{ik} f_k(t)\right)^* y[t+i-1] \\ &= \mathrm{y}[\mathrm{t}\text{-}1] + \bar{\vec{\psi}}^T[t]\vec{\gamma}^* \end{aligned}$$

Where

$$\begin{aligned} \vec{\psi}^T[t] &= \left[\mathrm{y}[\mathrm{t}] \quad y[t-1] \quad \ldots \quad y[t-p+1]\right] \otimes \left[f_o(t) \quad f_1(t) \quad \ldots \quad f_q(t)\right] \\ &= \vec{\varphi}^T[t] \otimes \vec{f}^T(t) \end{aligned} \tag{4.5}$$

$$\begin{aligned} \bar{\vec{\psi}}^T[t] &= \left[\mathrm{y}[\mathrm{t}] \quad y[t+1] \quad \ldots \quad y[t+p-1]\right] \otimes \left[f_o(t) \quad f_1(t) \quad \ldots \quad f_q(t)\right]^* \\ &= \bar{\vec{\varphi}}^T[t] \otimes \vec{f}^{*T}(t) \end{aligned} \tag{4.6}$$

$$\vec{\gamma}^T = \left[\vec{a}_1^T \quad \vec{a}_2^T \quad \ldots \quad \vec{a}_p^T\right], \quad \vec{a}_i^T = \left[a_{i0} \quad a_{i1} \quad \ldots \quad a_{iq}\right]$$

and the mean squared error

$$\varepsilon \doteq \frac{1}{2}\left\{\sum_{t=p-1}^{T-1} |\, e^f[t+1]]^2 + \sum_{t=1}^{T-p+1} |\, e^b[t-1]\,|^2\right\}$$

$$= \frac{1}{2}\left\{ \sum_{t=p-1}^{T-1} |y[t+1] + \vec{\psi}^{T}[t]\vec{\gamma}\,|^2 + \sum_{t=1}^{T-p+1} |\, y[t-1] + \bar{\vec{\psi}}^{T}[t]\vec{\gamma}^{*}\,|^2 \right\}$$

Let $\hat{\vec{\gamma}}$ be the estimation of $\vec{\gamma}$. The $\hat{\vec{\gamma}}$ that minimizes ε can then be found equal to

$$\hat{\vec{\gamma}} = -\left(\sum_{t=p-1}^{T-1} \vec{\psi}^{*}[t]\vec{\psi}^{T}[t] + \sum_{t=1}^{T-p+1} \bar{\vec{\psi}}[t]\bar{\vec{\psi}}^{*T}[t] \right)^{-1} \left(\sum_{t=p-1}^{T-1} \vec{\psi}^{*}[t] y[t+1] + \sum_{t=0}^{T-p} \bar{\vec{\psi}}[t] y^{*}[t-1] \right) \qquad (4.7)$$

Hence, the TVAR parameter estimates $\hat{\vec{a}}[t]$ are

$$\hat{\vec{a}}[t] = \begin{bmatrix} \hat{a}_1[t] \\ \hat{a}_2[t] \\ \vdots \\ \hat{a}_p[t] \end{bmatrix} = \left(I_{pxp} \otimes \vec{f}^{T}(t) \right) \cdot \hat{\vec{\gamma}} = Z(t) \cdot \hat{\vec{\gamma}}$$

Where $\otimes$ represent Kronecker Products, and I_{pxp} is an identity matrix, of *pxp* size.

Note that in the derivation for the TVAR parameter $\hat{\vec{a}}[t]$ as above, a property of the Kronecker Products [Graham, 1981] was used. Some properties of the Kronecker products are summarized in the appendix.

Next, we show that for the proposed approach, two basic functions spanning the same subspace yielded the same TVAR parameter estimate and hence the frequency estimate. Let $\hat{\vec{a}}[t]$ be the parameter estimates as $\hat{\vec{a}}[t] = Z(t) \cdot \hat{\vec{\gamma}}$ from using the basic function $\vec{f}(t)$. Let another basic function $\vec{u}(t)$ span the same subspace with $\vec{f}(t)$, that is $\vec{u}(t) = \mathrm{A}\,\vec{f}(t)$. Similar to the equation (4.7), if $\tilde{\vec{\gamma}}$ is the minimizer of the least square error from using the $\vec{u}(t)$ basic function,

$$\tilde{\vec{\gamma}} = -\left(\sum_{t=p-1}^{T-1} \vec{\psi}_u{}^{*}[t]\vec{\psi}_u{}^{T}[t] + \sum_{t=1}^{T-p+1} \bar{\vec{\psi}}_u[t]\bar{\vec{\psi}}_u{}^{*T}[t] \right)^{-1} \left(\sum_{t=p}^{T} \vec{\psi}_u{}^{*}[t] y[t+1] + \sum_{t=0}^{T-p} \bar{\vec{\psi}}_u[t] y^{*}[t-1] \right)$$

Since

$$\vec{\psi}_u[t] = \varphi[t] \otimes \vec{u}(t) = \varphi[t] \otimes \mathrm{A}\vec{f}(t) = I_{pxp}\varphi[t] \otimes \mathrm{A}\vec{f}(t) = (I_{pxp} \otimes \mathrm{A})(\varphi[t] \otimes \vec{f}(t))$$
$$= \Xi\vec{\psi}(t) \quad \text{, where } \Xi = I_{pxp} \otimes \mathrm{A}$$

Similarly, $\vec{\bar{\psi}}_u[t] = \Xi\vec{\bar{\psi}}(t)$, and

$$\vec{\tilde{\gamma}} = -\left(\sum_{t=p-1}^{T-1} \Xi \cdot \vec{\psi}^*[t]\vec{\psi}^T[t] \cdot \Xi^T + \sum_{t=1}^{T-p+1} \Xi \cdot \vec{\bar{\psi}}[t]\vec{\bar{\psi}}^{*T}[t] \cdot \Xi^T \right)^{-1} \left(\sum_{t=p-1}^{T-1} \Xi \cdot \vec{\psi}^*[t]y[t] + \sum_{t=1}^{T-p+1} \Xi \cdot \vec{\bar{\psi}}[t]y^*[t] \right)$$
$$= -(\Xi^T)^{-1} \left(\sum_{t=p-1}^{T-1} \vec{\psi}^*[t]\vec{\psi}^T[t] + \sum_{t=1}^{T-p+1} \vec{\bar{\psi}}[t]\vec{\bar{\psi}}^{*T}[t] \right)^{-1} \left(\sum_{t=p-1}^{T-1} \vec{\psi}^*[t]y[t+1] + \sum_{t=1}^{T-p+1} \vec{\bar{\psi}}[t]y^*[t-1] \right)$$
$$= (\Xi^T)^{-1}\hat{\vec{\gamma}}$$

Therefore

$$\tilde{\vec{a}}[t] = \left(I_{pxp} \otimes \vec{u}^T(t)\right) \cdot \vec{\tilde{\gamma}} = \left(I_{pxp} \otimes \left(\mathrm{A}\vec{f}(t)\right)^T\right) \cdot \left(\Xi^T\right)^{-1}\hat{\vec{\gamma}}$$
$$= \left(I_{pxp} \otimes \vec{f}^T(t)\mathrm{A}^T\right) \cdot \left(I_{pxp} \otimes A^T\right)^{-1}\hat{\vec{\gamma}}$$
$$= \left(I_{pxp} \otimes \vec{f}^T(t)\right)\left(\mathrm{A}^T A^{-T}\right)\hat{\vec{\gamma}}$$
$$= \left(I_{pxp} \otimes \vec{f}^T(t)\right)\hat{\vec{\gamma}}$$
$$= \hat{\vec{a}}[t]$$

Since $\hat{\vec{a}}[t] = \tilde{\vec{a}}[t]$ and the time-varying frequencies are extracted from these time-variant parameters, the frequency estimates from these two sets of basis functions, which equally span the same subspace are exactly the same.

4.4 Chapter summary

Table 4.1 is a summary of the results from our tests. It is obvious that we cannot decisively select the best single basis function that is suitable for all signal tests. It is more or less dependent on the characteristics of signals. If the signal is a chirp or has a

frequency that varies linearly, all the five basis functions are suitable as the basis for the parameter expansion. If the signal has a frequency that varies periodically, the Fourier and cosine the function are the best fits. However, in general, if the characteristics of the real signals were not known, we recommend the Fourier function as the basis expansion of the TVAR parameters, since the Fourier function yielded reasonable accuracy in the frequency estimation for all five nonstationary signals. We also recommend that the dimension $q \sim 10$ or 12 should be used with the Fourier function.

Table 4.1: Summary of the best functions and the suitable dimensions that yield the least error for each signal test.

	Suitable dimension q*	Best Basis function
Signal test 1	4	Any, except cosine function**
Signal test 2	8	Any
Signal test 3	8	Cosine and Fourier
Signal test 4	12	Fourier
Signal test 5	12	Cosine and Fourier

Remark: *Dimension was considered suitable in that it is the smallest, but yields approximately the least error in frequency estimation (i.e. increasing q higher than this number would not yield much difference in estimation error).

** This is only for the dimension $q = 4$. For $q > 4$, all functions (include cosine function) were equally good in estimating the time-varying frequency of signal test 1.

CHAPTER 5

Limitations of the Modified Basis Function Method

The proposed method, the modified basis function approach was shown to improve the frequency estimation, especially when the model order was over-determined. However, there were some conditions and limitations in using the proposed method for estimating the time-varying frequency or the spectrum of non-stationary signals. The conditions and limitations are stated below. Note that the Fourier basis function and an expansion dimension of q =12 are used.

1. Signals must be free from direct component (DC component).

This limitation is due to the fact that in a linear system, the autoregressive parameters represent only the oscillating characteristics of the system. Since the proposed method employs the autoregressive model, whose parameters are allowed to vary with time, it could not correctly represent a signal that contains a DC component. Therefore, the proposed approach may fail to estimate the time-varying frequency of the non-stationary signal, if the signal has a large DC component. Figure 5.1 shows the frequency estimate of a chirp signal in a noise-free environment by using the proposed approach when the signal has a DC and no DC components.

In general, signals may have a DC component. A removal of this DC component is a must. This can be accomplished by using a high pass filter for pre-processing the signal before applying the proposed method.

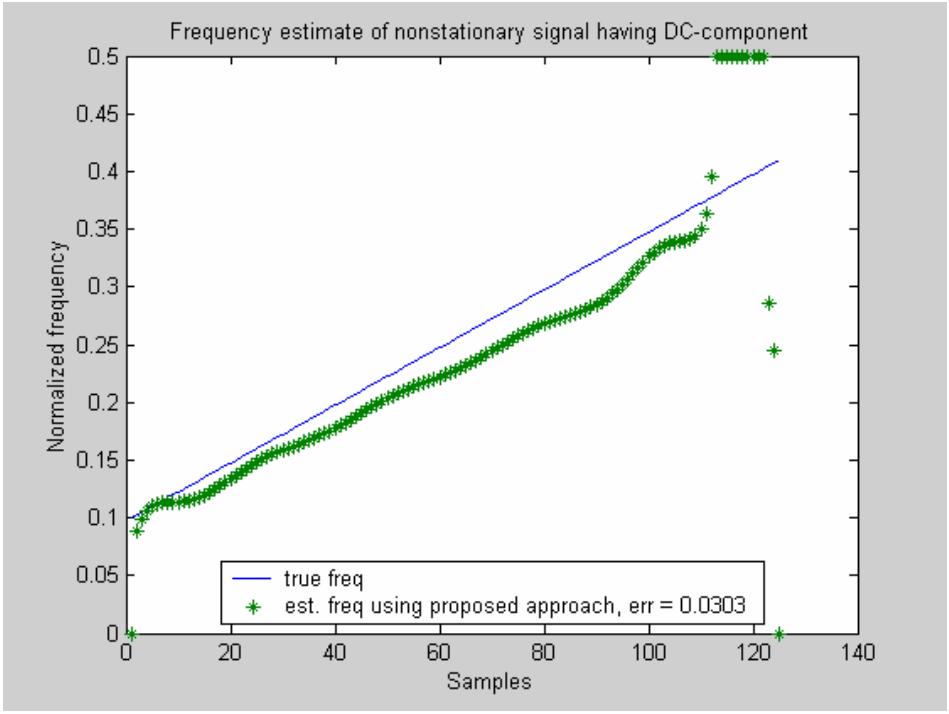

(a)

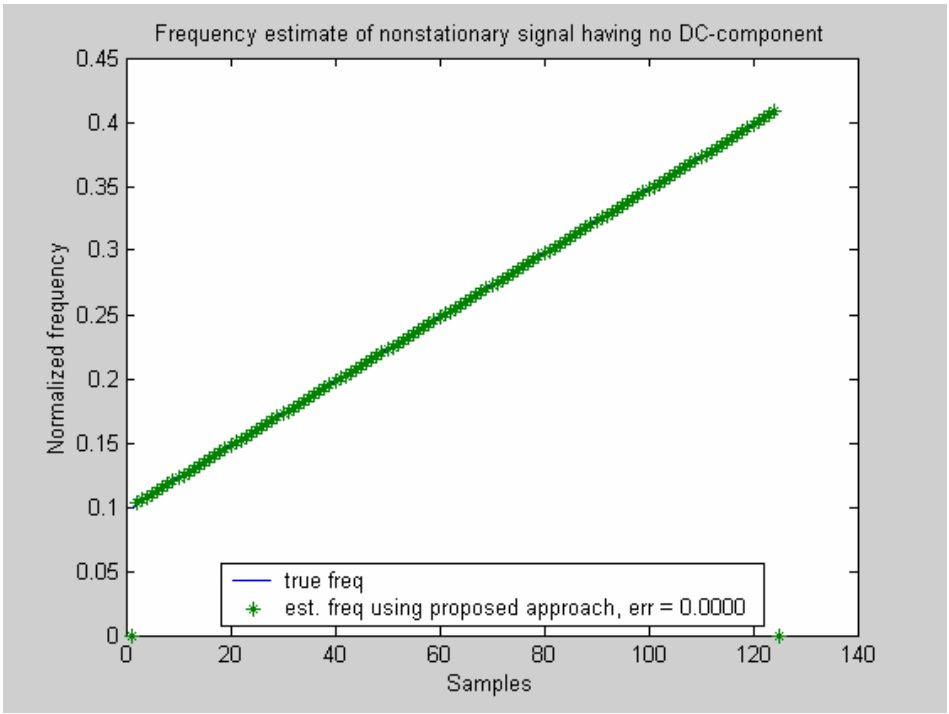

(b)

Figure 5.1: Frequency estimate of a chirp signal, $x = \cos(0.01\pi t^2 + 0.002\pi t) + 0.3$ having a DC component (a), and signal $x = \cos(0.01\pi t^2 + 0.002\pi t)$ having no DC component (b) and sampling rate Fs = 4Hz.

2. The model order p must be determined, if it is not pre-known.

When the number of the time-varying component is unknown, the determination of the model order is necessary, especially when the signal is clean or of a very low noise (SNR >20 dB). This is because when the signal is noise-free or of very low noise and the high order is used, the matrix **C** in equation (3.17) may becomes nearly a singular matrix, and then its inversion becomes invalid. Even when the inversion of **C** is valid, the high model order might cause a spurious in the time-varying spectral estimation. For noisy signals that have SNR ≤ 20 dB, the determination of the TVAR model order is less required, because the bigger the model order that is used, the better the time-varying spectral estimates that are obtained. This was already observed and mentioned in Chapter 3. However, right model order is also needed for the noisy signal, because if the model order is too high, spurious may occurs.

Few available approaches in the selection of the TVAR model order are available. For example, the Akaike information criterion [Kozin and Nakajima, 1980], the Baysian approach [Rajan and Rayner, 1996], and the maximum likelihood estimation [Eom, 1999] are utilized for the calculation of the model order in the TVAR model. The details of these methods are directed to those papers, respectively. Described below is the maximum likelihood method for the determination of the TVAR model order [Eom, 1999], summarized in the following, where the vector $\vec{c}$ in the estimation is modified to comply with our proposed method.

Step-1: Calculate $\vec{z}[t] = \vec{\varphi}[t-1] \otimes \vec{f}(t)$, $\vec{\bar{z}}[t] = \vec{\bar{\varphi}}[t+1] \otimes \vec{f}(t)$ where vector $\vec{f}[t]$, $\vec{\varphi}[t]$, and $\vec{\bar{\varphi}}[t]$ are defined below, and $\otimes$ is the Kronecker multiplication defined in Appendix A-2.

$$\vec{\varphi}^T[t] = \begin{bmatrix} y[t] & y[t-1] & \dots & y[t+p-1] \end{bmatrix}$$
$$\vec{\bar{\varphi}}^T[t] = \begin{bmatrix} \mathrm{y[t]} & y[t+1] & \dots & y[t+p-1] \end{bmatrix}$$
$$\vec{f}^T[t] = \begin{bmatrix} f_o[t] & f_1[t] & \dots & f_q[t] \end{bmatrix}$$

Step-2: Compute $\vec{c} = -\left(\sum_{t=p}^{T} \vec{z}[t]\vec{z}^T[t] + \sum_{t=0}^{T-p} \vec{\bar{z}}[t]\vec{\bar{z}}^T[t] \right)^{-1} \left(\sum_{t=p}^{T} \vec{\psi}[t]y[t] + \sum_{t=0}^{T-p} \vec{\bar{\psi}}[t]y[t] \right)$.

Step-3: Estimate $\hat{\beta} = \frac{1}{N} \sum_{t=0}^{T} \left[y[t] - \vec{c}^T \vec{z}[t] \right]^2$.

Step-4: Obtain the cost function

$$J(p,q) = \frac{p(q+1) + 2 - N}{2} \log(2\pi\hat{\beta}) - \frac{1}{2} \log\left(\left| \sum_{t=0}^{T} \vec{z}[t]\vec{z}^T[t] \right| \right).$$

Step-5: Choose the model order $p=p_{opt}$ and the expansion dimension $q=q_{opt}$ that maximize the cost function $J(p,q)$, where $p_{opt} \in \{2,4,...,p_{\max}\}$ and $q_{opt} \in \{0,1,...,q_{\max}\}$.

Note that this calculation consumes a lot of processing time, if p_{max} and q_{max} are set too high. However the results in Chapter 4 showed that the Fourier function was overall the best as a basis function with the expansion dimension of q~10 or ~12. When the Fourier function is used and the dimension is fixed at q=12, the computational expense for the model selection can be reduced.

3. The length N of recorded signal must satisfy $pq \leq 0.2N$.

This limitation on the length resulted from the parsimony principle • being the rule of the thumb suggested in [Niedzwiecki, 2000]. For a signal that consists of a single time-frequency component, the rule of the thumb $pq \leq 0.2N$, where N is the length of the recorded signal, can be used. For the signal that has multiple time-frequency components, the condition $pq << N$ should be used. Figure 5.2 and figure 5.3 show time-varying spectral estimates of nonstationary signals in a noise-free and noisy (20 dB SNR) situations. This signal has two chirp frequency components that vary linearly and close to each other (0.01Fs). Figure 5.4 shows the spectral estimate of another nonstationary signal that consists of two frequency components varying nonlinearly with time and only 0.01Fs apart from each other. The $pq << N$ were satisfied in the calculation. In the noise-free case, we used the exact model order $p = 4$ in the spectral estimation, but in a noisy-situation a very high model order ($p = 16$) has to be used. As seen, a high frequency-resolution for the time-varying spectral estimation is yielded by using the proposed approach, either in a noise-free or 20 dB noisy case. Note that although the resolution of the spectral estimate in Figure 5.4 (b) is not so good compared to another in a noisy case such as that in figure 5.3, its resolution could be better, if a longer length and higher model order were utilized. However, increasing the length and the model order would consume large computation time.

• see a foot note in Chapter 3 for some detail

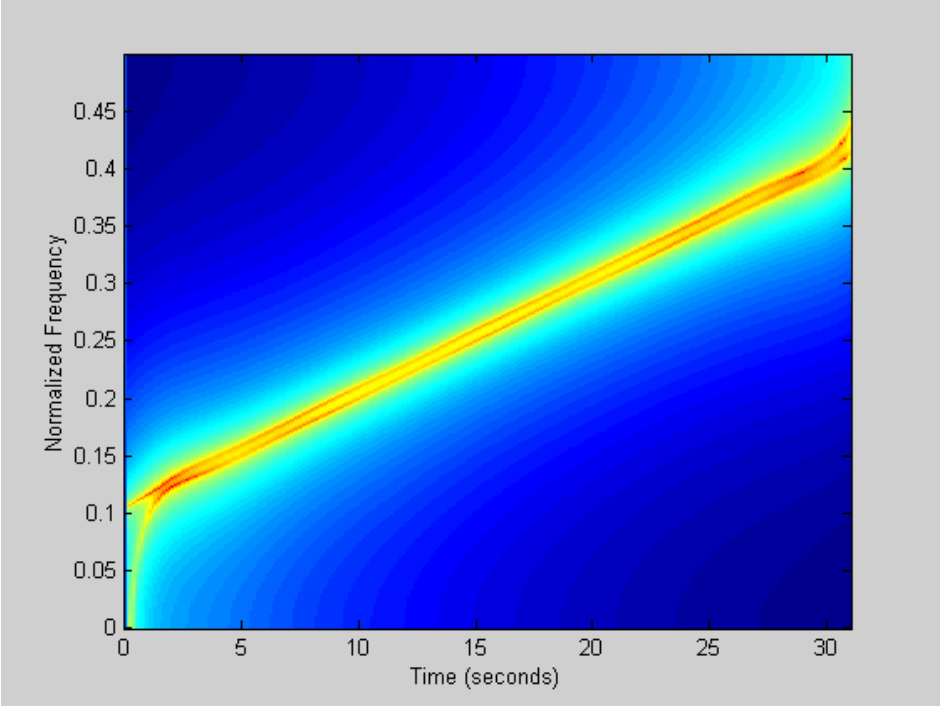

(a) use $p = 4$, sampling rate Fs = 25Hz

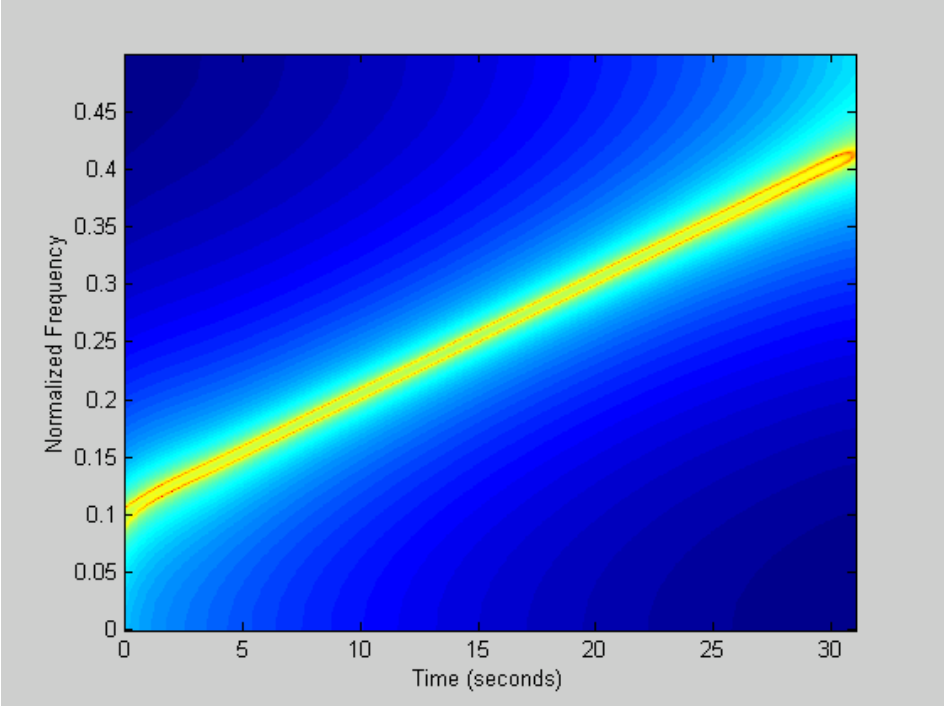

(b) use $p = 4$, sampling rate Fs = 50Hz.

Figure 5.2: Spectral estimate of the noise-free signal 1, having two chirp components close to each other, a) when the signal length is 776 samples, and b) when the signal length is 1551 samples

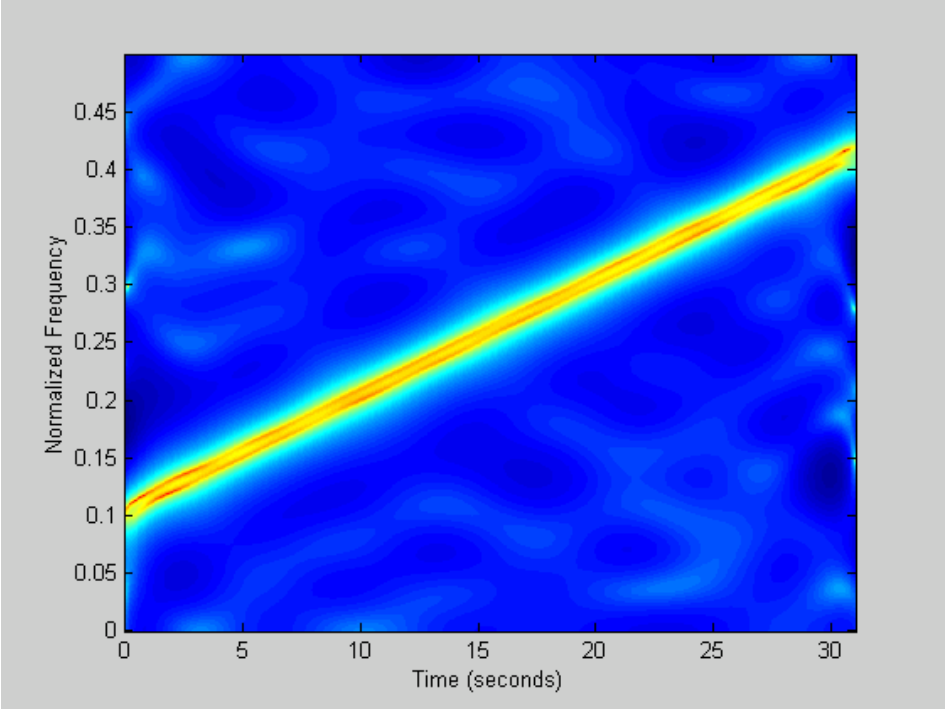

(b) from noisy signal, use p = 16, Fs = 50Hz.

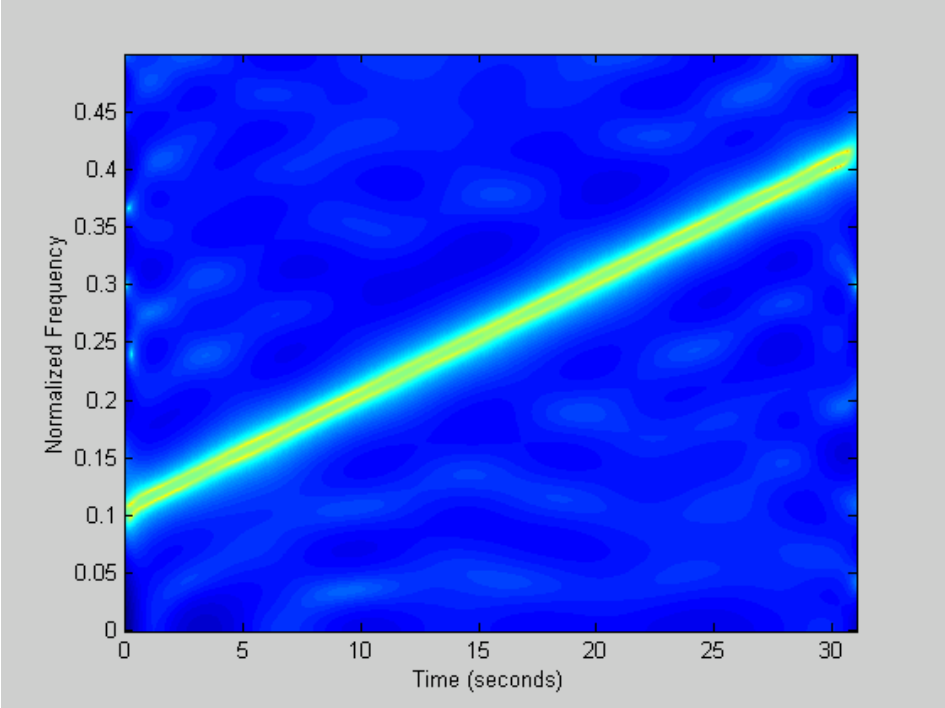

(c) from noisy signal 1, use p = 16, Fs = 80Hz.

Figure 5.3: Spectral estimates of the noisy signal, having 2 chirp components close to each other, (a) for signal length equal to1151 samples, and (b) for signal length equal to 2481 samples.

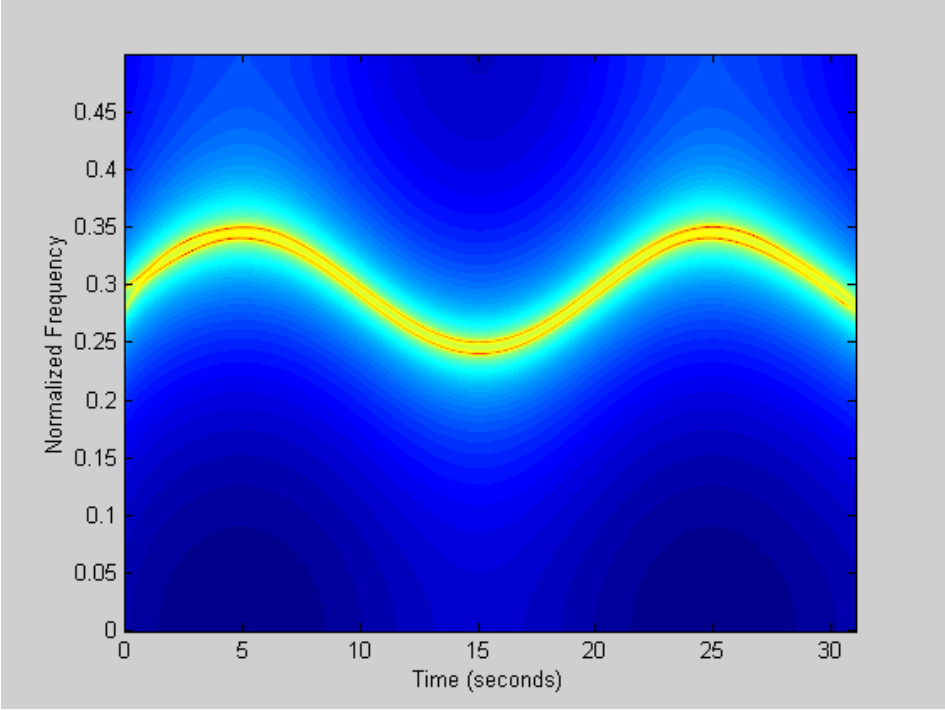

(a) noise-free, use p = 4, Fs = 50.

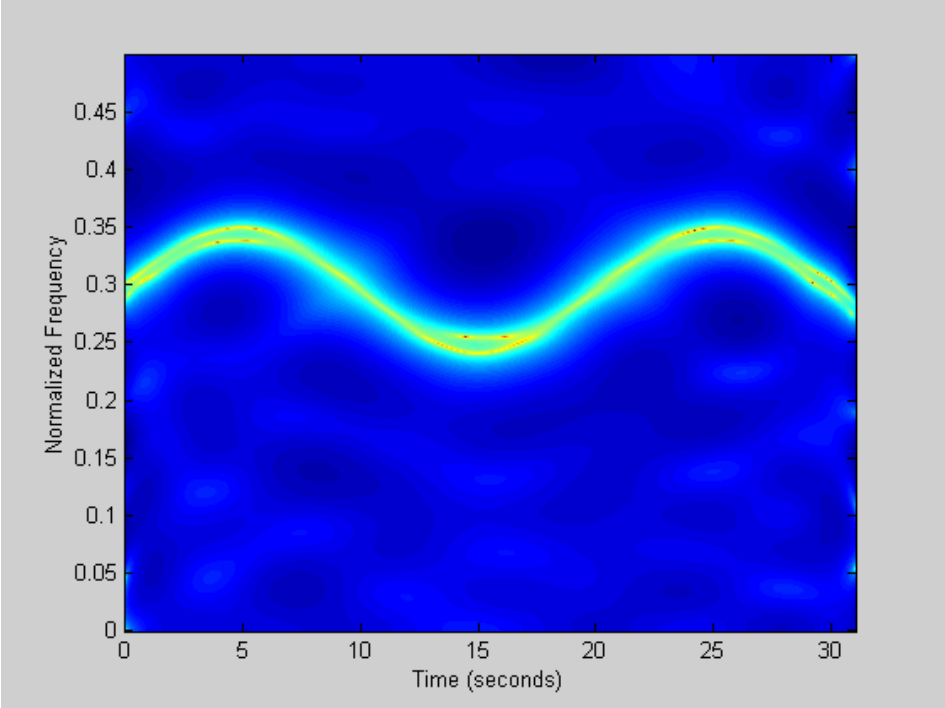

(b) noisy , use p = 16, Fs = 80.

Figure 5.4 Time-varying spectral estimates of a nonstationary signal that consists of two nonlinear time-frequency components close to each other, for (a) noise-free and (b) noisy environments.

4. Jeopardy from the spectral estimation at the location of the spectral crossing.

While the proposed approach is capable of providing high frequency resolution, the estimation of the time-varying frequency at the location of the spectral crossing between the time-frequency components may not be accurate. Figure 5.5 displays the spectral estimate of a non-stationary signal that has two time-frequency components crossing each other. One frequency component is chirp like, and the other frequency component varies periodically. As seen, the spectral lines are discontinuous and mis-tracked at some intersections in either noise-free or noisy situations. Notice that in the noisy case, where the high model order was used, there are some spurious peaks located at the beginning and the ending of the signal length, seen in figures 5.5 (c).

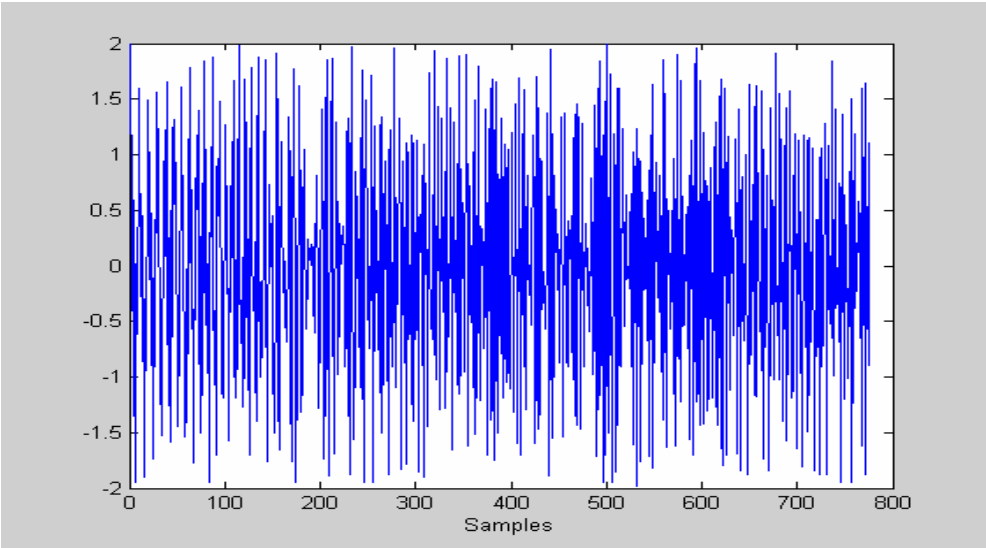

(a) A non-stationary signal that has crossing time-frequency components

Figure 5.5 Spectral estimate of the nonstationary signal (a) having two time-varying frequency components that cross each other at some locations, in noise-free (b) and 20dB-SNR noisy (c) environment.

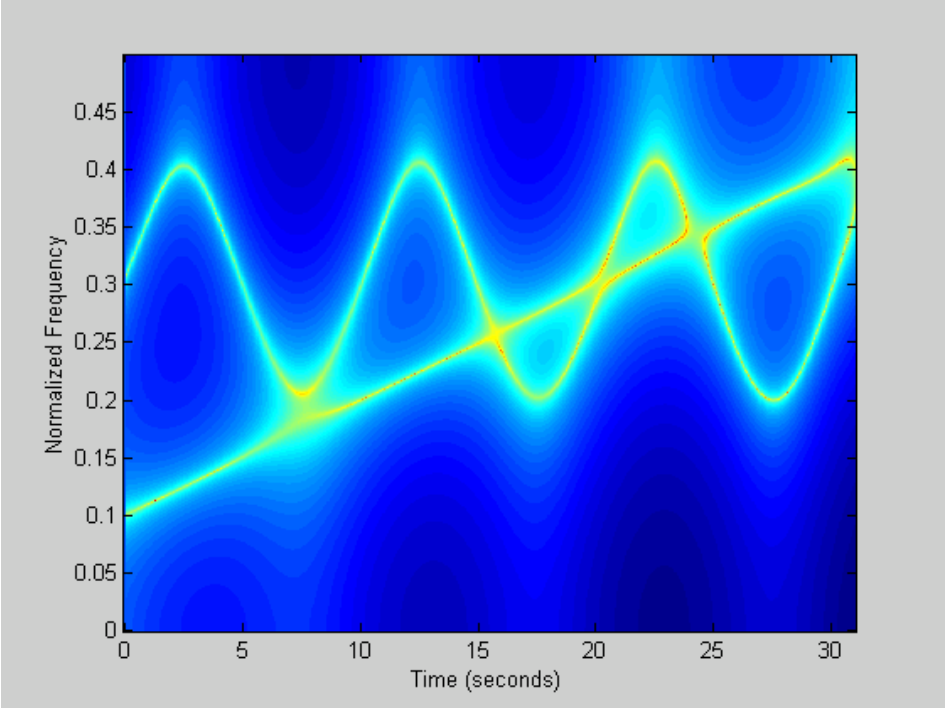

(b) Noise-free case, use p = 4, Fs =25Hz

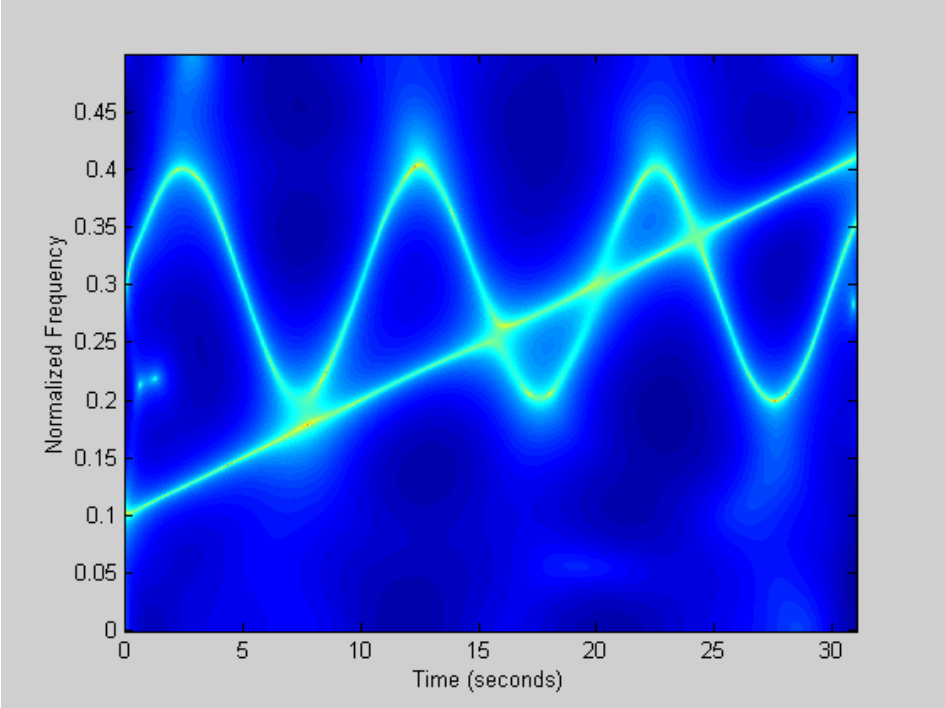

(c) Noisy case, use p = 12, Fs = 50

Figure 5.5 Spectral estimate of the nonstationary signal (a) having two time-varying frequency components that cross each other at some locations, in noise-free (b) and 20dB-SNR noisy (c) environment. (Continued)

Despite all these limitations, two important advantages of the proposed approach are desirable. First, the resolution can be very high. Second, compared to the WVD, we do not need to be concerned about the artifact or the cross term between two or more frequency components. The cross terms between the frequency components, or the interaction between negative and positive frequency components of a real signal are undesirable. Figure 5.6 shows the cross term of the positive and the negative frequency components of the real signal that was used in figure 5.1(b). As seen, the Wigner-Ville distribution has a high resolution, but suffered from the cross-term. The Choi-Willams distribution is able to get rid of the cross term, but it comes with the price of a less resolution.

Chapter summary

Although the proposed method does improve the accuracy in the frequency estimation, several limitations are mentioned in this chapter. Some limitations include a requirement that the signal has no DC-component, a signal length that should not be shorter than $p \cdot q / 0.2$, and the number of the time-frequency components that, if unknown, must be estimated. In the noisy case, the big order of the TVAR model can be used, since the high order of the TVAR model can suitably represent the signal with an additive white noise (proof in appendix). However, if the model order is too high, spurious peaks occur. Furthermore, at locations where there are intersections between the time-frequency components, the proposed approach may not be able to track the frequencies. Reasons for this inability at the intersection are unclear, but a similar result was also observed in Figure 3 in Eom [1999].

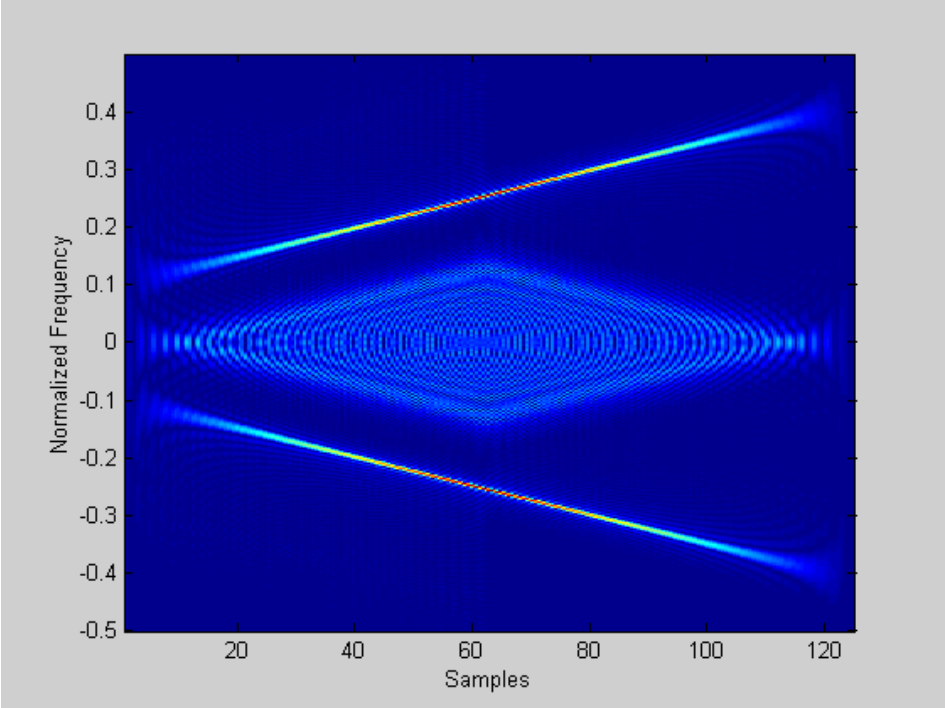

(a) The Wigner-Ville distribution

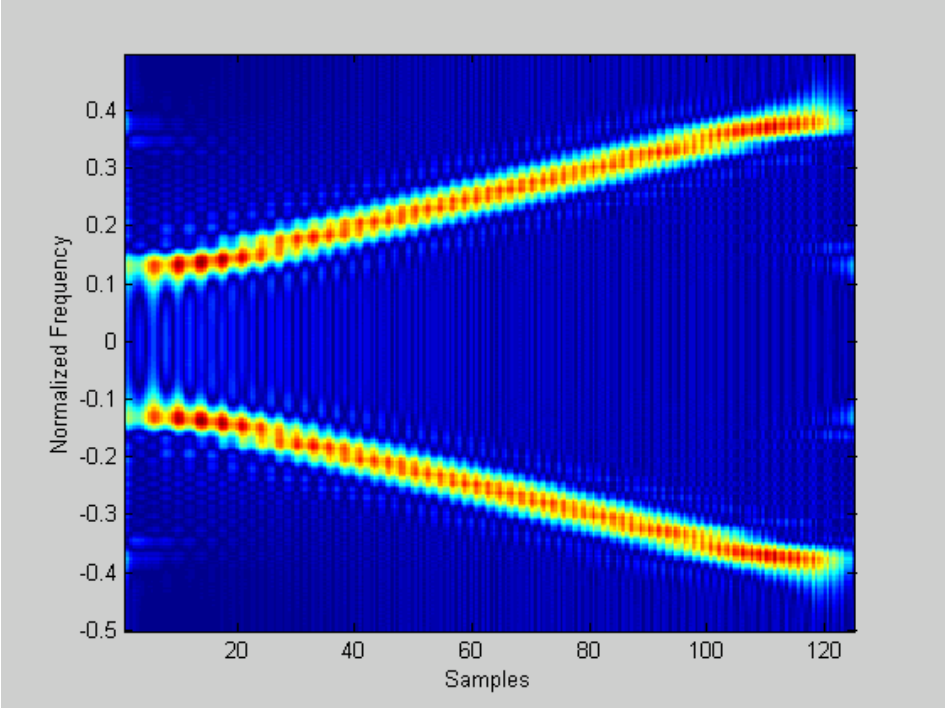

(b) The Choi-Williams distribution

Figure 5.6: Time-frequency distribution of a signal used in fig 5.1-b, by using the Wigner-Ville distribution (a), the Choi-Williams (b).

CHAPTER 6

Demonstration: The Time-Varying Spectral of a Violin Vibrato

This chapter demonstrates the use of the proposed approach (proposed approach 2 in chapter 3) to analyze the time-varying spectrum of a nonstationary acoustic signal. The violin vibrato is used as an example.

6.1 Introduction

Vibrato is a tonal effect in music where one or more characteristics of a sound is repeatedly or periodically raised and lowered over a range for the duration of that sound. The vibrato is used to refer to the frequency modulation and the term *tremolo* is used to refer to the amplitude modulation in [Hall, 1980]. However, it is mentioned in [Rossing et al., 2002] and [Beament, 1997] that the term *tremolo* for the amplitude modulation is improperly used because in music it refers to the rapid alternation between two notes. The vibrato is broadly used by musicians or singers for adding warmth to a musical tone and capable of hiding a defect in a wavering sound, such as voices from several singers singing together, or the voice from a nervous singer.

The violin vibrato is generated by rocking a finger on a string back and forth on the finger board when playing a note. This somewhat periodically changes the length of the violin string, and results in a periodic tone change or frequency modulation. However, because of the resonance in the violin's body, the frequency deviation causes amplitude variation or modulation [Rossing et al., 2000; Fletcher and Rossing, 1998].

Therefore, the violin vibrato involves not only a frequency modulation, but also amplitude modulation. Some studies including [Ando and Yamakuchi, 1993; Beauchamp, 1974; Fletcher and Sanders, 1967] used the short-time Fourier (STFT) analysis to display the existence of frequency and amplitude modulation of the violin partials. Mellody and Wakefield [2000] employed the modal distribution, a time-frequency method, to estimate both the frequency and the amplitude of the violin partials. It is said that the frequency modulation of the vibrato mostly occurs around 6 or 7 Hz [Hall, 1980], and a deviation of the frequency from the center frequency of the violin vibrato is ±15 cents[1] in average.

In this chapter, only the frequency modulation is estimated, since the frequency and the amplitude cannot be simultaneously achieved by using the proposed approach. We demonstrate using the proposed approach to estimate the time varying spectrum of violin vibrato.

6.2 Method

6.2.1 Violin signal and vibrato

The violin sound was obtained from an internet website www.violinafrica.co.za. The sound is in mono, 8 bit digital sounds sampled at a rate of 22 kHz, and of 20.6 seconds length. The violin vibrato was chosen at two different pitches. Both were of 454 ms in length.

---

[1] Cent is the smallest unit in music scale, One cent is one-hundredth of a semitone in log10-scale.
$1\text{cent} = \sqrt[100]{semitone} = \sqrt[1200]{octave}$.

6.2.2 TVAR model and the modified basis function approach for the time-varying spectral estimation.

In contrast to the spectrogram and the time-frequency distribution in which a signal is analyzed in the frequency domain, the TVAR model with the basis function directly employs the waveform of the nonstationary signal in the time domain. The spectral information of the nonstationary signal is reserved via the time-varying parameters of the TVAR model. The following are the steps in estimating the time-varying spectrum of violin vibratos using the proposed approach, explained in Chapter 3.

Step 1: High pass filtering of the violin signal to get rid of the DC component.

This process is required for the proposed approach since it failed to estimate when the signal contained a DC component. However, in using a high pass filter, a cut off frequency must be chosen. For the violin, it is not difficult to choose the cut off frequency, since the violin sound cannot go so low and typically produces frequencies higher than 200 Hz [Hall, 1980]. Therefore, a frequency cutoff at 200 Hz is used for a high pass filter. The type of the filter has no significant difference in the spectral estimation using the proposed approach, since the proposed approach is not sensitive to the phase change of the nonstationary signal. However, we chose to use the Type-2 Chebyshev filter, since it allows a very steep cut-off slope and has equiripple in the stop band, but monotonicity in the pass band.

Step 2: Estimation of the TVAR model order p.

For the low noise or the noise-free signal, the order of the TVAR model needs to be determined. If the number of spectrum peaks is unknown, the model order selection,

such as the maximum likelihood model order selection in Chapter 5 can be used. Fortunately, for the violin signal the fundamental and the harmonic frequencies are well separated, so the number of spectral peaks is easily determined. For example, the Fourier transform of the violin note B_5^b, is shown in Figure 6.1. There are 4 dominant spectral peaks, hence a suitable model order $p = 8$ can be used. Note that a band pass filter could also be used to get rid of the DC component and limit the number of harmonics. Also the noise at the low and high frequencies is reduced, if the band pass filter is used.

Step 3: Time-varying spectral estimation.

The proposed approach 2 in Chapter 3 is used. The Fourier function is used as a basis function and the expansion dimension is $q = 12$. The calculation for the time-variant parameters of the TVAR model and the time-varying spectral density are summarized in the following process:

i. Form $\bar{\varphi}^T[t] = \begin{bmatrix} \mathrm{y[t]} & y[t-1] & \dots & y[t-p+1] \end{bmatrix}$

$$\bar{\bar{\varphi}}^T[t] = \begin{bmatrix} \mathrm{y[t]} & y[t+1] & \dots & y[t+p-1] \end{bmatrix}$$
$$\vec{f}^T[t] = \begin{bmatrix} f_o[t] & f_1[t] & \dots & f_q[t] \end{bmatrix}$$

ii. Obtain $\bar{\psi}^T[t] = \bar{\varphi}^T[t] \otimes \vec{f}^T[t]$, $\bar{\bar{\psi}}^T[t] = \bar{\bar{\varphi}}^T[t] \otimes \vec{f}^{*T}[t]$

iii. Compute

$$\hat{\bar{\gamma}} = -\left(\sum_{t=p-1}^{T-1} \bar{\psi}^*[t]\bar{\psi}^T[t] + \sum_{t=1}^{T-p+1} \bar{\bar{\psi}}[t]\bar{\bar{\psi}}^{*T}[t] \right)^{-1} \left(\sum_{t=p-1}^{T-1} \bar{\psi}^*[t]y[t+1] + \sum_{t=1}^{T-p+1} \bar{\bar{\psi}}[t]y^*[t-1] \right)$$

iv. Estimate the time-variant parameters of the TVAR model

$$\hat{\bar{a}}[t] = \begin{bmatrix} \hat{a}_1[t] \\ \hat{a}_2[t] \\ \vdots \\ \hat{a}_p[t] \end{bmatrix} = \left(I_{pxp} \otimes \bar{f}^T(t)\right) \cdot \hat{\bar{\gamma}}$$

v. Calculate the time-varying spectral density of the nonstationary signal $y[t]$.

$$S_{yy}[t, f] = \frac{\sigma_w^2}{\left|1 + \sum_{i=1}^{p} a_i[t] e^{-j2\pi f \cdot i}\right|^2}$$

where σ_w^2 is the variance estimate of the white noise input.

$$\sigma_w^2 \sim \sigma_e^2 = \frac{1}{T-p} \sum_{t=p+1}^{T} \left(y[t] + \sum_{i=1}^{p} a_i[t] y[t-i] \right)^2 .$$

6.3 Frequency analysis of the violin vibrato.

The time-varying spectrum of the violin signal was calculated via the block estimation by using the block width equal to the length of the violin signal, which is 10k samples. Results from using the proposed method to estimate the time-varying spectrum of the note with the vibrato are shown in figure 6.1(c) and 6.2(c), which display 453 millisecond sections of the vibrato notes B_5^b and D_6 (fundamental frequency 932.3 and 1174.7 Hz respectively). The frequency modulation can be noticed from the plot using the TVAR approach due to its high resolution representation, which is in contrast to that of using the Fourier transform (figure 6.1a and 6.2a), or the short-time Fourier transform (figure 6.1b and 6.2b). The Fourier transform yielded no information about the time variation of the frequencies. The STFT can track the time variation, but has a frequency

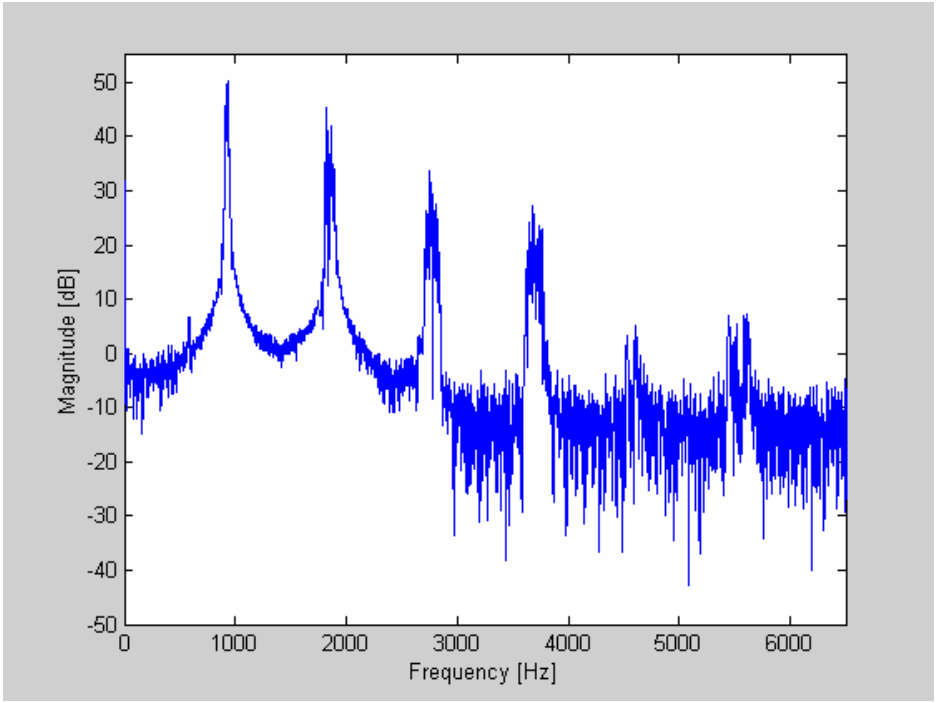

(a) Spectrum using Fourier transform- frequency modulation cannot be seen.

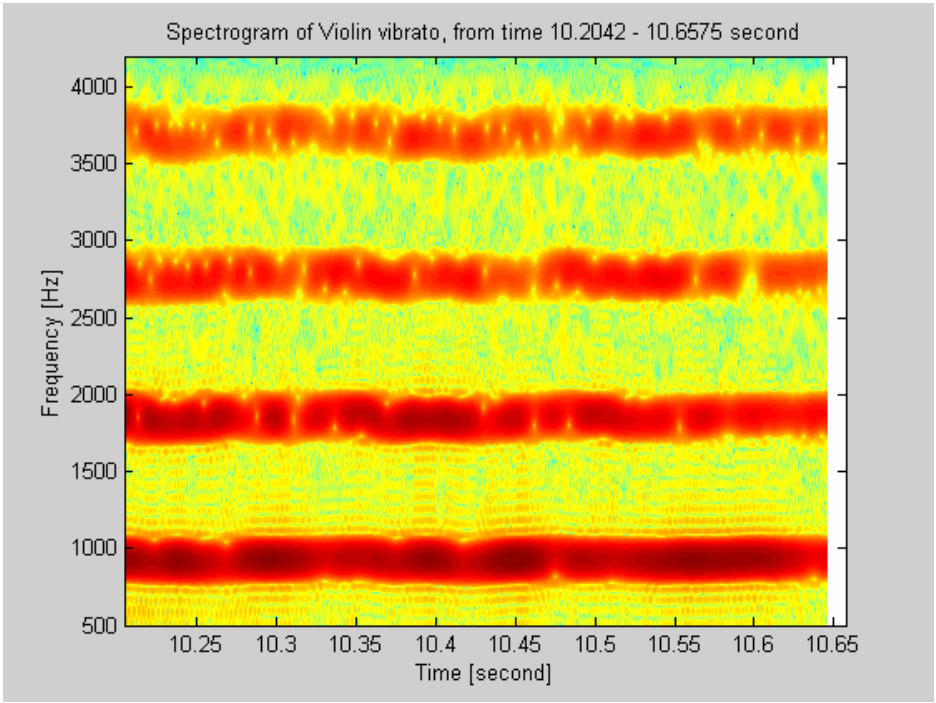

(b) Spectrogram using STFT and Kaiser window length-256, with overlap-250

Figure 6.1: Time-varying spectrum of violin vibrato note B_5^b, using (a) Fourier transform (b) STFT and (c) TVAR model and modified basis function approach – first four harmonics.

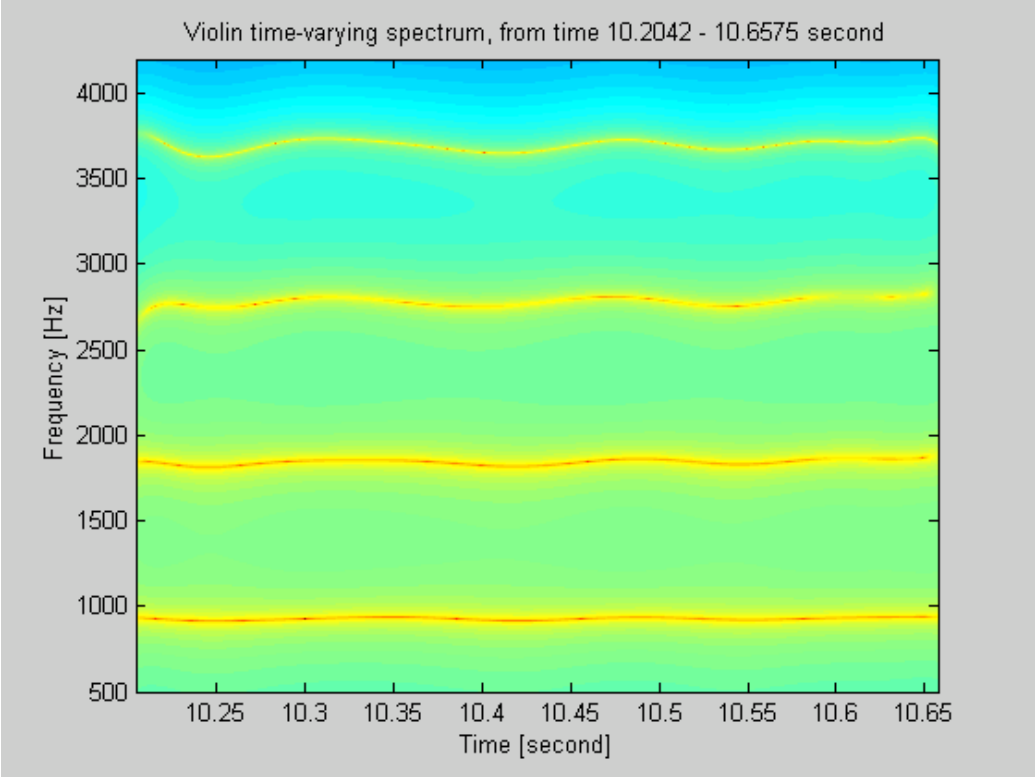

(c) Time-varying spectrum using TVAR model with modified basic function approach

Figure 6.1: Time-varying spectrum of violin vibrato note B_5^b, using (a) Fourier transform (b) STFT and (c) TVAR model and modified basis function approach – first four harmonics (continued)

resolution limitation, depending on a chosen window length. If the long window length was used, the resolution could be good, but the time-variation frequency could not be seen.

The modulation rate of the vibrato, from using the proposed method, is about 6 Hz. The harmonic has the same modulation rate as the fundamental frequency. It should be noticed that the results shown in the figure display only a few harmonics for each of the notes. The total number of harmonics for a note can be as much as 20 or more, depending on the note and the sampling frequency.

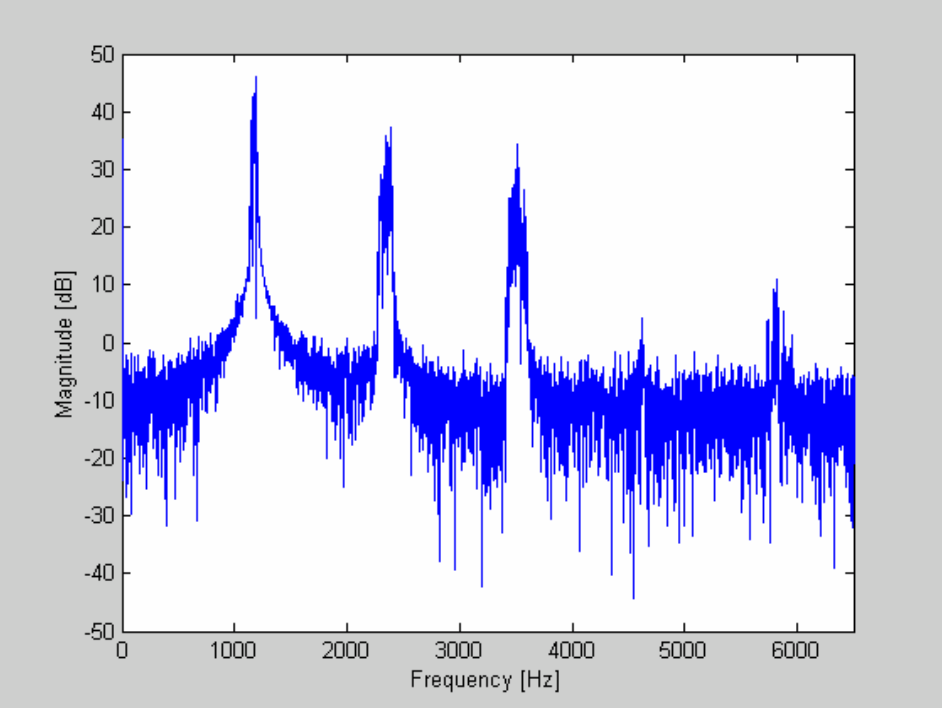

(a) Spectrum using Fourier transform- modulation cannot be seen.

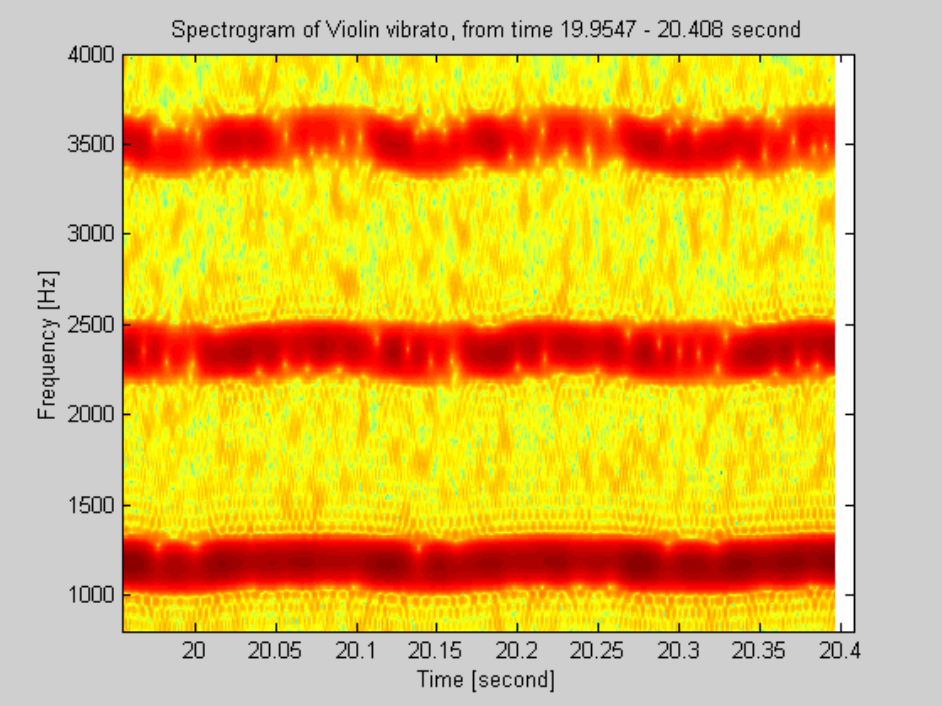

(b) Spectrogram, using STFT with Kaiser window length-256, with overlap-250

Figure 6.2: Spectral estimate of the violin vibrato note D_6, using (a) the Fourier transform, (b) the STFT, and (c) the TVAR model and the modified basis function approach - first three harmonics

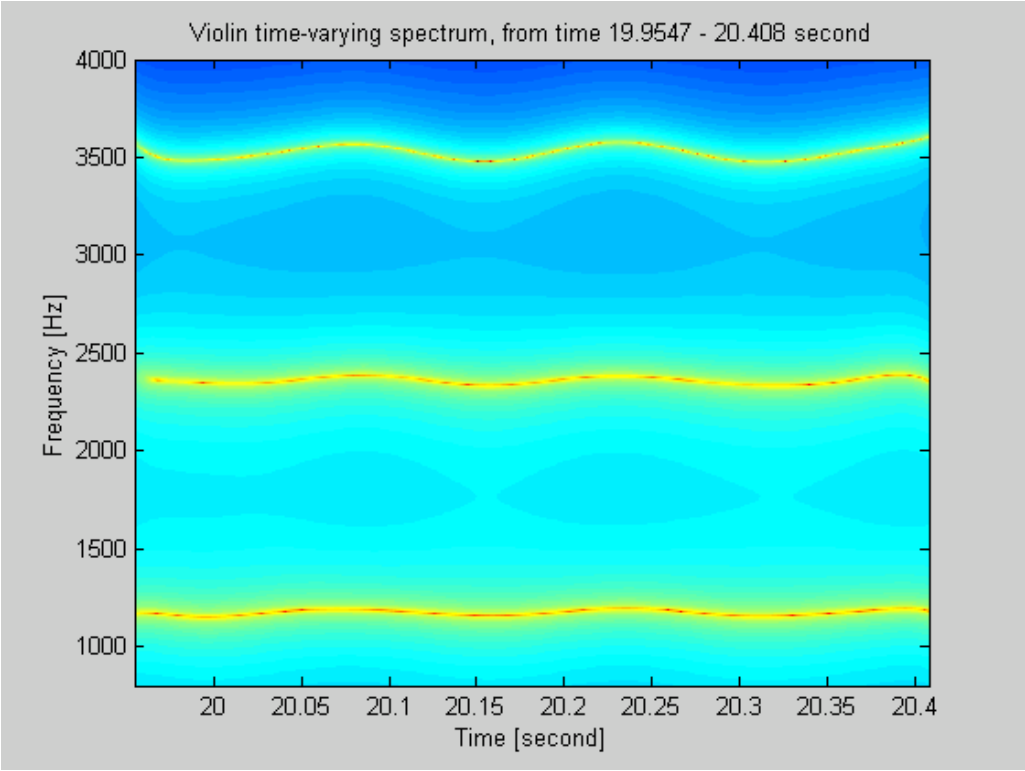

(c) Time-varying spectrum using the TVAR model and the modified basis function approach.

Figure 6.2: Spectral estimate of the violin vibrato note D_6, using (a) the Fourier transform, (b) the STFT, and (c) the TVAR model and the modified basis function approach - first three harmonics (continued)

Figure 6.3 displays a result from the peak-picking of the spectrogram and the time varying spectrum. As shown, both the TVAR with the modified basis function and the STFT spectral lines, vary with time. However, the TVAR with the modified basis function yielded smoother spectral peaks than that from the STFT.

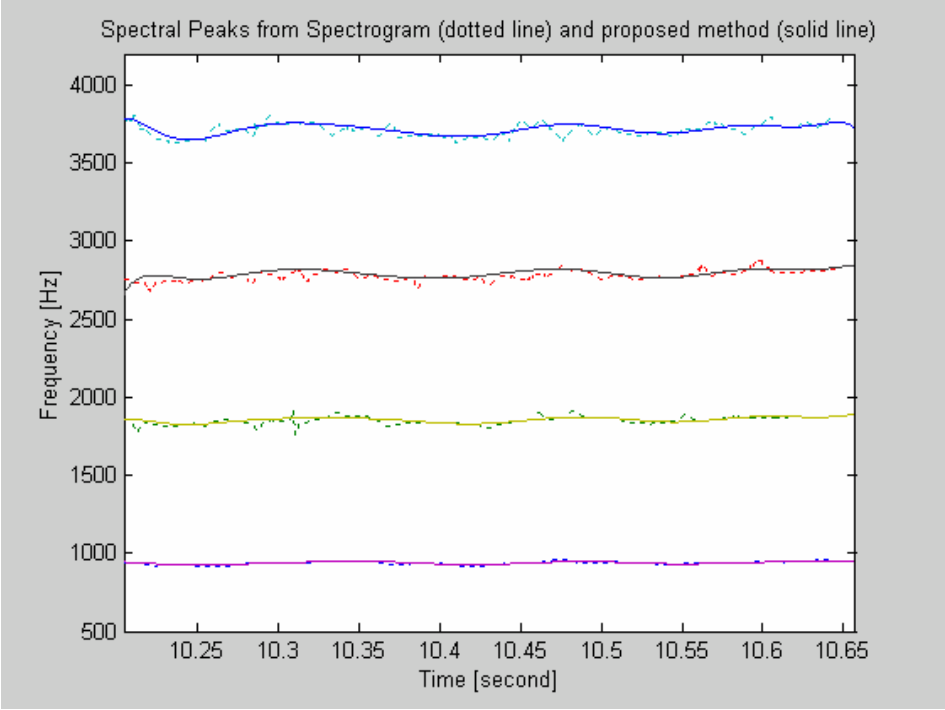

(a) For note B_5^b

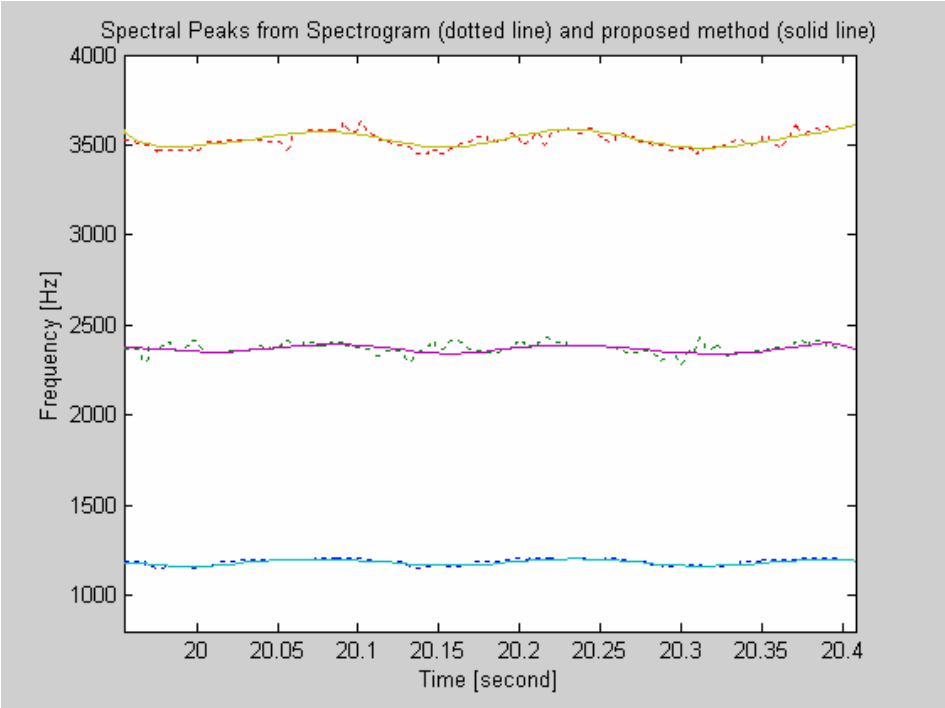

(b) For note D_6

Figure 6.3 Lines of spectral peaks from the spectrogram (dotted line) and the proposed approach (solid line)

Also noticeable is the frequency deviation in each partial. Table 6.1 is a summary of the mean frequency and the frequency deviation of the first four harmonics of the note B_5^b, and the first three harmonics of the note D_6. As shown, the mean frequencies of the partials are approximately integer-multiple to the mean of the fundamental frequency. However, the frequency deviations for each partial are different. The higher partial seems to have higher frequency deviation than the lower partial or the fundamental frequency. The reason for this is not obvious to us, but it might involve a non-linearity and a transient of the string vibration.

Table 6.1: Mean frequency and frequency deviation of each partial for the notes B_5^b and D_6

	Note B_5^b		Note D_6	
	Mean frequency	Frequency deviation (peak-to-peak)	Mean frequency	Frequency deviation (peak-to-peak)
Partial 1	0.937 kHz	25 Hz	1.182 kHz	40 Hz
Partial 2	1.860 kHz	45 Hz	2.368 kHz	55 Hz
Partial 3	2.793 kHz	65 Hz	3.532 kHz	95 Hz
Partial 4	3.715 kHz	80 Hz	-	-

6.4 Chapter summary

A demonstration of using the proposed approach, the TVAR model with the modified basis function approach, to analyze a real non-stationary acoustic signal was

given. A violin vibrato was used as an example. Results from using the proposed method were compared to those from using the STFT. It was observed that line spectra from the TVAR parameters were smoother and of higher frequency resolution than that from the STFT. The vibrato rate was about 6 Hz, which confirmed the findings of other researchers that the vibrato rate would be 6 Hz or 7 Hz. The frequency deviations for all harmonics are not equal. It seems to increase nonlinearly with the harmonic number. A further theoretical study might be needed so that this increase in frequency extent can be precisely explained. However, this is beyond the scope of this thesis.

CHAPTER 7

Conclusion

7.1 Thesis summary

Estimation of the time-variant coefficients of the TVAR model could be done by using either the adaptive algorithm or the basis function method. The adaptive algorithm allowed the time-variant coefficients to be on-line estimated, while the basis function method yielded parameter estimates via the block computation. The time-varying frequency of a non-stationary signal was extracted from the time-varying parameters of the TVAR model representing that non-stationary signal. It was shown that the time-varying frequency could be estimated by using the adaptive algorithm, if the frequency variation with time was slow, and an additive white noise was low. The basis function method was capable of estimating a frequency that quickly or broadly varied with time, but not it was so good in tracking a frequency jump.

A new modification for the basis function approach was presented for estimating the time-varying frequency of nonstationary signals which has modurate (15 dB) to high (20 dB or higher) signal-to-noise ratio. By utilizing both the forward and the backward estimators, and applying a constraint that equalizes the forward and the backward time-varying parameters, an improvement to the basis function approach for frequency estimation were obtained, especially when the order of the TVAR model was over-determined.

Several basis time-functions were compared in estimating the time-varying frequency of the non-stationary signals. The non-harmonic Fourier function, from our tests, was overall the best for the basis function expansion, and the expansion dimension of the order 10 or 12 should be used with the Fourier function. Some limitations of the modified basis function approach were requirements that the signal has no DC-components, the signal length should not be shorter than 5 times $p \cdot q$, and the number of the time-frequency components, if unknown, must be determined.

A demonstration using the modified basis function approach for the frequency analysis of an acoustic signal was given. Violin vibrato was used as an example. It was shown that the time-varying spectral estimates had a very high frequency resolution. Lines of spectral peaks from using the TVAR model and the modified basis function approach were smooth, and the frequency modulations of the violin vibrato were obviously seen. These were contrasted with the traditional analysis of the STFT that yielded a lower frequency resolution and the frequency modulation of the vibrato was not easily seen.

7.2 Future research

The results in this thesis have justified a proposed method, the TVAR model with the modified basis function approach, as a new technique to explore the characteristics of nonstationary acoustic signals, especially the time-frequency variation. The modified basis function approach, although using a set of predefined time-basis functions, yields smooth spectral line estimates with very high frequency resolution. This is a very useful

advantage of the proposed approach because, in some cases, the spectrum variation of a short nonstationary signal may not be easily observed with the existing analysis techniques (such as the Fourier transform, the STFT, the TFD or the phase-lock-loop (PPL)), but could be easily seen by using the modified basis time function approach. For example, in our demonstration, the violin vibrato was analyzed and the time-frequency plots were shown. The frequency modulation was clearly noticed with the modified basis function approach, but not with the STFT. Also it was found that the frequency variations for each partial were different and nonlinear. This characteristic of the frequency fluctuation cannot be easily observed by using the STFT. To explain the nonlinear frequency variation of the violin vibrato, a further study is needed.

The TVAR and the modified basis function approach are not only useful to violin vibrato analysis, but also to the analysis of other musical instruments, such as drum and other string instruments. Other applications, which are not in music area, are also possible. For example, works were found which used the basis function approach for predictive speech coding [Liporace, 1975; Hall, 1980], Doppler frequency estimation [Girault al etc., 2000], ultrasound attenuation estimation [Girault al etc., 1998], and communication channel fading [Tsatsanis and Giannakis, 1996]. The modified basis function could be adapted and used in similar applications to these as well.

Other possible applications are feature extraction and vibration monitoring. Since information about a system's characteristics is contained in the time-variant parameters of the TVAR model, the TVAR parameters are virtually the signature of the system. They could be processed through a neural network, or a classifier, to determine or to monitor

the system's condition. How good and early the fatigue condition of the system can be detected is an open problem.

APPENDIX

A. Transforming the equation (3.9) or (3.15) to the matrix relation (3.17).

Expanding the summation for $k = 0,1,...q$ in (3.9) or (3.15),

$$\sum_{i=1}^{p}\left(\begin{bmatrix} c_{0l}(1,j) & c_{1l}(2,j) & \cdots & c_{ql}(p,j) \end{bmatrix} \begin{bmatrix} a_{i0} \\ a_{i1} \\ \vdots \\ a_{iq} \end{bmatrix} \right) = -c_{0l}(0,j), \quad j = 1,2,...p \text{ and } l = 0,1,...,q$$

$$\sum_{i=1}^{p}\left(\begin{bmatrix} c_{00}(i,j) & c_{10}(i,j) & \cdots & c_{q0}(i,j) \\ c_{01}(i,j) & c_{11}(i,j) & \cdots & c_{q1}(i,j) \\ \vdots & \vdots & \ddots & \vdots \\ c_{0q}(i,j) & c_{1q}(i,j) & \cdots & c_{qq}(i,j) \end{bmatrix} \begin{bmatrix} a_{io} \\ a_{i1} \\ \vdots \\ a_{iq} \end{bmatrix} \right) = -\begin{bmatrix} c_{00}(0,j) \\ c_{01}(0,j) \\ \vdots \\ c_{0q}(0,j) \end{bmatrix}, \quad j = 1,...,p$$

$$\sum_{i=1}^{p} \Phi(i,j)\vec{a}_i = -\vec{\chi}_j, \quad j = 1,...,p \tag{A-1}$$

where $\Phi(i,j) = \begin{bmatrix} c_{00}(i,j) & c_{10}(i,j) & \cdots & c_{q0}(i,j) \\ c_{01}(i,j) & c_{11}(i,j) & \cdots & c_{q1}(i,j) \\ \vdots & \vdots & \ddots & \vdots \\ c_{0q}(i,j) & c_{1q}(i,j) & \cdots & c_{qq}(i,j) \end{bmatrix}$, $\vec{a}_i = \begin{bmatrix} a_{i0} \\ a_{i1} \\ \vdots \\ a_{iq} \end{bmatrix}$, and $\vec{\chi}_j = \begin{bmatrix} c_{00}(0,j) \\ c_{01}(0,j) \\ \vdots \\ c_{0q}(0,j) \end{bmatrix}$

Again, expand the summation for $i = 1,...,p$ and $j = 1,...,p$ in (A-1). Equations (3.9) and (3.15) is finally in a matrix form as

$$\begin{bmatrix} \Phi(1,1) & \Phi(2,1) & \cdots & \Phi(p,1) \\ \Phi(1,2) & \Phi(2,2) & \cdots & \Phi(p,2) \\ \vdots & \vdots & \ddots & \vdots \\ \Phi(1,p) & \Phi(2,p) & \cdots & \Phi(p,p) \end{bmatrix} \begin{bmatrix} \vec{a}_1 \\ \vec{a}_2 \\ \vdots \\ \vec{a}_p \end{bmatrix} = - \begin{bmatrix} \vec{\chi}_1 \\ \vec{\chi}_2 \\ \vdots \\ \vec{\chi}_p \end{bmatrix} \qquad \text{(A-2)}$$

$$\downarrow \qquad \downarrow \qquad \downarrow$$

$$\mathbf{C}_{(p(q+1))x(p(q+1))} \qquad \mathbf{a}_{(p(q+1))x1} \qquad \mathbf{d}_{(p(q+1))x1}$$

or $\mathbf{Ca = d}$

Which is the matrix relation (3.17) □

B. Properties of Kronecker Products [Graham, 1981]

Let A and B be vectors or matrices. The properties of Kronecker products are listed as following:

1 $A \otimes B = \begin{bmatrix} a_{11}B & a_{12}B & \dots & a_{1n}B \\ a_{21B} & a_{22}B & \dots & a_{2n}B \\ \vdots & \vdots & & \vdots \\ a_{m1}B & a_{m2}B & \dots & a_{mn}B \end{bmatrix}$

2 $A \otimes (\alpha B) = \alpha (A \otimes B)$

3 $(A + B) \otimes C = A \otimes C + B \otimes C$ and $A \otimes (B + C) = A \otimes B + A \otimes C$

4 $(A \otimes B) \otimes C = A \otimes (B \otimes C)$

5 $(A \otimes B)^T = A^T \otimes B^T$ and $(A \otimes B)^{-1} = A^{-1} \otimes B^{-1}$

6 $(A \otimes B) \otimes (C \otimes D) = AC \otimes BD)$

C. The TVAR process with the infinite model order validly represents the TVMA or the TVARMA process with a finite model order.

To prove this, we will simply show that both the TVMA(1) and the TVARMA(1,1) can be changed into the TVAR form with the infinite order. The transfer function of the TVMA(1) process is

$$H_{MA}(z) = d_0[t] + d_1[t]z^{-1} \tag{A-3}$$

Let $$d_0[t] + d_1[t]z^{-1} = \frac{1}{1 + c_1[t]z^{-1} + c_2[t]z^{-2} + \ldots}$$

$$= \frac{1}{C(z)}$$

where the term in the right side is the transfer function of the TVAR(∞), and $C(z)$ is the z-transform of $c_k[t]$ with respect to *k*. That is

$$C(z) = \mathrm{Z}\{z_k[t]\} = \frac{1}{d_0[t] + d_1[t]z^{-1}}$$

$$= \frac{1/d_0[t]}{1 + d_1[t]/d_0[t]\, z^{-1}}$$

take the inverse z-transform of $C(z)$,

$$c_k[t] = \frac{1}{d_0[t]}\left(-\frac{d_1[t]}{d_0[t]}\right)^k, \text{ k = 0, 1, 2, } \ldots \tag{A-4}$$

Therefore, the TVMA(1) are equivalent to the TVAR(∞), in which the infinite TVAR coefficients $c_k[t]$ must be defined as equation (A-4). □

For the TVARMA(1,1) process, its transfer function is

$$H_{ARMA}(z) = \frac{1 + b_1[t]z^{-1}}{1 + a_1[t]z^{-1}} \tag{A-5}$$

Let
$$\frac{1 + b_1[t]z^{-1}}{1 + a_1[t]z^{-1}} = \frac{1}{1 + c_1[t]z^{-1} + c_2[t]z^{-2} + \ldots}$$

$$= \frac{1}{C(z)} = H_{AR}(z)$$

$$C(z) = Z\{z_k[t]\} = \frac{1 + a_1[t]z^{-1}}{1 + b_1[t]z^{-1}}$$
$$= 1 + \frac{(a_1[t] - b_1[t])z^{-1}}{1 + b_1[t]z^{-1}}$$

and the inverse z-transform of $C(z)$ is

$$c_k[t] = \begin{cases} 1 & , \ k = 0 \\ (a_1[t] - b_1[t])(-b_1[t])^{k-1} & , \ k = 1,2,3,.... \end{cases} \tag{A-6}$$

Hence the TVARMA(1,1) process is equivalent to the TVAR(∞), in which the TVAR parameters are defined in the equation (A-6). □

D. Show that a TVAR process with the additive white noise is equivalent to a TVARMA signal.

Let the signal $x[t]$ be the impulse response of the TVAR(m) processes, and $y[t] = x[t] + w[t]$ where $w[t]$ is the additive white noise. The spectral density of $x[t]$ is

$$P_{xx}(t,\omega) = \frac{1}{\left|1 + \sum_{k=1}^{m} a_k[t]e^{-jk\omega}\right|^2} = \frac{1}{D(t,\omega)}$$

The power spectral density of $y[t]$ is

$$P_{yy}(t,\omega) = P_{xx}(t,\omega) + \sigma_w^2 = \frac{1}{\left|1 + \sum_{k=1}^{m} a_k[t] e^{-jk\omega}\right|^2} + \sigma_w^2$$

$$= \frac{1 + \sigma_w^2 D(t,\omega)}{\left|1 + \sum_{k=1}^{m} a_k[t] e^{-ik\omega}\right|^2},$$

which is actually the power spectral density of a TVARMA(m,m) process. Therefore, the TVAR(m) process in the additive white noise becomes a TVARMA(m,m) process, whose coefficients in the numerator of the TVARMA transfer function depend on the power spectral density of the signal and the noise variance. □

REFERENCES

[Ando and Yamakuchi, 1993] S. Ando and K. Yamaguchi, "Statistical study of spectral parameters in musical instrument tones," *J. Acoust. Soc. Am.*, Vol. 94, No. 1, pp 37-45, 1993.

[Beament, 1997] J. Beament, *The Violin Explained*, Oxford, 1997.

[Beauchamp, 1974] J. W. Beauchamp, "Time-variant spectral of violin tones," *J. Acoust. Soc. Amer.*, Vol. 56, No. 3, pp. 995-1004, 1974.

[Beex and Shan, 1999] A.A Beex and P. Shan, "A time-varying prony method for instantaneous frequency estimation at low frequency," *Proceeding of the 1999 IEEE International Symphosium on Circuits and Systems*, Vol 3, pp. 5-8, 1999.

[Boashash, 1992] B. Boashash, "Estimating and interpreting the instantaneous frequency of a signal. II: Algorithms and applications," *Proceeding of the IEEE*, Vol. 80, No. 4, pp. 540-568, 1992.

[Charbonnier et al., 1987] R. Charbonnier, M. Barlaud, G. Alengrin, and J. Menez, "Results on AR Modeling of Nonstationary Signals," *Signal Processing*, Vol. 12, No. 2, pp 143-151, 1987.

[Cohen,1995] L. Cohen, *Time-Frequency Analysis*, Prentice Hall, Chapter 3, Englewood Cliffs, NJ: 1995.

[Datta, 1995] B. N. Datta, *Numerical Linear Algebra*, Brooks/Cole, Pacific Grove, CA: 1995 .

[Eom, 1999] K.B. Eom, "Analysis of Acoustic Signatures from Moving Vehicles Using Time-Varying Autoregressive Models," *Multisignal Systems and Signal Processing*, Vol 10, pp 357-378, 1999.

[Fletcher and Rossing, 1998] N. H.Fletcher and T. D. Rossing, *The Physics of Musical Instruments- 2nd edition*, Springer-Verlag, NY 1998.

[Fletcher and Sanders, 1967] H. Fletcher and L.C. Sanders, "Quality of violin vibrato tones," *J. Acoust. Soc. Am.*, Vol. 41, No. 6, pp 1543-1544, 1967.

[Girault et al., 2000] J. M. Girault, D. Kouame, A. Ouahabi, and F. Patat, "Estimation of the blood Doppler frequency shift by a time-varying parametric approach." *Ultrasonics*, 38, pp. 682-687, 2000.

[Girault et al., 1998] J.M Girault, F. Ossant, A Ouahabi, D. Kouame, and F. Patat, "Time-Varying Autoregressive Spectral Estimation for Ultrasound Attenuation in Tissue

Characterization," *IEEE Transactions on Ultrasonics, Ferroelectrics, and Frequency Control*, Vol. 45, No. 3, pp. 650-659, 1998.

[Graham, 1981] A. Graham, *Kronecker Products and Matrix Calculus with Applications - Chapter 2*, John Wiley & Sons, 1981.

[Hall et al., 1983] M.G. Hall, A.V. Oppenheim, and A.S. Willsky, "Time Varying Parametric Modeling of Speech," *Signal Processing*, Vol. 5, pp 267-285, 1983.

[Hall, 1980] D. E. Hall, *Musical Acoustics: An introduction*, Wadsworth, CA, 1980.

[Haykin, 1996] M. H. Hayes, *Statistical Digital Signal Processing and Modeling,* John Wiley and Sons, NY: 1996.

[Kay, 1988] S.M. Kay, *Modern Spectral Estimation*, Prentice Hall, Englewood Cliffs, NJ: 1988.

[Kozin and Nakajima, 1980] F. Kozin and F. Nakajima, "The Order Determination Proplem for Linear Time-Varying AR Models," *IEEE Transactions on Automatic Control*, Vol. AC-25, No. 2, pp 250-257, 1980.

[Liporace, 1975] L.A. Liporace, "Linear Estimation of Nonstationay of Nonlinear Signals," *J. Acoust. Soc. Amer*., vol. 58, no. 6, pp 1288-1295, 1975.

[Marple, 1987] S.L. Marple, *Digital Spectral Estimation*, Prentice Hall, Englewood Cliffs, NJ: 1987.

[Mellody and Wakefield, 2000] M. Mellody and G. H. Wakefield, "The Time-frequency characteristics of violin vibrato: Modal distribution analysis and synthesis," *J. Acoust. Soc. Am*., Vol 107, No 1, pp. 598-611, 2000.

[Niedzwiecki, 2000] M. Neidzwiecki, *Identification of Time-varying Processes*, John Wiley & Sons, Chicester, England, 2000.

[Rao, 1970] T. Subba Rao, "The fitting of nonstationary time series models with time-dependent parameters," *J.Royal Statist. Soc. Series B*, Vol. 32, No.2, pp312-322, 1970.

[Rajan and Rayner, 1996] J. J. Rajan and P. J. W. Rayner, "Generalized Feature Extraction for Time-Varying Autoregressive Model," IEEE Transactions on Signal Processing, Vol. 44, No. 10, pp 2498-2507, 1996.

[Rossing at al., 2002] T. D. Rossing, F. R. Moore, and P. A. Wheeler, *The Science of Sound*, Addison Wesley, CA, 2002.

[Swanson, 2000] D.C. Swanson, *Signal Processing for Intelligent Sensor Systems*, Marcel Dekker, 2000.

[Therrien, 1992] C. W Therrien, *Discrete Random Signals and Statistical Signal Processing*, Prentice Hall, Englewoood Cliffs, NJ: 1992.

[Trefethen and Bau, 1997] L. N. Thefethen and D. Bau, III, *Numerical Linear Algebra*, Siam, Philadephia, PA: 1997.

[Tsatsanis and Giannakis, 1996] M. K. Tsatsanis and G. B. Giannakis, " Modelling and Equalization of Rapidly Fading Channels," *International Journal of Adaptive Control and Signal Processing*, Vol. 10, pp. 159-176, 1996.

VITA

Chukiet Sodsri was born in Nakhon Pathom, Thailand, on March 9, 1971. He earned a Bachelor's degree in physics in May 1993 from Silpakorn University, Thailand, where he graduated with honors. He worked as an engineer for Melco Manufactruring Company, an electronic firm in Thailand, from 1993 to 1995. In 1996, he was granted a scholarship from the Royal Thai Government to continue his study in the United State. In 1998, Mr. Sodsri received a Master's degree in electrical engineering from The George Washington University, Washington DC. He earned a Ph.D. in acoustics from The Pennsylvania State University in 2003.